UNIVERSITÀ
DEGLI STUDI
FIRENZE

DOTTORATO DI RICERCA IN INGEGNERIA INDUSTRIALE

CICLO XXXII

COORDINATORE Prof. De Lucia Maurizio

Modellazione e Simulazione di Reti di Distribuzione del Gas Naturale in presenza di Iniezione di Idrogeno

Settore Scientifico Disciplinare ING-IND/09

Dottorando
Dott. *Adolfo Dominique*

Tutore
Prof. *Carcasci Carlo*

Coordinatore
Prof. *De Lucia Maurizio*

Anni 2016/2019

DOCTORATE IN INDUSTRIAL ENGINEERING

XXXII CYCLE

Modelling and Simulation of Natural Gas Distribution Networks in the presence of Hydrogen Injection

Candidate

Adolfo Dominique

Supervisor

Prof. *Carcasci Carlo*

2016/2019

Abstract

The 2050 long-term strategy, defined by the European Commission, leads towards zero greenhouse gas emissions by 2050. Reduction of carbon dioxide emissions can be achieved substituting high carbon fossil fuels (coal and oil) with natural gas, renewable sources and green fuels. In the next years, the gas system will play a central and crucial role in the global energy market. Due to modifications of international gas trade flows and rise of demand, the existing gas infrastructures will necessarily have to be expanded, upgraded and renovated in the immediate future. Furthermore, power-to-gas technology is a potential solution to support and accelerate the penetration of renewable sources and the decarbonization of the energy sector. The excess of power generated by renewable energy sources is used by power-to-gas facilities to produce alternative green fuels. The resulting gas, such as hydrogen or synthetic natural gas, can be injected and stored into the existing gas grid. Subsequently, the green low/zero-carbon fuel blended with the traditional natural gas would enable to reduce carbon dioxide emission of industrial, commercial and residential gas customers.

In this new scenario, it is essential to study, model and simulate the integration and operation of gas networks in the energy system. It is also very important to evaluate the impact of alternative fuel injections on the properties and composition of the gas delivered to the users connected to the gas grid.

In this thesis, a steady-state and dynamic one-dimensional gas network tool, named "Gas Network Solver", is developed. The research focuses on mathematical modelling of city gate station (source), pipe, reducing station, valve, demand node and interchange node elements, which compose a gas distribution network. Particular attention is dedicated to the implementation of the mathematical model of the gas and the algorithm for quality tracking in order to analyse and simulate multiple types of gas sources.

The tool proposed is validated by comparing results of three test cases to solutions obtained with a commercial software application, named "Scenario Analysis Interface for Energy Systems" (SAInt), and data from other models available in the literature.

Finally, a case study considering a real medium-pressure and low-pressure gas distribution network, composed by about 2289 elements and located in a hilly area of central Italy, is analysed. After the simulation and analysis of the network in the actual scenario, a possible solution to decarbonize the network is carried out. The installation of a power-to-gas facility, associated effects on behaviour of the network and quality of the gas delivered are studied. The investigation also aims to evaluate the maximum amount of hydrogen injectable respecting gas standards defined by the Italian Regulatory Authority for Energy, Networks and Environment.

Contents

Nomenclature

Mathematical Symbols

A	Pipe cross-section area	$[m^2]$
c	Speed of sound	$[m/s]$
C	Generic quantity transported	$[-]$
D	Pipe diameter	$[m]$
DD	Diffusion coefficient	$[m^2/s]$
$\dot{E}$	Energy flow	$[MJ/s]$
g	Gravitational acceleration	$[m/s^2]$
HHV	Higher heating value	$[MJ/Sm3]$
L	Pipe length	$[m]$
$\dot{m}$	Mass flow rate	$[kg/s]$
M	Molecular weight	$[kg/kmol]$
p	Pressure	$[Pa]$
Pe	Peclet number	$[-]$
$\dot{Q}$	Standard volumetric flow rate	$[Sm^3/h]$
R	Gas constant	[J/mol K]
Re	Reynolds number	$[-]$
SG	Specific gravity	$[-]$
t	Time	$[s]$
T	Temperature	$[K]$
UFL	Upper flammability limit	[%]
v	Flow Velocity	$[m/s]$
VFL	Lower flammability limit	[%]
WI	Wobbe index	$[MJ/Sm^3]$
x	Space direction	$[m]$
y	Mole fraction	$[-]$
Y	Generic flow variable	$[-]$
Z	Compressibility Factor	$[-]$
Δp	Pressure drop	$[Pa]$
Δt	Time step	$[s]$
Δx	Spatial discretization	$[m]$
ε	Pipe surface roughness	$[m]$
θ	Pipe inclination angle	[°]
λ	Darcy friction factor	$[-]$
μ	Dynamic viscosity	$[\mu Pa\ s]$
ξ	Viscosity parameter	$[-]$
ρ	Density	$[kg/m^3]$

Acronyms

H2	Hydrogen
LNG	Liquefied natural gas
NG	Natural gas
NWG	Gas network solver
P2G	Power to gas
SAInt	Scenario analysis interface for energy systems
SMR	Steam-methane reforming
SNG	Synthetic natural gas
TSO	Transmission system operator

Subscripts

0	Standard conditions
c	Critical property
dmd	Demand
g	Gas
in	Inlet
max	Maximum
mix	Mixture
out	Outlet
k	Specie
u	Universal gas
r	Reduced property
set	Setpoint value
x	Spatial direction

Chapter 1

Introduction

Global warming is a severe problem for the planet. The emission of gases causes the greenhouse effect, which traps heat radiating from Earth to space. This effect has produced, in the last decades, a rise of about $2\ ^{\circ}C$ in the average temperature of the Earth.
In the last years, sustainable policies of countries, climate actions and commissions strategies have led to substitute hydrocarbon fuel, such as oil and coal, with natural gas which is lower carbon fuel. The use of natural gas as primary energy provides a halving of CO2 emissions. However, this solution is not able to satisfy the high targets defined by the EU 2050 long term strategy [1.1]. Therefore, the introduction in the energy market of alternative green fuels, such as biogas, hydrogen and synthetic natural gas, is necessary to achieve zero-carbon emission and mitigate climate effects.
The fluctuation of wind and solar sources generates the loss of a large amount of energy. The surplus of electricity generated can be used by power-to-gas facilities to produce green pure hydrogen gas. The injection of the resulting fuel into gas networks would contribute to decarbonise the gas system and mitigate climate change. However, due to its characteristics, hydrogen highly impacts on behaviour of gas networks and properties of the gas delivered to users.
In this new scenario of the gas system, modelling and simulation of gas networks, in particular in the presence of alternative sources, is essential for gas companies.

1.1 Natural Gas Overview

Due to climate change and policies objectives, the global energy market is in the midst of a sustainable transformation. The trend of total world energy demand, assessed for the past years and forecasted for the next years, is shown in figure 1.1. Nowadays, most of the energy is required

and consumed by residential users, industries, and the transport sector. Due to economic and technological development, the world's energy consumption is projected to rise at a pace between 1 and 2% per year. In 2050, the target year for several climate predictions and energy strategies [1.1], the total amount of energy required by customers will be about $446\ EJ/yr$. However, the maximum peak demand of $462\ EJ/yr$ is estimated in 2033. After that, a quite reduction in energy usage is expected because of an increase in users' devices efficiency and a decrease in the transport sector consumption.
As shown in figure 1.2, a significant part of the increase in demand will be supplied by the rise of renewable sources (wind and solar PV) and natural gas. At the same time, a reduction of high carbon sources is expected. However, in 2050 oil and coal sources will still provide about 28% of the total energy demand because of common use in less economically developed countries.

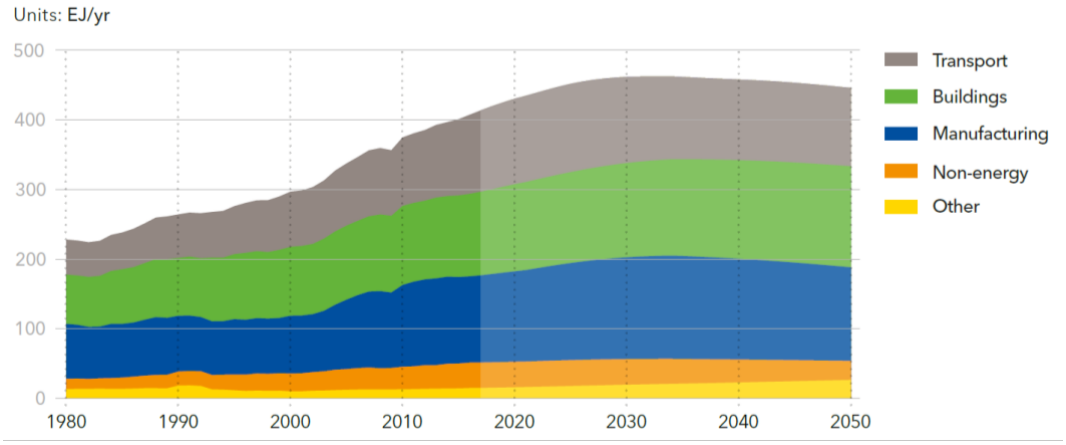

Figure 1.1: World final energy demand by sector [1.2].

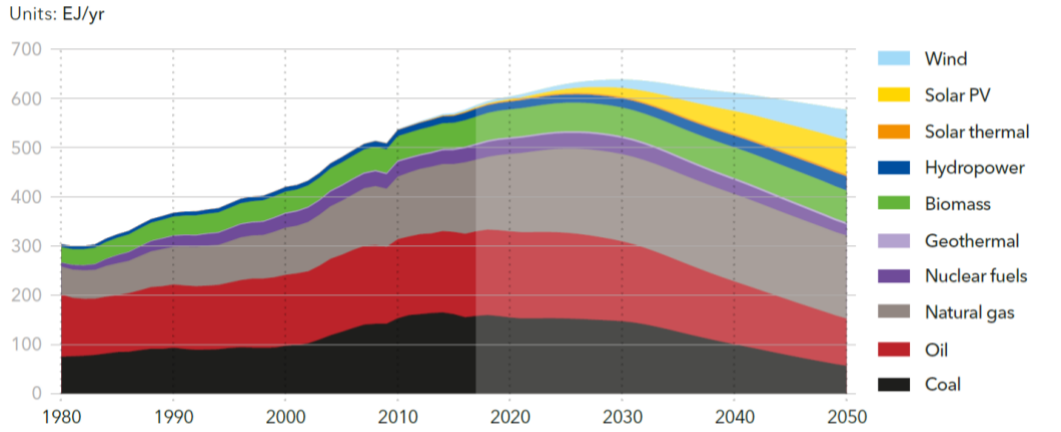

Figure 1.2: World primary energy supply by source [1.2]

Figure 1.3 shows the primary energy consumption by sources in 2050 for the different world regions. As mentioned above, natural gas and renewable sources in the next future will replace high-carbon fossil fuels. In 2050, for many of the world regions (Europe, America, Middle East, North Africa, North East Eurasia and South East Asia), NG will dominate the energy market with a percentage between 25 and 57 of the total energy produced. For policies strategies, only in two regions, other sources will be the primary energy. In the OECD Pacific region (Japan, Republic of

Korea, Australia and New Zealand), about 26 and 13% of the energy demand will be covered respectively by wind and solar PV renewable sources because of the strong promotion of RES to reduce carbon emissions. Instead, as a consequence of the very large consumptions, oil and coal will supply about 30% of the energy requested by users in Greater China.

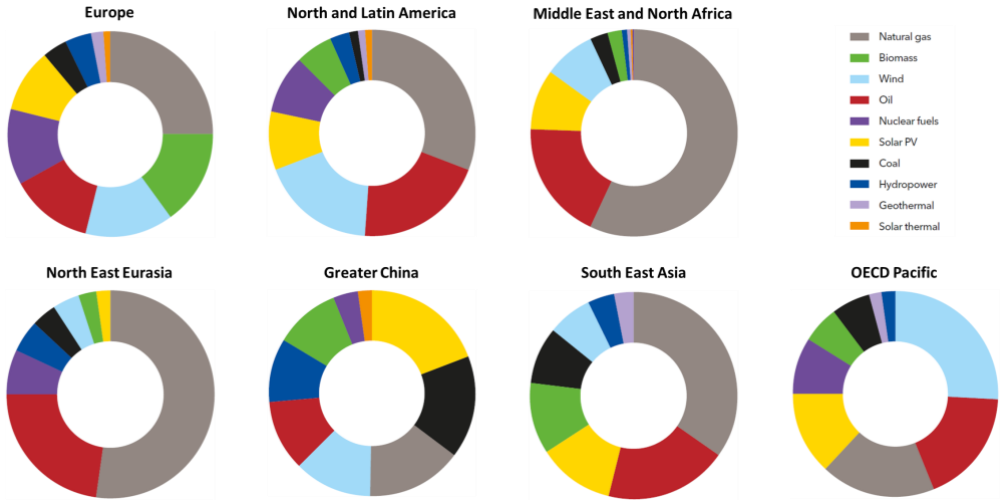

Figure 1.3: Primary energy consumption by source in 2050 for the world regions [1.2].

In 2033, natural gas will provide to users the maximum amount of energy ($5'500\ Gm^3/yr$), which corresponds to an increment of 19% than today (figure 1.4). The main natural gas customers are and will be power generation, followed by residential users and manufacturing industries. In the next 10 years, a significant increment of the NG demand, by these 3 principal sectors, is expected. Thereafter, the consumption of natural gas will be substantially constant or slightly decreasing until 2050. Of particular note, an expected increase until 2030 of the natural gas consumption in the form of CNG for light-vehicle and LNG for maritime navy and heavy-vehicle. In 2050, about 10% of all vehicles of the transport sector will be powered by motors based on natural gas fuels.

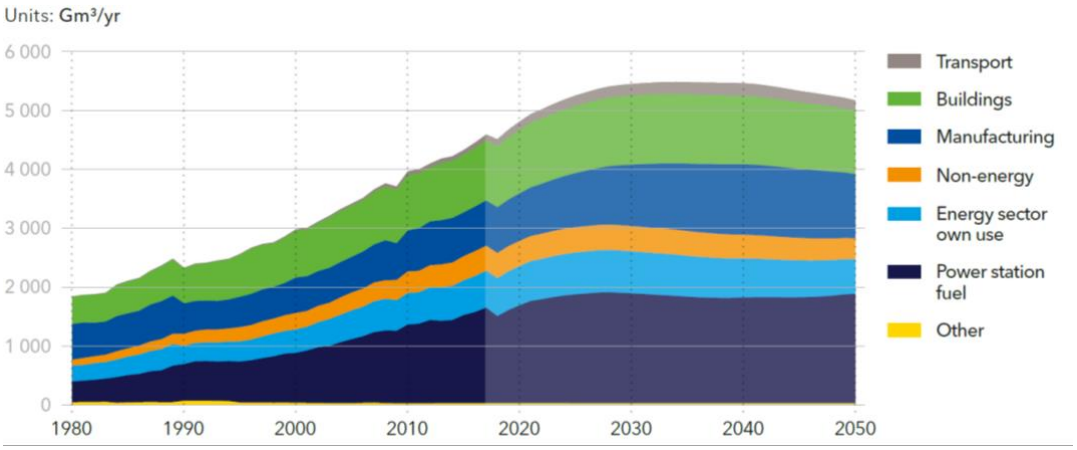

Figure 1.4: World natural gas demand by sector [1.02]

Natural gas resources are widely distributed around the world (figure 1.5). However, the main gas reserves are located in the Commonwealth of Independent States (CIS), Middle East and North America. Africa and Latin America, even if they do not have the biggest reserves, are the regions with the largest number years of technically recoverable resources. As a consequence of gas reservoirs and customers located around the world, gas trade flows between countries and regions are massive. From production sites to the places of use, the natural gas can be transported by LNG carriers or onshore/offshore pipelines (figure 1.6).

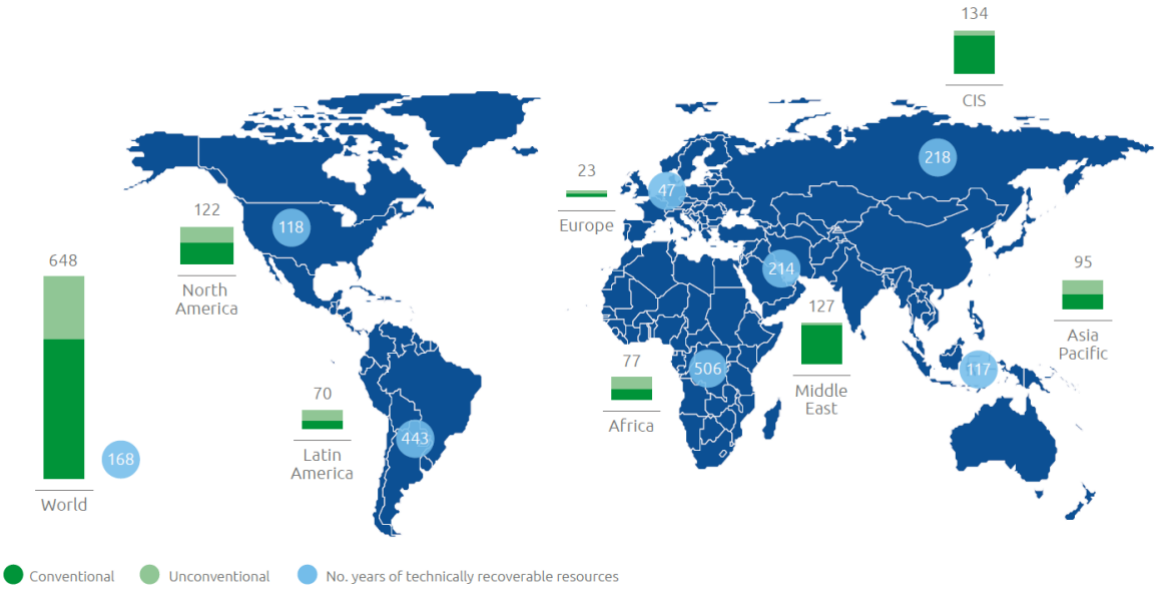

Figure 1.5: Natural gas total technically recoverable resources by region (tcm) [1.3].

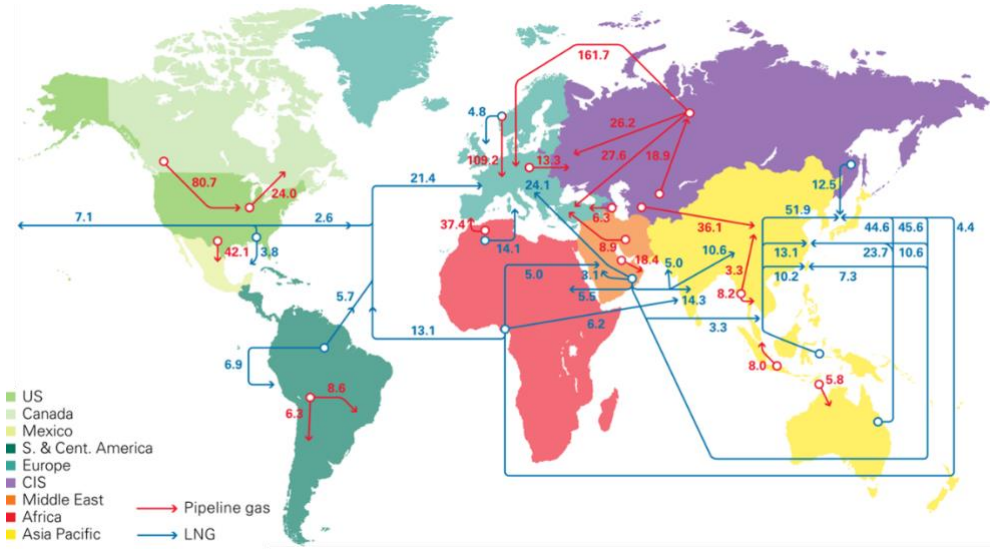

Figure 1.6: Natural gas trade flows worldwide for the year 2017 (bcm) [1.4].

Natural gas systems are very large complex structures, which aim to treat, transport, storage, distribute the gas and lastly increase/decrease gas pressure (figure 1.7). The first stage of the supply

chain is the production stage, where natural gas plants extract the gas situated in underground reserves, remove contaminants (CO_2, H_2S, heavy hydrocarbons, etc.) and sometimes liquefy the gas. After that, long onshore/offshore pipelines and LNG carries are responsible for moving and transferring the natural gas from one country to another (supply stage). Inside a country, the gas infrastructure is composed by high-pressure pipelines (transmission stage), medium-pressure networks (local transmission) and low-pressure subnetworks (local distribution). In these 3 pressure levels subsystems, the gas is compressed by compressor stations, stocked into underground storage, decompressed and measured by city gate stations and reducing stations. All these processes are necessary to deliver the gas at the correct pressure level to a wide variety of users.

Large industries and gas power plants, which require a fuel gas with high pressure and are located in suburban areas, are connected to the transport network. Medium-pressure networks supply the gas to reducing stations (source for LP grids), CNG fuelling stations, large commercial customers, medium and small industries. Finally, the gas is delivered at the lowest pressure levels to residential users (homes), medium and small commercial customers.

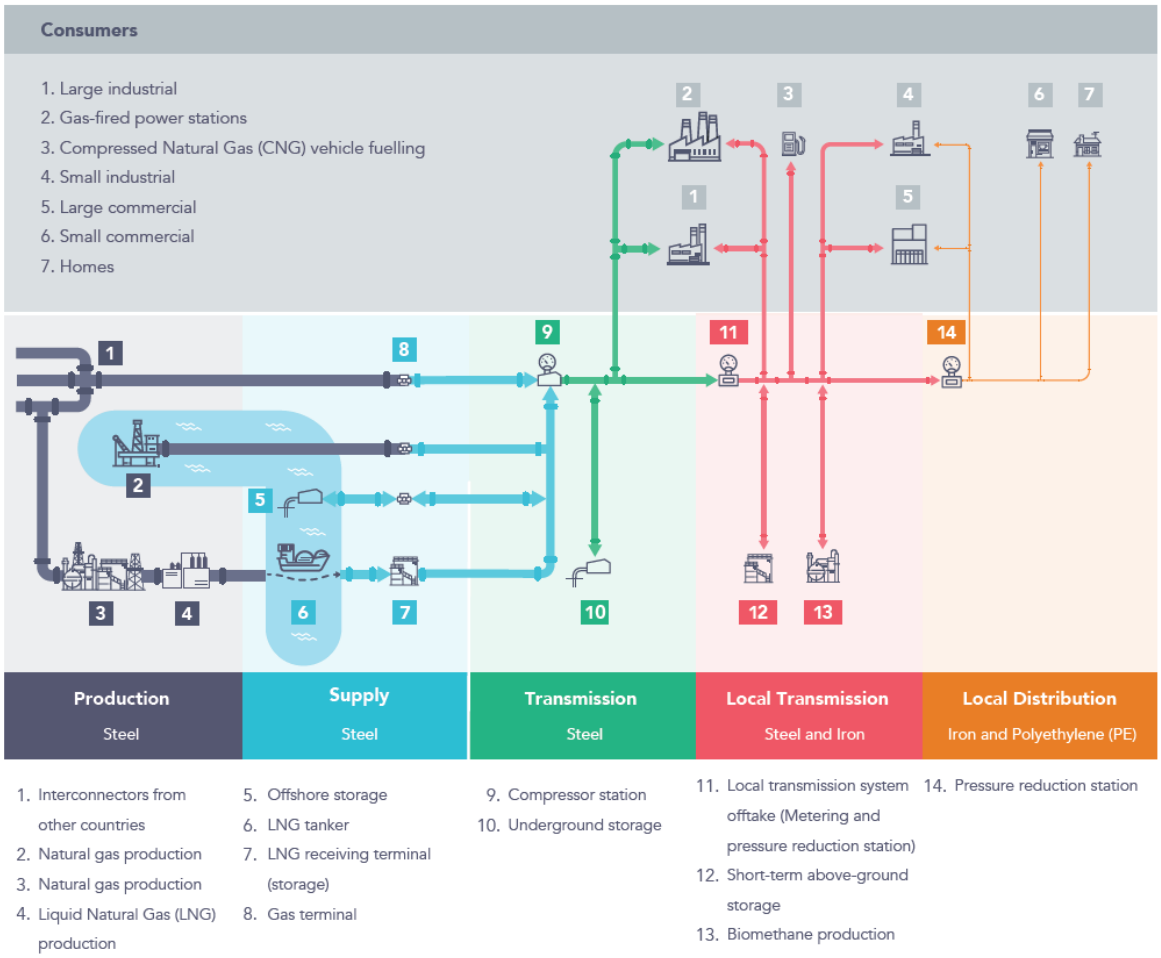

Figure 1.7: Schema of a generic whole gas system [1.5].

Given the complexity of the natural gas system, emissions of methane and CO2 from the supply chain are highly variable and sometimes large in magnitude. However, the main source of greenhouse gas (GHG) emissions associated with natural gas is from end-use combustion (cooktop burners and boilers). Carbon dioxide (CO2) pollutions emitted by the combustion of natural gas fuel are about $184\ gCO_2eq/kWh$. Figure 1.8 shows that this value is considerably lower than CO_2 combustion emissions of other fossil fuels. Using natural gas respect to coal, the emissions produced are approximately halved. Therefore, the natural gas, as a low-carbon fuel, is strongly promoted in the world, especially in Europe. As previously shown, it is already substituting the other hydrocarbon fuels (oil and coal) to reduce greenhouse gases and mitigate climate change.

Figure 1.8: Combustion emissions for the different of fossil fuels [1.5].

1.1.1 Alternative fuels

Nowadays and in coming years, natural gas is and will be the widely used source of energy around the world. This fuel has various sustainable advantages in the form of low localised pollution and lowers greenhouse intensity than oil and coal. However, for the emissions target defined by the EU 2050 long-term strategy [1.1] and other countries policies, substituting heavy hydrocarbons with natural gas it is not sufficient to reduce and prevent climate change.

Decarbonising of the gas system is a potential and essential solution to reduce greenhouse gas emission and especially CO_2 emissions. This goal can be achieved partly (1° step) and fully substituting (2° step) the traditional natural gas flowing into gas networks with green gases.

Figure 1.9 shows the main alternative fuels (biomethane, hydrogen, synthetic methane and synthetic natural gas) which can replace natural gas in the European energy market. In particular, hydrogen will play a crucial role in the decarbonisation of the gas network and so to achieve the zero-carbon emission objective defined by the European Commission [1.1]. Respect to natural gas and the other alternative gases, it is the only fuel gas which directly does not produce carbon dioxide emission during the combustion process. However, hydrogen has a more complex supply

chain because there are no resources in nature, and its properties are very different from those of natural gas.

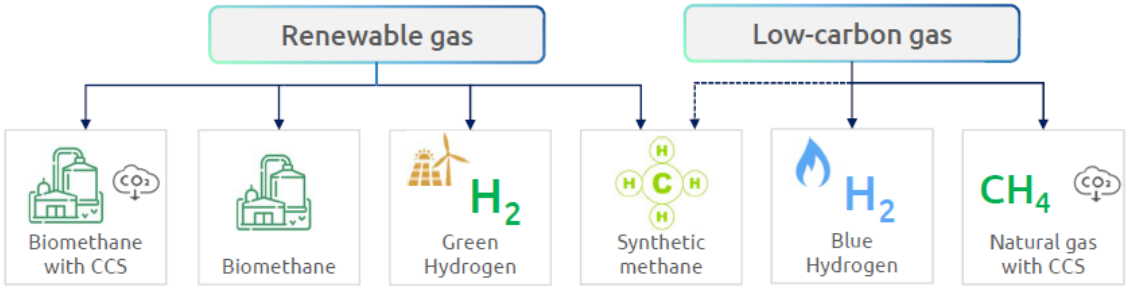

Figure 1.9: Potential renewable gas in Europe [1.6].

Hydrogen can be produced by several methods, as shown in figure 1.10. Currently, steam methane reforming is the primary technique used to produce H_2 gas. A reaction between methane and steam at high-temperature ($800\ °C$) and medium-pressure ($30\ bar$) generates a mixture composed of hydrogen and carbon gases. After that, CO, CO_2 and other impurities are removed to produce pure H_2 fuel. Coal and biomass gasification are also common process employed to produce hydrogen fuel. However, as SMR, this process forms carbon gases which must be captured and stored.
Nowadays, only about 4% of the total H_2 gas production is done by electrolysis. It is a process carbon-free which, using electricity, splits the water into hydrogen and oxygen. Depending on the type of electrolyser used, the energy conversion has an efficiency in the range $65 \div 80\%$ [1.5]. However, thanks to the possibility to use electricity generated by renewable sources, this solution (P2G) is becoming of interest by gas, electricity and hydrogen companies.

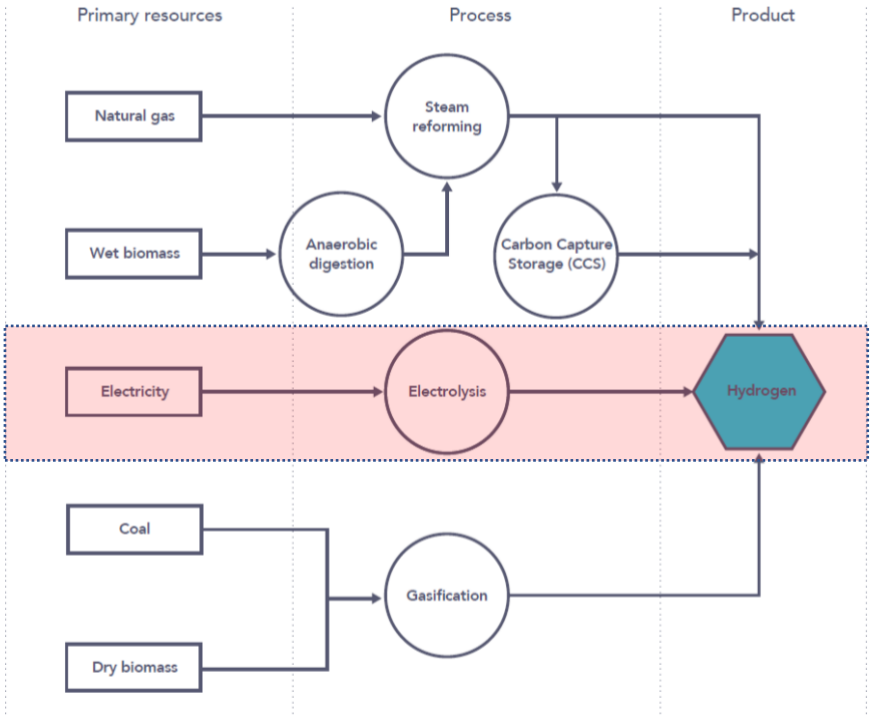

Figure 1.10: Process and resources to produce hydrogen [1.5].

Fluctuating and intermittent renewable sources, such as wind and solar, produce electricity which is only partially used by the electric grid. The surplus of energy can be used by power-to-gas systems to produce, by water electrolysis, hydrogen gas. Therefore, the resulting green zero-carbon fuel could be directly injected into the existing gas grid (figure 1.11).
Figure 1.12 shows principal geographical areas of high availability of wind and solar energy in Europe. Theoretically, there is a large amount of RES and consequently a potential production of green hydrogen from P2G technology. Using the European gas transmission network, this gas could be stored and transported from production sites to other countries which usually import the traditional natural gas.

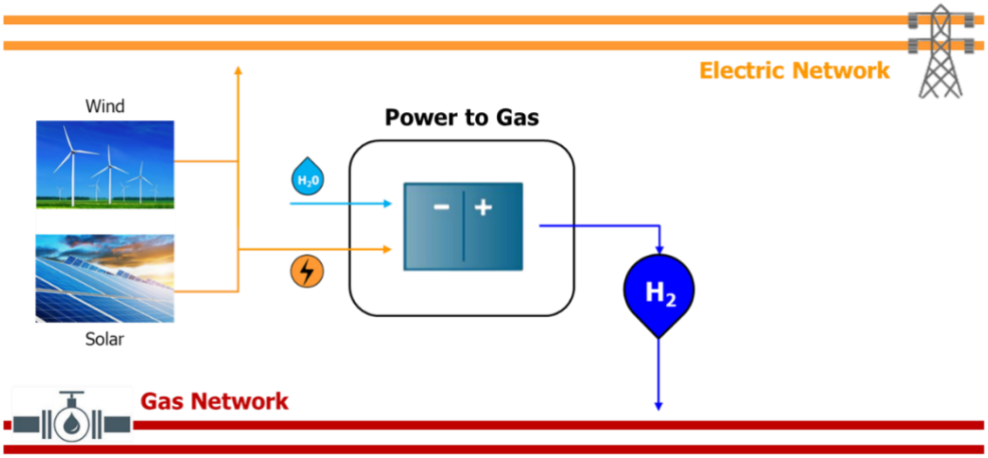

Figure 1.11: Schema of a power-to-gas solution to produce hydrogen fuel.

Figure 1.12: Overview of potential hydrogen production hubs in Europe [1.6].

1.1.1.1. Natural gas and Hydrogen mixture

Gas network elements and combustion devices of users connected to the grid were designed and realized to operate with natural gas. Although, the composition and properties of natural gas change according to the source's origin, values are usually included in a limited range. Due to the different characteristics of the pure hydrogen gas, a mixture of natural gas and H_2 can have properties very far from those of NG. Therefore, transport, storage and use of green hydrogen produced by power-to-gas facilities into gas networks is a great and difficult challenge.

Nowadays, the maximum allowed percentage of H_2 into the gas flowing into existing gas infrastructure is a big open-ended question of great interest to researchers. A small fraction of hydrogen has also a significant impact on network behaviour and characteristics of gas delivered to the users.

From a regulatory point of view, there is no specific standard which regulates properly this new scenario. National regulatory authorities of European countries have different viewpoints. In Germany and the UK, different values of concentration of H_2 up to 10% (mole fraction) are allowed [1.7]. In the gas standards [1.1] defined by the Italian Regulatory Authority for Energy, the injections or concentration of H_2 or other alternative fuel into the natural gas mixture are not mentioned. Interestingly, any concentration of alternative fuel could be allowed into Italian gas network until that SG, HHV and WI values of the gas mixture are included in the defined ranges.

In the scientific literature, few researchers tried to answer this question analysing with theoretical and/or experimental studies different compositions of a natural gas and hydrogen mixture.

Deymi-Dashtebayaz [1.7] analysed the properties of an NG and H_2 mixture for several compositions of the natural gas used for the blending. The hydrogen blended into the gas mixture has been varied from 0 to 10 molar percentage to estimate the effect of H_2 in a plausible range.

The natural gas compositions studied are the 5 primary Iran mixtures, which have a percentage of methane (CH_4) between 80.01 and 90.04% and other contaminants as carbon dioxide (CO_2) and Hydrogen sulfide respectively in the range $0 \div 8.41\%$ and $0 \div 6.32\%$.

Figures 1.13 and 1.14 show variation of the main fuel properties (SG, HHV and WI) as a function of the molar fraction of hydrogen into the mixture for the 5 Iran gas composition studied. The blending of H_2 into the mixture has not negligible effect on specific gravity, higher heating value and so Wobbe index of the gas fuel. Increasing the percentage of hydrogen, the specific gravity of the blending gas decreases with the same trend for all the compositions of the natural gas considered. Due to the very low SG value of the H_2 gas, the density of the natural gas has a limited effect on the reduction rate with the percentage of hydrogen. The energy density (HHV), shown in MJ/Nm^3 unit, also decreases up to 6.69% for hydrogen molar concentration in the range $1 \div 10\%$. Maximum differences are evaluated for the Kangan NG composition, which has the maximum higher heating value ($38.42\ MJ/Nm^3$). As a consequence of its definition (ration between HHV and square of SG), the WI of mixtures analysed decreases with the hydrogen fraction. In the range of H_2 percentage investigated, the trend is quite linear and maximum variations estimated are between 2.08 and 2.42% respect to the reference values (100% NG).

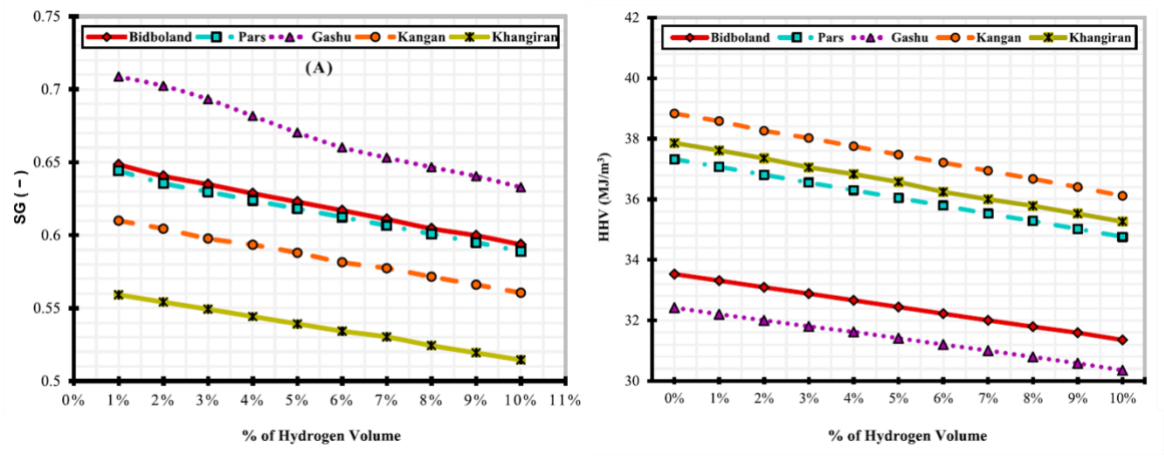

Figure 1.13: Specific gravity and HHV for the various NG compositions with H_2 % [1.7].

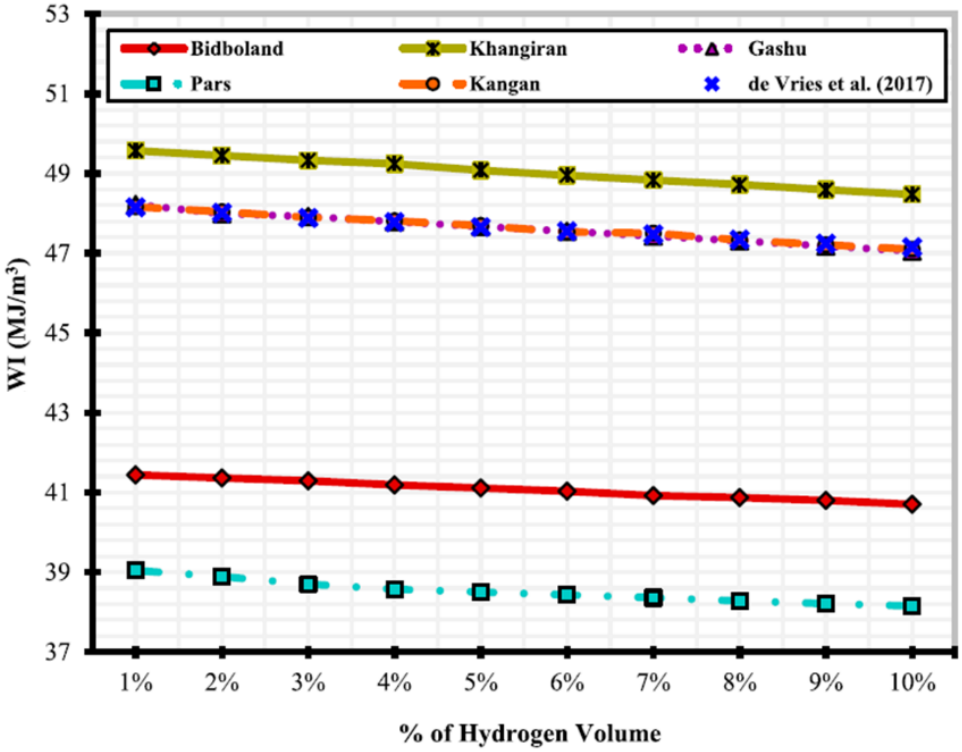

Figure 1.14: Wobbe index for the various NG compositions with H_2 % [1.7].

Variations of the lower and upper flammability limit for the different NG and H_2 compositions analysed are shown in figure 1.15. The higher flammability of hydrogen fuel produces a rise of the LFL and UFL values of the mixture when H_2 is blended with natural gas. For the hydrogen fraction investigated, the variation evaluated for the upper flammability is up to 1.6%. Conversely, effects on the lower flammability limit are limited ($< 0.5\%$).

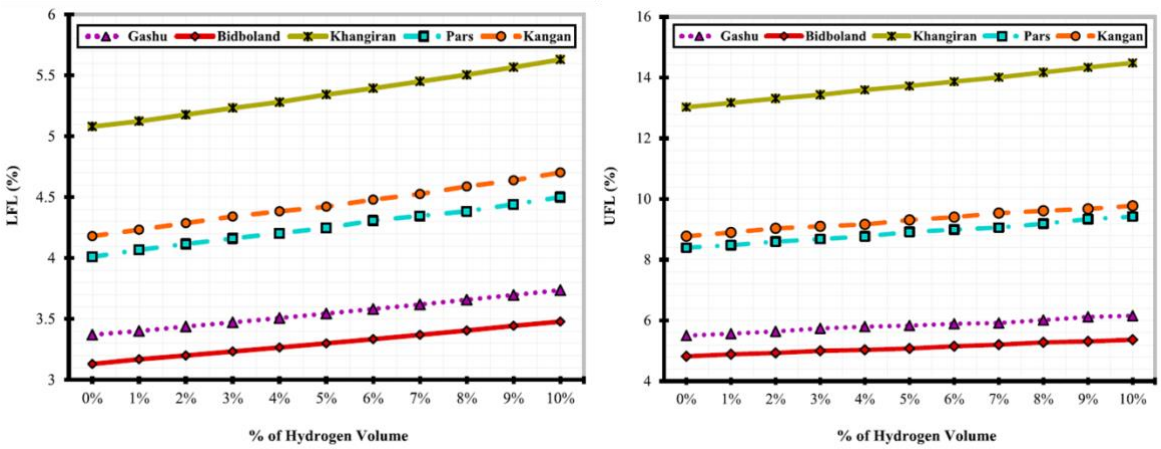

Figure 1.15: LFL and UFL variations for the various NG compositions with H_2 % [1.7].

Experimental studies on a representative natural gas cooktop burn were carried out by Zhao [1.8] to analyse the effects on the combustion performances of an H_2 fraction into the mixture. The maximum percentage of hydrogen investigated in this study was defined as the maximum amount without encountering a significant operability issue.

Figure 1.16 shows the schema and imagine of the test rig. A commercial burner with a heating load of $2.666\ kW$ and a self-aspirating technology was selected. The natural gas used is composed of 95.8% of methane (CH_4), other hydrocarbons (C_{2+}), 1.9% of carbon dioxide ($C0_2$) and 0.3% of nitrogen (N_2).

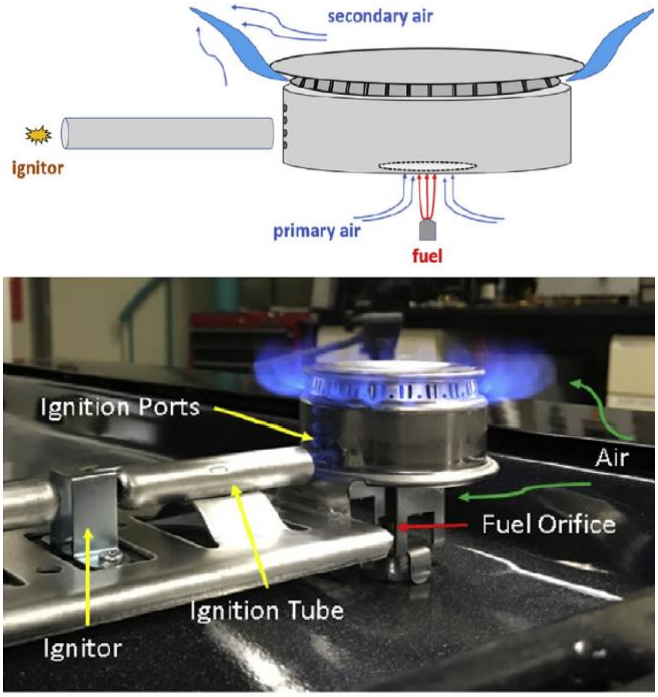

Figure 1.16: Schema and imagine of the cooktop burner tested by Zhao [1.8].

The ignition time as a function of the molecular percentage of hydrogen into the mixture is shown in figure 1.17. Values measured for cold conditions are higher than hot conditions, independently

from the fraction of H_2 into the gas mixture. Increasing the hydrogen blended up to 15%, the ignition time slightly decreases for both conditions of the burn. Thereafter, an intermittent flashback of the flame (figure 1.18), which determines the limit concentration of H_2, occurs.

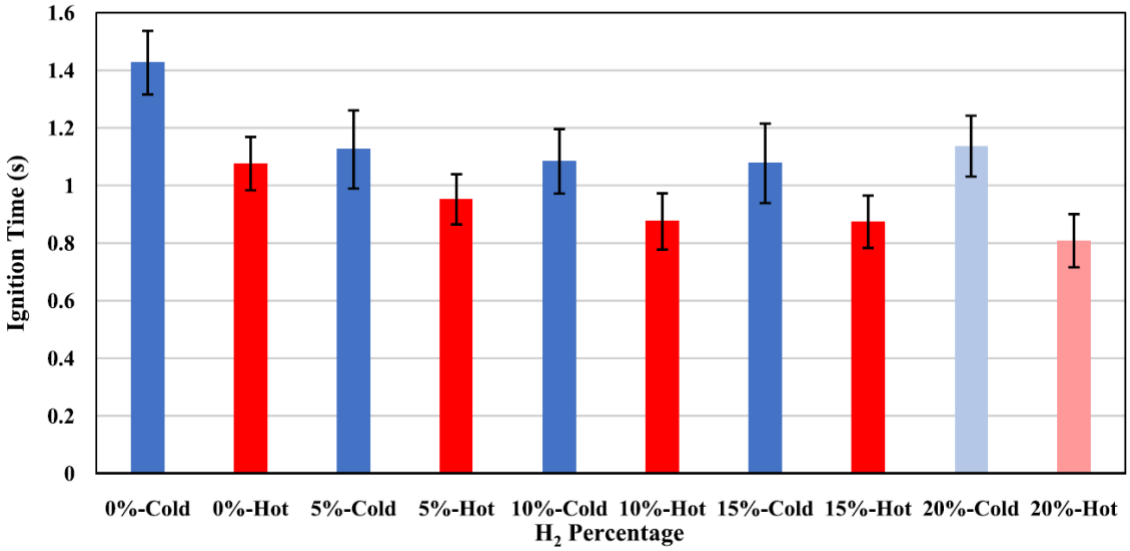

Figure 1.17: Ignition time of the cooktop burner [1.8] for different molar H_2 %.

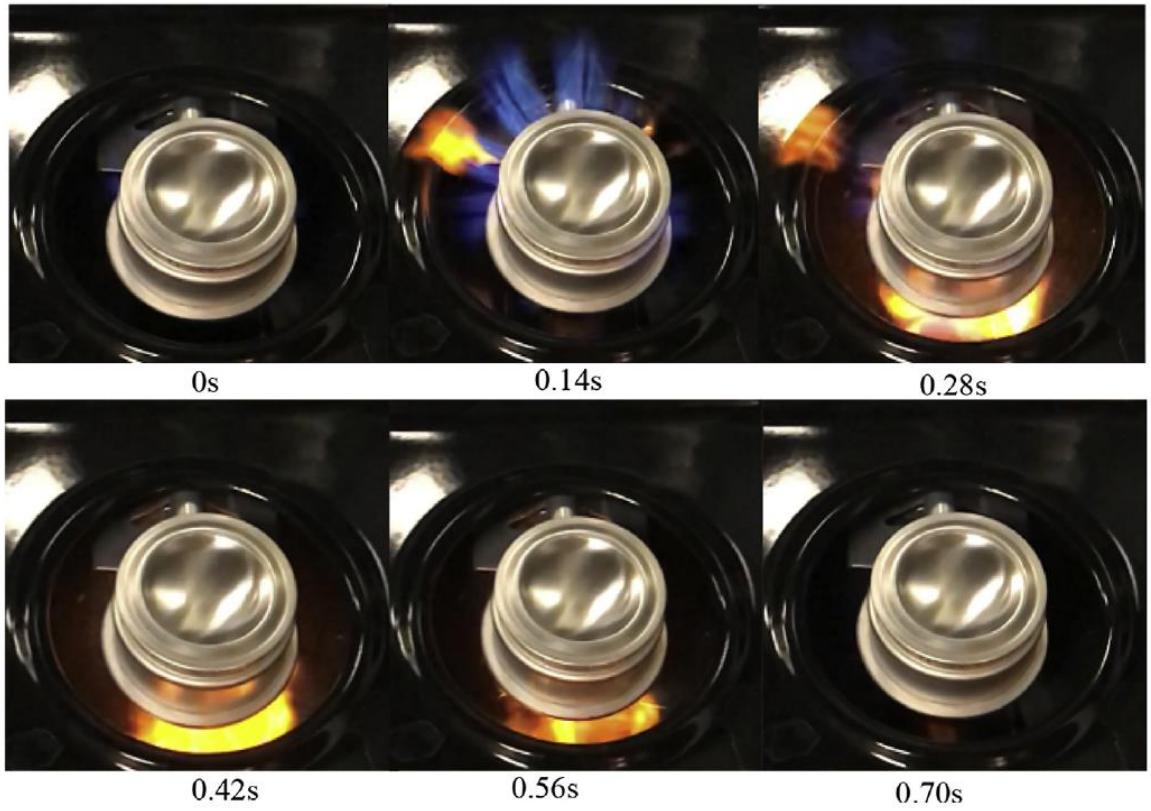

Figure 1.18: Flashback procedure by the cooktop burner [1.8] for a mixture with 20% of H2.

Figure 1.19 shows the cooktop burner flame structure observed for H_2 fraction between 0 and 80%. In this test, the burn is igniting with a fuel of pure NG and after that, the hydrogen gas is added to the mixture until the established concentration. A light blue flame is observed in the case of pure natural gas. Low fractions of hydrogen into the mixture have a small effect on the shape and colour of the flame. For intermediate values of H_2, light blue and quite invisible flame characteristics of the hydrogen flame were noted. The flashback of the flame occurs when the hydrogen percentage is increased from 75 to 80%.

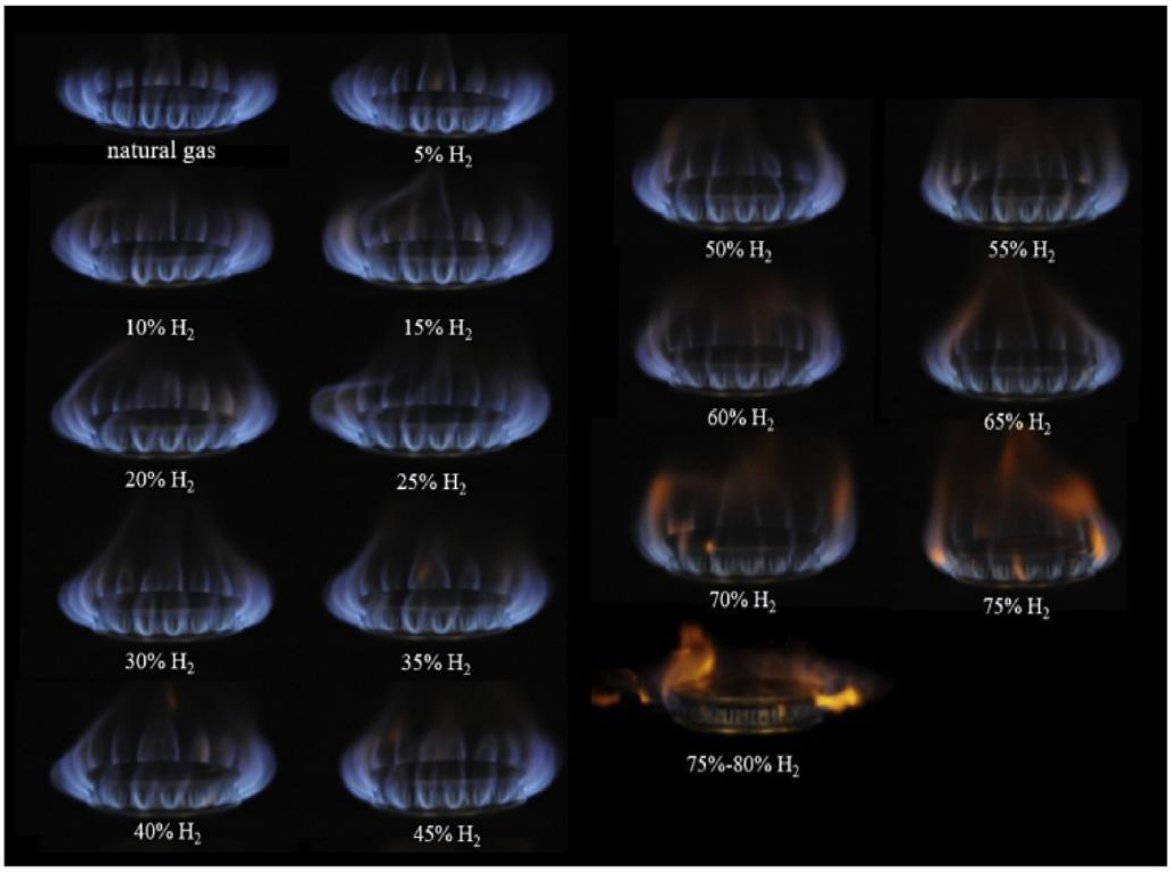

Figure 1.19: Flames characteristics of the cooktop burner [1.8] for different molar H2 %.

As shown in figure 1.20 and 1.21, the use of hydrogen into a cooktop burner also determines differences in terms of combustion noise intensity and temperature of the burn. The increment on the sound pressure level of the flame is pronounced only for concentrations of hydrogen higher than 75%. Conversely, the burn temperature quite increases with the amount of hydrogen into the mixture. An H_2 fraction of 75% produces a significant increment of the burn temperature of about $25\ °C$.

Finally, there were shown pollutants emitted by the cooktop burner for different levels of hydrogen blended. As shown in figure 1.22, the emission of NO_x, CO and UHC measured decrease with hydrogen addition. Conversely, the effect on NO emission of hydrogen into the mixture is negligible respect to the other pollutants.

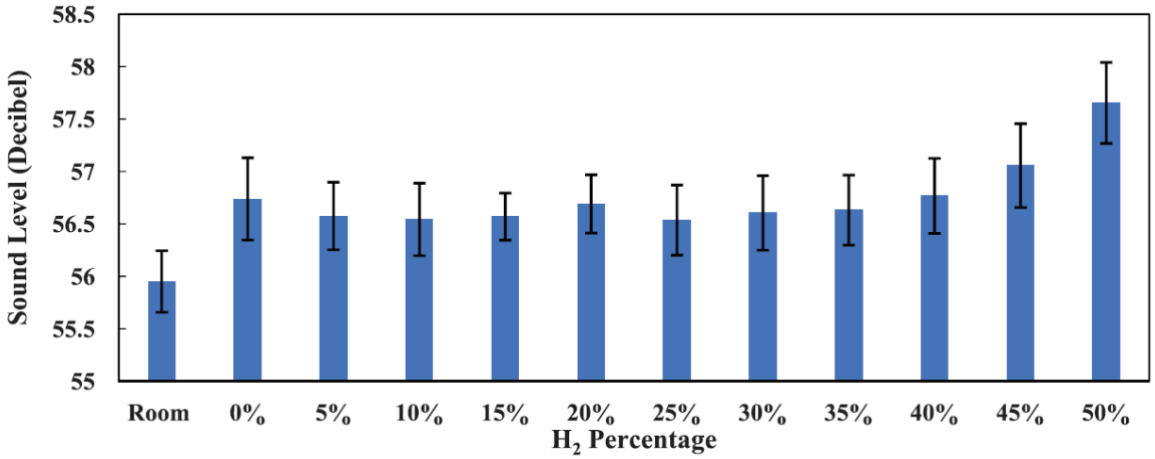

Figure 1.20: Combustion noise level of the cooktop burner [1.8] for different molar H2 %.

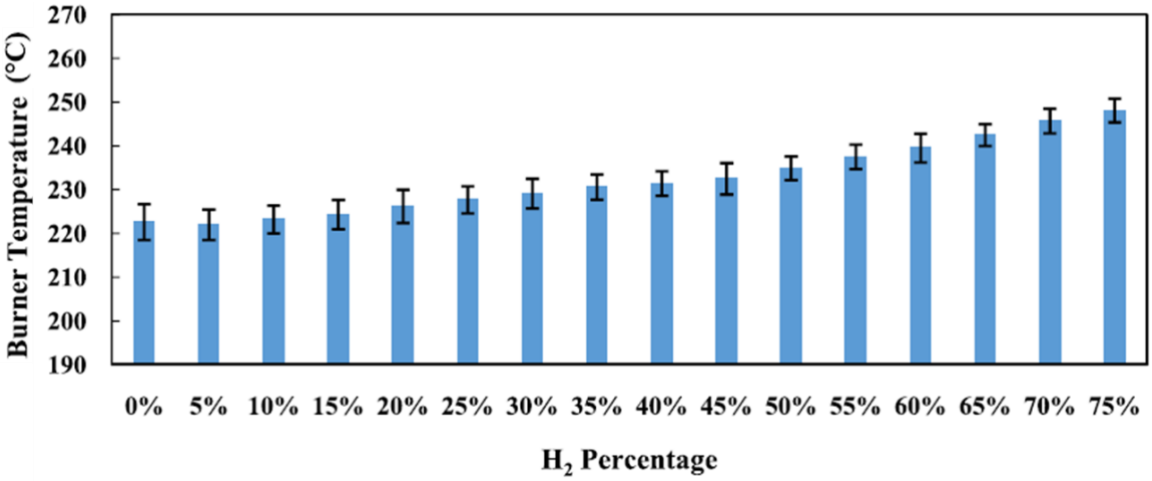

Figure 1.21: Temperature of the cooktop burner [1.8] for different molar H2 %.

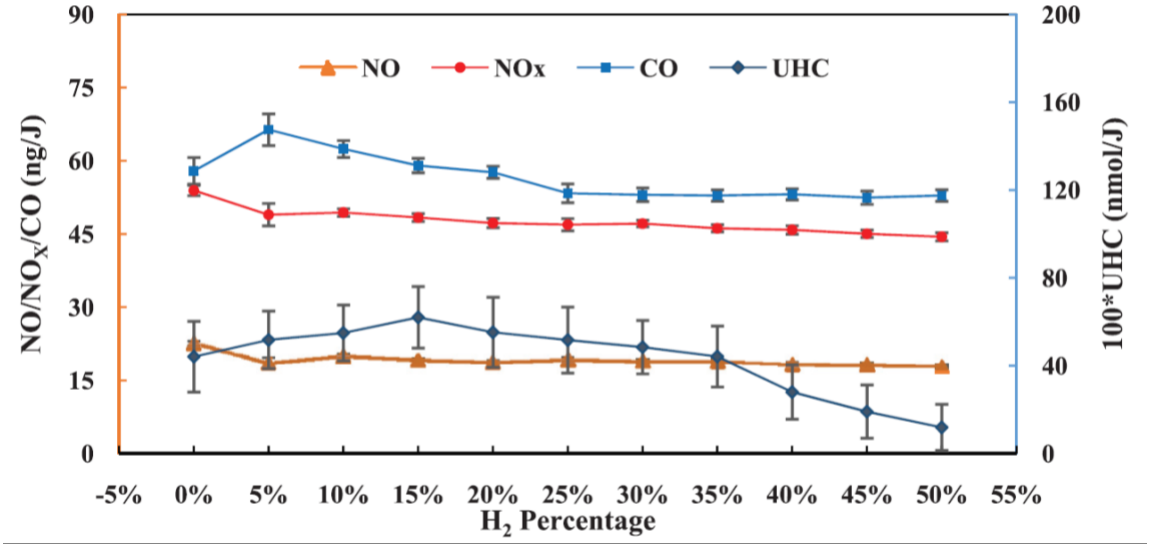

Figure 1.22: Emissions of the cooktop burner [1.8] for different molar H2 %.

1.2 Gas network models

Gas networks are massive infrastructure responsible for transporting and distributing large amounts of energy from production fields to a wide variety of consumers. Considering their main role in the global energy scenario, numerical tools are useful and essential for owner companies. Optimal design and management of these complex systems allow companies to operate efficiently by reducing costs, guarantee users' requests and respect standards defined by gas regulators [1.1]. Due to increasing consumption and changes of worldwide trade flows of the natural gas, expansion, upgrading and renovation of the existing gas networks are necessary. Mathematical models, which are capable to analyse several possible ways and find the best solution, are crucial in this case and they can provide strong support for gas companies.
On the technical side, the main objective of a gas network tool is to provide a realistic mathematical model of the components of the system and predict the behaviour of the network in nominal, dynamic and emergency scenarios. In particular, a computer programme, setting boundary conditions, calculates the variables of the problem (pressure, velocity, mass flow rate and temperature) at each element of the network. After solving the mathematical problem, the fluid dynamics properties are used to evaluate and provide for all demand nodes main parameter values of the gas quality delivered (specific gravity, higher heating value and Wobbe index), which mainly influence performances and combustion characteristics of users' devices connected to the gas network.

1.2.1 State of art

In the last decades, the problem of describing the behaviour of the gas flowing into a network has been of high importance and a subject of study by several academic and industrial researchers.
Steady-state models are usually applied to gas network scenarios where the pressure of sources and gas withdrawn by nodes are assumed constant or change slowly in time. Conversely, dynamic simulations of the network are essential during a daily variation in gas demand or transient scenarios such as a quick reduction of the pressure imposed by a supply node, a compressor station or a reducing station. In these conditions, due to the unsteady nature of the gas flow, the amount of gas storage in pipes is significant and has a crucial role in the network behaviour. However, the solution of unsteady governing equations of a gas flow involves the implementation of advanced numerical schemas and more computation resources to run the simulations.
Therefore, steady-state tools are usually employed for analysing, designing and optimizing gas network composed of hundreds or thousands of elements. Instead, simpler gas systems such as transport pipelines or part of medium-pressure distribution networks are typically modelled by dynamic computational software and simulated in several unsteady scenarios.
Nowadays, the substitution of hydrocarbon fuels with green gases produced by renewable sources is a crucial issue for the decarbonisation of the global energy system. In this context, a feasible pathway is to store and transport, into the gas grid, the hydrogen or synthetic natural gas produced by the surplus of renewable sources. For this reason, analyses of gas networks must focus on the compatibility between unconventional "green" gases and the traditional natural gas. It is also

important to study the impact of alternative fuel injections on network behaviour and properties of the gas delivered to users.

Bermúdez [1.10] developed the GANESO™ software with a graphical user interface, which is used by gas companies for simulation and optimization process of gas transport networks. During the problem modelling, it is possible to select different compressibility factor equations (SGERG88 or AGA8) and friction factor correlations (Colebrook or Weymouth). The modelling, simulation and optimization of the full Spanish transport network, which is composed by 500 nodes, 500 pipes, 4 compressor stations and 6 regasification plant, was carried out by authors with the aim of exhibit the accuracy, reliability and performance of the tool proposed.

An accurate and fast numerical method for the simulation of pipelines under non-isothermal steady-state scenario was proposed by López-Benito [1.11]. Two different methods were implemented to evaluate the friction factor and so the pressure drops into the pipeline. When the roughness of the internal surface is not available, the λ value is indirectly calculated using measured values of the pressure. Conversely, the GERG 1.19 correlation is employed to determine the friction factor if the characteristics of the pipeline are available. In this article, a real Spain pipeline owned by Enagas company with different pipe inclination and several withdraws was tested as a case of study.

Szoplik [1.12] developed a steady-state gas network of a small Polish city to establish a mathematical correlation between the required pressure of supplier and the gas demand by users in different periods of the year. The real data of users' consumption, air temperature for thousands of hours in the different season of the year were used as input for the simulation.

A comparison of different formulations (AGA, Panhandle A, Panhandle B, and Weymouth) of the flow equation was performed by Bagajewicz [1.13]. The author also proposed a new generic metamodel useful in optimization problems. In literature, several authors developed a simplified non-iterative equation to calculate the pressure drop and flow in a pipe. For these formulations also a transmission factor, independently from the roughness of the pipe, is used instead of the friction factor. Due to the inaccuracies of the approximate formulations, a nondimensional arbitrary parameter named "pipe efficiency" is added to the equation with the purpose of achieving results comparable with experimental data. However, the results of the case studied show that pressures evaluated by the several models are different from each other. Instead, the metamodel uses the Colebrook equation to calculate the friction factor and a non-linear regression of experimental data to obtain coefficient values of the correlation. Therefore, when the composition of the gas and characteristics of the pipe are well-known, accurate pressure and flow values are obtained.

Cavalieri [1.14] proposed a model with the possibility of simulating multiple pressure levels of a real gas distribution network. The new formulation reported includes the correction for pipes inclination and the pressure-driven mode, which set as boundary conditions the pressure at demand nodes. In this case, the tool developed was used to simulate the steady-state behaviour of a non-trivial realistic gas network composed of 67 nodes and 88 pipes with several pressure levels.

A lot of models in literature [1.11, 1.12, 1.14] use the well-known Newton-Raphson method to find the solution to the problem. Instead Ekhtiari [1.15], with the aim of increment the efficiency and stability of the computational method, introduced a novel methodology to solve the non-linear system of equations of a steady-state network. Equations of the elements are associated with a

non-linear matrix which is solved iteratively. As a case of study, he modelled and simulated the Irish gas transportation network with 109 nodes and 112 pipes.

Pambour [1.16, 1.17] developed a dynamic tool, named Scenario Analysis Interface for Energy Systems (SAInt), to study the unsteady isothermal behaviour of gas transport network or coupled electricity and gas systems. Underground storage, liquefied natural gas terminal, compressor stations and reducing stations can also be simulated in the model presented. The Hofer and Papay formulations were implemented to calculate respectively the friction factor and the compressibility factor of the gas. Tool developed was applied by authors to simulate the Bulgarian-Greek national transport network during a typical variable gas flow demand of $48h$.

One-dimensional isothermal and non-isothermal gas flow through a pipeline was modelled and studied by Osiadacz [1.18] and Chaczykowski [1.19]. When the gas flowing into a pipe is subject to slow fluctuations, it has sufficient time to achieve the temperature of the ground. Therefore, an isothermal dynamic model can be used to simulate correctly the problem. Conversely, during a rapid transient scenario, a thermal model of the pipe is necessary to predict properly the behaviour of the network. Results of the tests show that the temperature of the gas has a significant impact on the property of the gas and consequently on pressure and flow value evaluated.

Helgaker [1.20] implemented and validated a gas network model which can simulate high-pressure off-shore pipelines. In particular, he focused his study on a $650\ km$ pipeline to investigate the effect of friction factor, compressibility factor and heat transfer models used. Results of the case studied shows that the use of Colebrook-With or GERG formulation for the λ parameter and one of the several equations of state in the literature (Soave-Redlich-Kwong, Benedict-Webb-Rubin-Starling, Peng-Robinson and GERG88, etc.) produce variations on the pressures evaluated into the pipeline. The thermal model used (steady or unsteady) has a significant impact on the calculation of the gas temperature but also the mass flow. Due to the heat accumulation effect considered, the unsteady heat transfer models correctly calculate the temperature profile along the pipeline respect to the traditional steady model.

A natural gas computer programme, which solves unsteady continuity and momentum equations using the method of characteristics, was proposed by Trabelsi [1.21]. Simulations carried out in the article show that this unconventional method, simple to implement, easy to solve and without convergence problems, evaluates pressure and flow evolutions during the time in good agreement with values calculated by a traditional numerical model.

Taherinejad [1.22] presented a new model based on the electrical analogy, which can predict the behaviour of gas flowing into a pipe using a system of algebraic and first-order ordinary differential equations. However, an additional arbitrary and dimensionless parameter, named "capacity factor", must be introduced to consider the line pack of pipes, and so to evaluate correctly dynamic effects. The new model was validated by comparing the case simulated with several numerical data available in the literature. Results show that pressure and flow values during the time are calculated correctly when a capacity factor of 3 is set.

Abeysekera [1.23] developed a steady-state model for simulating gas networks in the presence of localized injection of green gases. A low-pressure distribution network composed of 11 nodes and 14 pipes was simulated in several scenarios. Biogas or pure hydrogen were injected at the main supply node or a decentralized node to analyse the impact of the location on the network behaviour.

A numerical tool used to simulate the steady-state and non-isothermal behaviour of transmission pipeline networks with multiple natural gas, synthetic natural gas and hydrogen sources, was proposed by Pellegrino [1.24]. This model was applied to a natural gas network with 80 nodes, 80 pipes. Different scenarios were investigated to define the best solution. The first with 1 H_2 injection node, the second only with 1 SNG injection node, and the third with 3 injections nodes of hydrogen and synthetic natural gas.
Elaoud [1.25] studied how an upstream hydrogen injection influences pressure and velocity of the gas in high-pressure looped networks during steady-state and transient scenarios. The network simulated by the author is composed of 1 source node, which supplies at $70\ bar$ a homogeneous natural gas and hydrogen mixture, 6 demand nodes, 2 junctions and 12 pipes. In this model, a quality tracking model was not implemented because it was not necessary. The H_2 is previously mixed with the natural gas and so only gas quality is flowing in all elements of the network.
A mixed-integer linear programming model useful for the reformation and expansion of existing real gas networks was implemented by Wang [1.26]. When hydrogen is blended with natural gas, properties of the gas and behaviour of the network change. Therefore, design parameters as pipes' diameter, pipes' wall thickness, supply nodes' pressure, etc. must be reconsidered and in some case adapted with the objective of guarantee the correct operation of the network in this new scenario. Result of the case studied shows that with a specific amount of hydrogen injected, the best operation of the network can be achieved by changing some pipelines, installing new compressor stations and increasing the pressure imposed by the existing compressor station and reducing stations.
Guandalini [1.27] developed a dynamic gas quality tracking model, which was used for simulating the downstream advancement of hydrogen injected in an intermediate point of a pipeline. The network selected for the model validation was a part of a transportation pipeline ($50\ km$) with two different demand nodes (industrial and residential) at the middle and at the outlet of the pipe. A variable amount of hydrogen is injected at a distance of $15\ km$ from the source node. Two consecutive days (1 week day and 1 weekend day) were simulated to investigate the impact of hydrogen injection in the presence of different gas flow demand.
A comparison between different numerical methods used to solve the gas quality transport problem was provided by Chaczykowski [1.28]. An implicit method was proposed to discretize the advective transport equation. Otherwise, a batch tracking algorithm was implemented to describe the movement of a particle through a pipe. Two real transmission pipelines were simulated to evaluate differences between the two model. Results show that the values obtained by the backward tracking method are more in agreement with measured values respect to the other method. Due to numerical diffusion problems, the implicit method is not capable of calculating correctly the profile of the composition at the outlet of the pipeline.

1.3 Research objectives

Nowadays, gas network models are crucial for a sustainable and optimal operation of the gas system. Simulation tools are useful for gas companies to predict and minimise failures, inefficiency and unsuitable of components of the network, respect gas standards and reduce management cost.

In the literature, several numerical models were proposed and developed to solve the one-dimensional governing equations of the gas flowing into gas networks. Most of these [1.10, 1.11, 1.13, 1.15, 1.16, 1.17, 1.18, 1.19, 1.20, 1.21, 1.22, and more other] were utilized for analysing critical issues and various scenarios of gas transportation pipelines in steady-state, dynamic, isothermal and non-isothermal conditions. Due to the lack of interest of gas from gas companies, in the past no more models were provided for the simulation of medium-pressure and low-pressure distribution networks[1.12, 1.14], which are complex infrastructure composed by hundreds of thousands of looped pipes. In the last years, only few researchers [1.8, 1.9, 1.23, 1.24, 1.25, 1.26, 1.27, 1.28] studied gas pipelines and gas distribution girds behaviour in the presence of hydrogen or alternative gas injections. As previously mentioned, the steady-state and dynamic models developed in this topic were applied on single high-pressure pipelines and on simplified (not very realistic) distribution looped networks.

The present thesis would cover the gap in the current literature by proposing a numerical tool able to model and simulate realistic gas distribution networks, composed by hundreds or thousands of elements, in steady-state and dynamic scenarios. Furthermore, the model can be used to analyse the impact of alternative fuel injections and evaluate the maximum amount of green gas that can be added to the network respecting gas standards. Finally, this research tries to promote the use of alternative fuels as a solution for decarbonising gas networks.

Bibliography

[1.1] European commission, "2050 long-term strategy", Brussels, COM 773 final (2018).

[1.2] L. A. Hovem, "Energy Transition Outlook 2019", DNV GL AS - Oil & Gas (2019).

[1.3] SNAM, IGU, BCG, "Global Gas Report 2019", Report (2019).

[1.4] BP, "Statistical Review of World Energy", 67° Edition (2018).

[1.5] J. Speirs, P. Balcombe, E. Johnson, J. Martin, N. Brandon, A. Hawkes, "A Greener Gas Grid: What are the options? ", Sustainable Gas Institute, Imperial College London (2017).

[1.6] SNAM, "The role of gas in the long-term energy scenario", Report Snam (2019).

[1.7] K. Altfeld, D. Pinchbeck, "Admissible hydrogen concentrations in natural gas systems", DIV Deutscher Industrieverlag GmbH, Gas for energy issue 3 (2013).

[1.8] M. Deymi-Dashtebayaz, A. Ebrahimi-Moghadam, S. I. Pishbin, M. Pourramezan, "Investigating the effect of hydrogen injection on natural gas thermo-physical properties with various compositions", Energy 167 (2019) 235–245.

[1.9] Y. Zhao, V. McDonell, S. Samuelsen, "Influence of hydrogen addition to pipeline natural gas on the combustion performance of a cooktop burner", International journal of hydrogen energy 4 (2019) 12239–12253.

[1.10] A. Bermúdez, J. González-Díaz, F. J. González-Diéguez, Á. M. González-Rueda, M. P. Fernández de Córdoba, "Simulation and optimization models of steady-state gas transmission networks", Energy Procedia 64 (2015) 130–139.

[1.11] A. López-Benito, F. E. Tenreiro, L. C. Gutiérrez-Pérez, "Steady-state non-isothermal flow model for natural gas transmission in pipes", Applied Mathematical Modelling 40 (2016) 10020–10037.

[1.12] J. Szoplik, "Improving the natural gas transporting based on the steady state simulation results", Energy 109 (2016) 105–116.

[1.13] M. Bagajewicz, G. Valtinson, "Computation of Natural Gas Pipeline Hydraulics", Ind. Eng. Chem. Res. 53 (2014) 10707−10720

[1.14] F. Cavalieri, "Steady-state flow computation in gas distribution networks with multiple pressure levels", Energy 121 (2017) 781–791.

[1.15] A. Ekhtiari, I. Dassios, M. Liu, E. Syron, "A Novel Approach to Model a Gas Network", Applied Science 9 (2019) 1047.

[1.16] K. A. Pambour, B. Cakir Erdener, R. Bolado-Lavin, and G. P. Dijkema, "SAInt - A novel quasi-dynamic Model for assessing Security of Supply in coupled Gas and Electricity Transmission Networks", Applied Energy 203 (2017) 829–857.

[1.17] K. A. Pambour, R. Bolado-Lavin, G. P. Dijkema, "An integrated transient model for simulating the operation of natural gas transport systems", Journal of Natural Gas Science and Engineering 28 (2016) 672–690.

[1.18] A. J. Osiadacz, "Simulation of transient gas flows in networks", Int. J. Numer. Methods Fluids 4.1 (1984) 13-24.

[1.19] M. Chaczykowski, " Transient flow in natural gas pipeline – The effect of pipeline thermal model", Applied Mathematical Modelling 34 (2010) 1051–1067.

[1.20] J. F. Helgaker, A. Oosterkamp, L. I. Langelandsvik, T. Ytrehus, "Validation of 1D flow model for high pressure offshore natural gas pipelines", Journal of Natural Gas Science and Engineering 16 (2014) 44–56.

[1.21] S. Trabelsi, L. Hadj-Taieb, S. Elaoud, "Modeling and Simulation of Transients in Natural Gas Pipelines", Springer Lecture Notes in Mechanical Engineering (2018).

[1.22] M. Taherinejad, S. M. Hosseinalipour, R Madoliat, "Dynamic simulation of gas pipeline networks with electrical analogy", J Braz. Soc. Mech. Sci. Eng. 39 (2017) 4431–4441.

[1.23] M. Abeysekera, J. Wu, N. Jenkins, M. Rees, "Steady state analysis of gas networks with distributed injection of alternative gas", Applied Energy 164 (2016) 991–1002.

[1.24] S. Pellegrino, A. Lanzini, P. Leone, "Greening the gas network - The need for modelling the distributed injection of alternative fuels", Renewable and Sustainable Energy Reviews 70 (2017) 266–286.

[1.25] S. Elaoud, Z. Hafsi, L. Hadj-Taieb, "Numerical modelling of hydrogen-natural gas mixtures flows in looped networks", Journal of Petroleum Science and Engineering 159 (2017) 532–541.

[1.26] B. Wang, Y. Liang, J. Zheng, R. Qiu, M. Yuan, H. Zhang, "A MILP model for the reformation of natural gas pipeline networks with hydrogen injection", International journal of hydrogen energy 43 (2018) 16141–16153.

[1.27] G. Guandalini, P. Colbertaldo, S. Campanari, "Dynamic modeling of natural gas quality within transport pipelines in presence of hydrogen injections", Applied Energy 185 (2017) 1712–1723.

[1.28] M. Chaczykowski, F. Sund, P. Zarodkiewicz, S. M. Hope, "Gas composition tracking in transient pipeline flow", Journal of Natural Gas Science and Engineering 55 (2018) 321–330.

Chapter 2

Theory and Models of the Gas Network Solver

In this chapter, it is developed the Gas Network Solver which is able to simulate the steady-state and dynamic behaviour of a gas network. Firstly, the gas network's problem is introduced, with a focus on the boundary conditions imposed at supply and demand nodes. Then, it is described characteristics and mathematical models of the gas fluid, linear (pipes, valves, reducing stations) and point (city gas stations and nodes) elements which compose a generic gas distribution grid. Finally, the gas quality tracking model developed, necessary to evaluate the properties and composition of the gas mixture at each node of the network, is presented. This model is essential in the presence of alternative gas injection to analyse its effects on the network's behaviour.

2.1 Gas distribution network problem and boundary conditions

A gas distribution network is responsible for transporting the gas from supply site to residential, industrial and commercial customers. The gas, injected into the network, flows in linear (pipes, valves and reducing stations) and point elements (junction nodes) connected and then is received by users.

City gate stations are the typical supply nodes of a gas distribution grid. Due to their characteristics, pressure, temperature and composition of the gas leaving the stations are usually known and set.

City gate stations are the typical supply nodes of a gas distribution grid. Due to the characteristics of them, the pressure, temperature and composition of the gas leaving the station are usually set and known.

Conversely, the mass flow rate is unknown because it depends on the gas requested by the downstream network. Interchange nodes are unconventional sources which, in injection mode, supply gas arriving from other networks or alternative gas (hydrogen, biogas and synthetic natural gas) produced by renewable plants. For them, the gas flow rate or power of the gas produced and injected into the grid is usually known and imposed as a boundary condition. The injection pressure is a function of the conditions of the element connected to this node.
Users of the network are connected to intermediate and final demand nodes. The gas extracted from these nodes depends on the consumption of users' devices. Considering a constant composition and higher heating value of gas delivered, the flow rate ($\dot{Q}_{dmd}$) can be set as a boundary condition (1) because it is proportional to the consumption. However, when gas composition and higher heating value depend on the time and position of the demand node, the energy approached is more appropriate to describe the problem. The energy requested by users ($\dot{E}_{dmd}$) is set as a boundary condition, and the gas flow rate is calculated (2) depending on the properties (HHV_g) of the local gas.

$$\dot{m}_{dmd} = \rho_{0g}\, \dot{Q}_{dmd}/3600 \tag{1}$$

$$\dot{m}_{dmd} = \rho_{0g}\, \dot{E}_{dmd}/HHV_g \tag{2}$$

The aim of modelling and simulating a gas network is to evaluate under steady-state and dynamic conditions: gas pressure and quality at each node; velocity and pressure drop of each pipe. These analyses are essential to predict the behaviour of networks, respect gas Standard [2.1] and guarantee the energy requested by customers.

2.2 Gas quality model

Natural gas (NG) is a mixture of hydrocarbon gases extracted from underground reserves located around the world. The principal component of the mixture is methane (CH_4). Its fraction corresponds to the 80 ÷ 99% of the natural gas. The remaining hydrocarbon gases are ethane (C_2H_6), propane (C_3H_8), butane (C_4H_{10}), pentane (C_5H_{12}) and hexane (C_6H_{14}). However, the mixture includes contaminant gas, such as carbon dioxide (CO_2), nitrogen (N_2) and helium (He).
The composition and properties of natural gas, which influence its combustion process, change according to the source's origin. In Italy, the natural gas extracted from underground reserves is up to 10% of the total national demand. The most significant amount of natural gas flowing into the Italian gas network is imported. Interconnection points between national and foreign pipelines are located in the north and south of the peninsula. Natural gas comes from Libyan, Algerian, Russian, North European pipelines. However, liquefied natural gas (LNG) regasification points are in centre-north coast of the Tyrrhenian and Adriatic Seas.
Table 2.1 shows the data of principal natural gas qualities present in Italy provided by the Italian Regulatory Authority for Energy, Networks and Environment [2.1]. The reference mixture is the Standard natural gas which is composed of a high percentage of methane and a low percentage of ethane, propane and nitrogen.

Table 2.1: Molecular gas composition of the mixtures of principal gas qualities in Italy [2.1].

	y_k [%]								
Source	CH_4	C_2H_6	C_3H_8	C_4H_{10}	C_5H_{12}	C_6H_{14}	CO_2	N_2	He
Standard NG	97.201	1.862	0.393	-	-	-	-	0.544	-
CH_4	100.000	-	-	-	-	-	-	-	-
Italian	99.348	0.098	0.300	0.006	-	0.005	0.039	0.472	0.002
Russian	96.401	1.675	0.512	0.152	0.029	0.017	0.303	0.898	0.013
Algerian LNG	90.631	7.480	1.190	0.291	0.006	0.001	0.001	0.399	0.001
North European	89.389	5.095	1.119	0.347	0.073	0.053	1.376	2.508	0.400
Algerian	88.120	7.866	1.223	0.160	0.023	0.012	1.606	0.890	0.100
Libyan	86.367	7.096	1.749	0.539	0.103	0.005	1.052	3.005	0.084

Global warming and world climate strategies lead to replacing non-renewable hydrocarbon fuels with green and eco-friendly gases produced by renewable sources.
Power to gas (P2G) systems and biogas plants produce alternative gases, such as hydrogen (H_2), biogas and synthetic natural gas (SNG). These gases can be injected into the national network and mixed with natural gas. Therefore, the presence of H_2, biogas and SNG sources also influence the properties and quality of the gas flowing into the network and delivered to users.
Nowadays, a great interest in the field is to evaluate the effects of gas quality on the network's behaviour. Different thermodynamic properties of the gas can alter the operability and efficiency of measuring instruments, network equipment and users' combustion devices.
The most commonly used parameters to characterise the gas quality are the specific gravity, the higher heating value and the Wobbe index.
The Specific gravity (SG) is the ratio (3) between the gas (ρ_{0g}) and air density (ρ_{0a}) at standard conditions ($T_0 = 20\,°C$, $p_0 = 101325.00\,Pa$). The standard gas density is proportional to the molecular weight of the gas mixture. Therefore, the SG parameter is used as an indicator of the gas composition.

$$SG = \rho_{0g}/\rho_{0a} \tag{3}$$

The higher heating value (HHV_g) is the total energy (MJ) released by $1\,Sm^3$ of the fuel considered during the combustion process. For a gas mixture, it is calculated, as the weighted sum (4) of the higher heating value of the components. Due to the different qualities of the gas into the network, the amount of gas flow rate delivered at the network nodes is not always adequate to satisfy

customers' fuel requested. Therefore, the transmission system operator (TSO), considering the higher heating value at each user of the network, should guarantee the energy request by users. The energy delivered ($\dot{E}_{dmd}$) at each node of the network can be evaluated by the product (5) of the standard volumetric flow rate ($\dot{Q}_{dmd}$) and the higher heating value of the gas mixture.

$$HHV_g = \sum_{k=1}^{n} y_k M_k HHV_k \tag{4}$$

$$\dot{E}_{dmd} = HHV_g \cdot \dot{Q}_{dmd} \tag{5}$$

The Wobbe index (WI) is defined as the ratio (6) between the higher heating value (HHV_g) and the quadratic square root of the specific gravity (SG). This derived parameter represents the quality of the gas and its interchangeability. It is used to compare different fuel gases, including natural gas and liquefied natural gas. If two gases with different composition have the same WI, the combustion parameters and energy of the users' devices do not change. Therefore, these two fuels can be interchangeable with each other, without affecting operability and performances of combustion systems. The gas safety management regulations [2.1] define the Wobbe index range ($47.2 \div 52.2\ MJ/Sm^3$) allowed to guarantee optimal combustion process of the devices connected to the grid.

$$WI = \frac{HHV_g}{\sqrt{SG}} \tag{6}$$

Data of molecular gas composition, provided by [2.2], are used to evaluate the gas parameters for the natural gas qualities in Italy. Figures 2.1, 2.2 and 2.3 show how properties (SG, HHV_g) and WI are highly dependent on gas origin. For example, the higher heating value of the Russian gas is 5% lower than the Algerian gas. Nevertheless, the Wobbe index and HHV_g of the eight compositions analysed are included between the minimum and maximum allowed values [2.1].

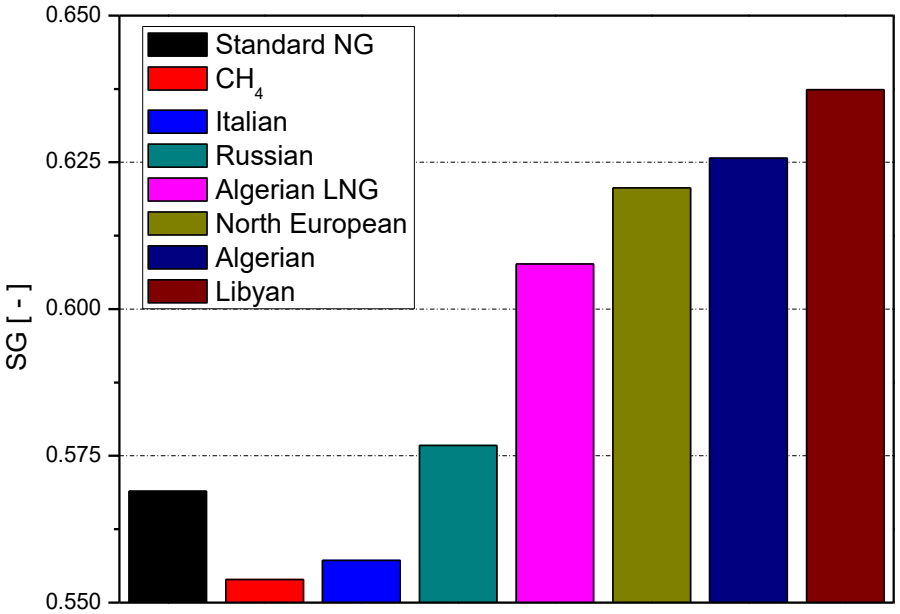

Figure 2.1: Specific gravity value for different NG composition.

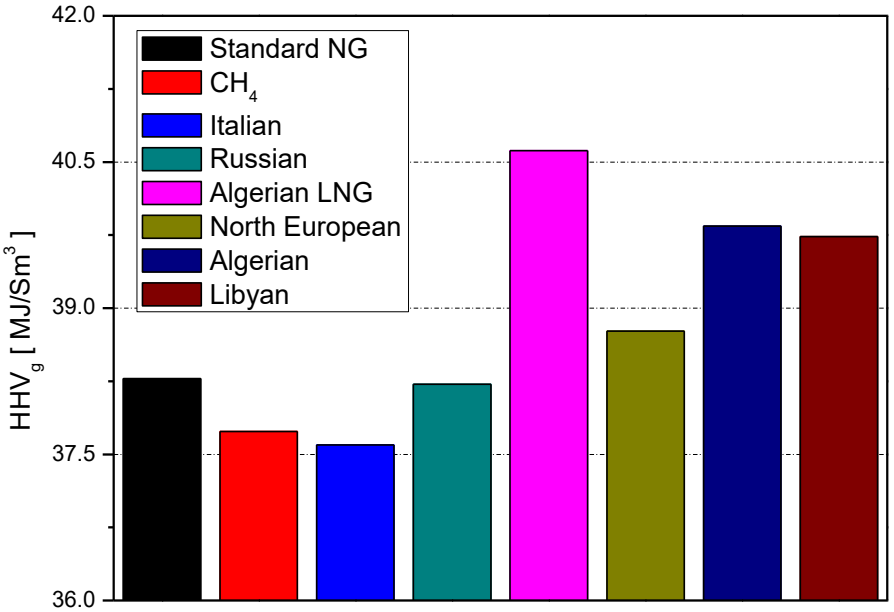

Figure 2.2: Higher heating value for different NG composition.

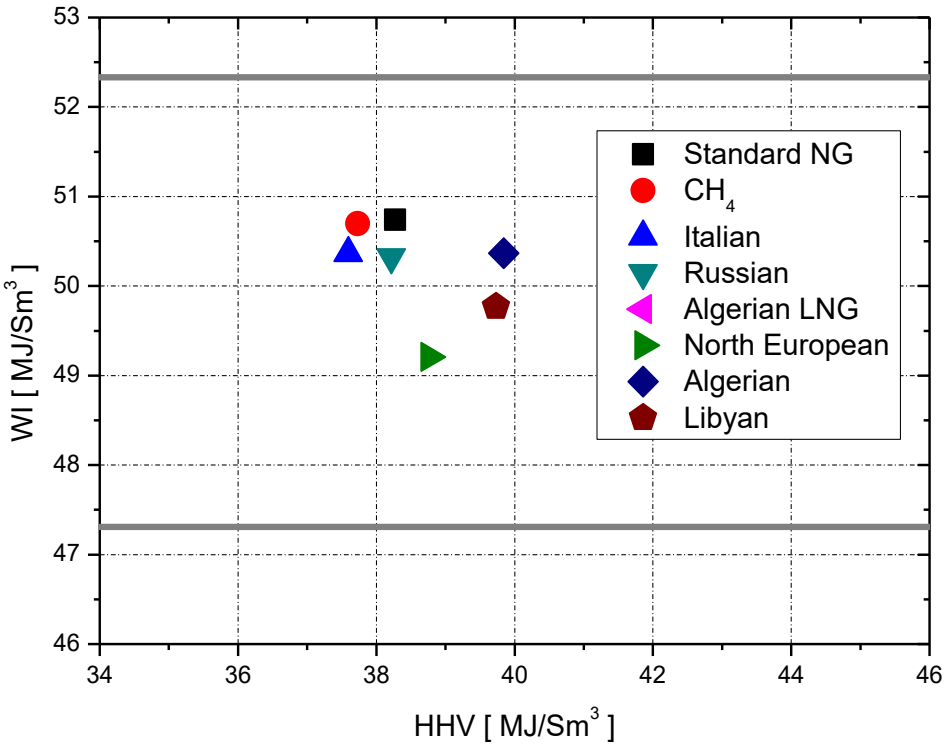

Figure 2.3: Wobbe index vs higher heating value for different NG composition.

Molar mass (M), specific gravity (SG), higher heating value (HHV_g) and Wobbe index (WI) of standard natural gas and hydrogen used to calculate the NG – H_2 mixture's parameters are listed in

table 2.2. The hydrogen is a fuel gas with very low mass density ($SG_{H2}/SG_{NG} = 0.10$) and specific energy that is about one-third of the natural gas. The Wobbe index of the hydrogen is lower than the minimum allowed value ($47.2\ MJ/Sm^3$). Therefore, a gas quality of pure hydrogen is not admissible with the standard and actual combustion devices connected to the gas grid.

Table 2.2: Gas properties of the standard natural gas and hydrogen.

Source	$M\ [kg/kmol]$	$SG\ [-]$	$HHV_g\ [MJ/Sm^3]$	$WI\ [MJ/Sm^3]$
Standard NG	16.4790	0.5690	38.28	50.74
H_2	2.0159	0.0696	12.08	45.79

Due to the different mass and energy density of the two gases, SG and HHV_g of the mixture decrease a lot with a small fraction of H_2, as displayed in figure 2.4 and 2.5. The SG_{mix}/SG_{NG} and HHV_{mix}/HHV_{NG} are respectively 0.35 and 0.49 when the hydrogen into the mixture is only a quarter of the natural gas.

Figure 2.6 shows the relationship between the higher heat value and the Wobbe index for the different compositions of the natural gas (NG) and hydrogen (H_2) mixture. Increasing hydrogen mass fraction, the HHV and WI of the gas mixture decrease. The Wobbe index is close to the minimum allowed value when the H_2 into the mixture is 5%. For a higher mass fraction of hydrogen, the gas quality does not respect the properties of users' demanded gas defined by the gas safety management regulations [2.1].

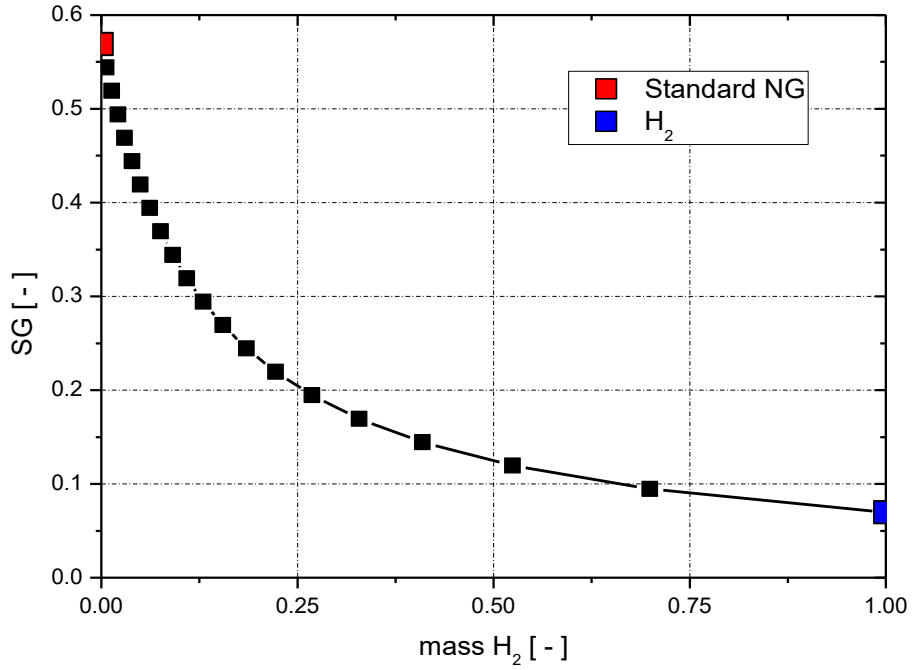

Figure 2.4: Specific gravity value for standard NG – H_2 mixture.

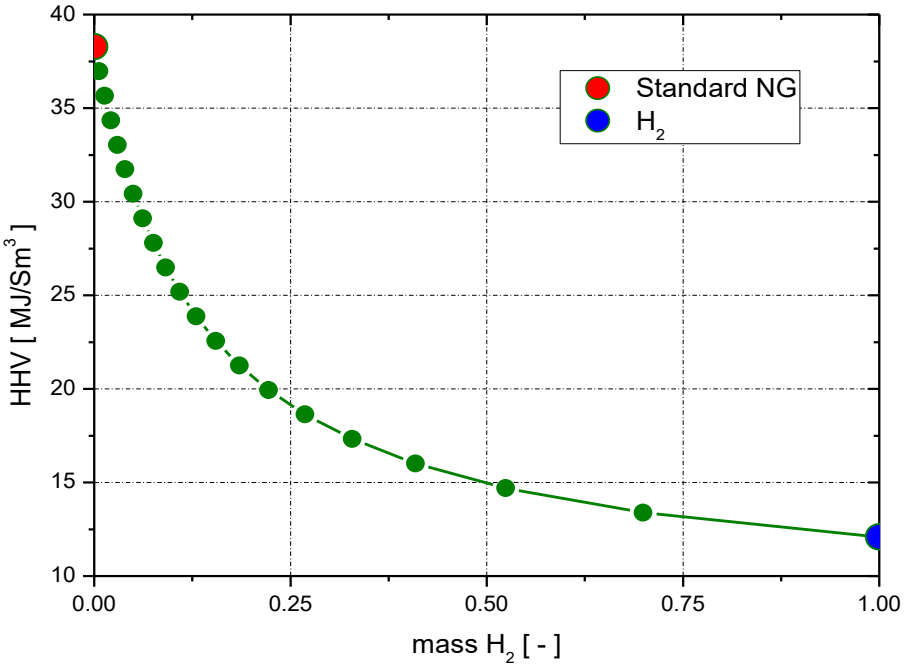

Figure 2.5: Higher heating value for standard NG – H_2 mixture.

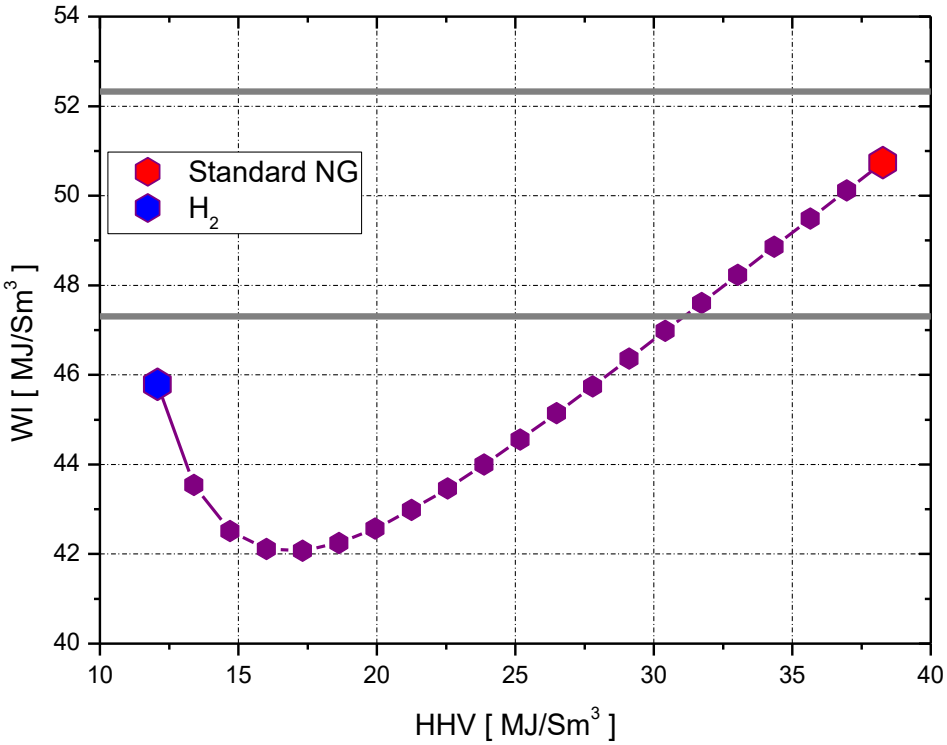

Figure 2.6: Wobbe index vs higher heating value for standard NG – H_2 mixture.

2.2.1 Equation of state

In fluid dynamics, the equation of state is necessary, with the flow governing equations, to completely describe the problem of the gas flowing into a network. This thermodynamic equation (7) relates pressure (p), density (ρ) and temperature (T_g) of the gas. When the behaviour of gas differs from the ideal gas, the compressibility factor should be used ($Z_g \neq 1$). For the other cases, setting the Z_g to one, the gas can be considered ideal.
The fluid flowing in gas networks is not a pure gas but a mixture of hydrocarbon gases and impurities. Therefore, the gas constant (R_g) is defined by the ratio between the universal gas constant and the weighted sum of the molecular weight (M_k) of the gas components (8).

$$\rho = p/Z_g R_g T_g \tag{7}$$

$$R_g = R_u / \sum_{k=1}^{n} y_k M_k \tag{8}$$

The ideal gas model, mathematically easy to develop, is inaccurate in gas network applications, as shown in figure 2.7. The compressibility factor of methane gas has variations up to 5% for low gas pressure ($0 \div 5\ bar_g$). Increasing the pressure of the gas, deviation from the ideal gas behaviour becomes more remarkable. The temperature of the gas also influences the compressibility factor. Only for higher temperatures, differences between the ideal and real gas models are negligible. Therefore, real gas behaviour is described by the equation of state and the compressibility factor, which depends on composition, pressure and temperature of the gas quality.

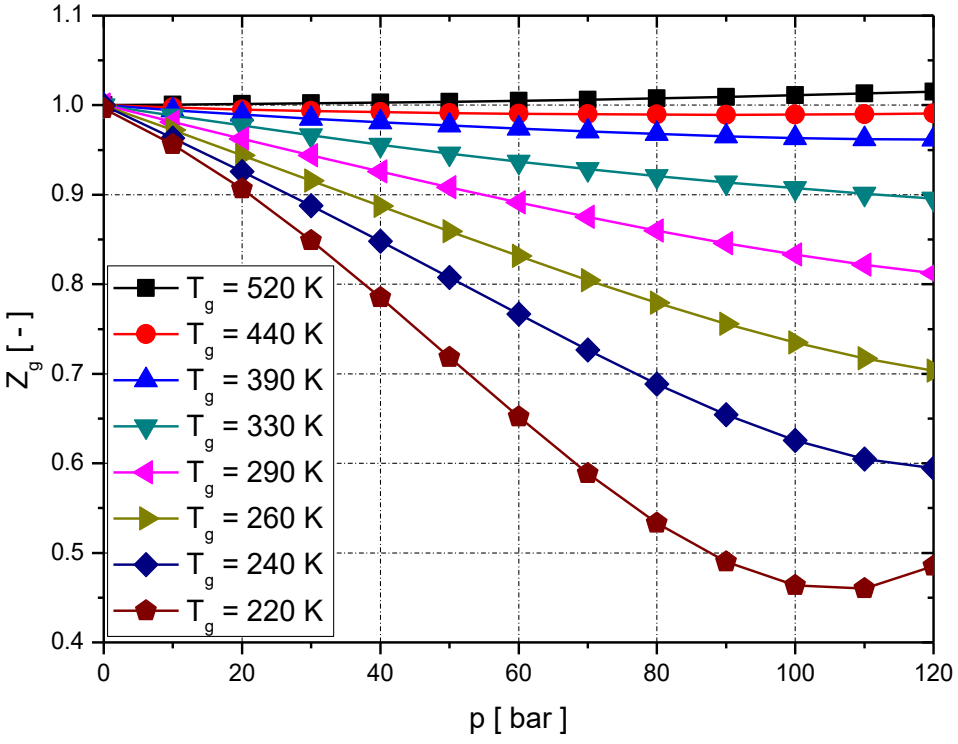

Figure 2.7: Compressibility factor for methane gas [2.3].

The real gas model proposed evaluates the compressibility factor (Z_g) of the mixture using the Papay equation [2.4]. Papay proposed a Z_g correlation (9) for natural gas composed of different hydrocarbon gases and valid for pressure up to $150\ bar_g$. The equation, used in several literature works [2.5, 2.6, 2.7] has two parameters, which are a function of the gas temperature (T_g), pressure (p) and quality (y_k).

$$Z_g = 1 - 3.52\, p_r\, e^{-2.260\, T_r} + 0.274\, {p_r}^2\, e^{-1.878\, T_r} \tag{9}$$

The T_r and p_r variables of the equation are, respectively, the reduced temperature and pressure of the gas mixture. Reduced properties are the ratio between the value and the critical value of properties (10, 11). For a mixture, introducing the concept of pseudo-critical properties, the critical pressure (p_c) and temperature (T_c) are calculated, such as the weighted sum (12, 13) of the critical property of the components.

$$T_r = T_g / T_c \tag{10}$$

$$p_r = p / p_c \tag{11}$$

$$T_c = \sum_{k=1}^{n} y_k\, M_k T_{c,k} \tag{12}$$

$$p_c = \sum_{k=1}^{n} y_k\, M_k p_{c,k} \tag{13}$$

2.2.2 Viscosity equation

When a gas or liquid flows in a pipe, particles, which are in relative motion, generate a frictional resistance force. Viscosity property is used to measure and quantify the resistance of fluid during its motion. In fluid dynamics problems, viscosity is a thermodynamic parameter necessary to determine the flow regime and consequently pressure losses due to shear stress.
Figure 2.8 shows the dynamic viscosity of natural gas fluid [2.8] for the temperature range of $241 \div 353\, K$ and the pressure range of $3 \div 140\, bar_g$. The gas viscosity increases with the pressure. Measurement values depend on the temperature for gas pressure up to $60\, bar_g$. Conversely, for high pressures, the dependence on the temperature is negligible.
In a gas network where the fluid composition is not constant and unique, the dynamic viscosity μ_g depends on gas conditions (p, T_g) and also composition (y_k). The model developed uses the Lucas method [2.2, 2.9] to evaluate the dynamic viscosity of the gas mixture. The viscosity parameter ξ_g of the gas mixture is calculated as a function (14) of the molecular weight M_g, critical temperature T_c and pressure P_c of the mixture. After that, the dynamic viscosity of the mixture μ_g is evaluated, as the ratio (15) of correct reduced temperature and the parameter ξ_g, where T_r is the reduced temperature of the mixture and $F_P^o\ F_Q^o$ are correction factors which take into account polarity and quantum effects.

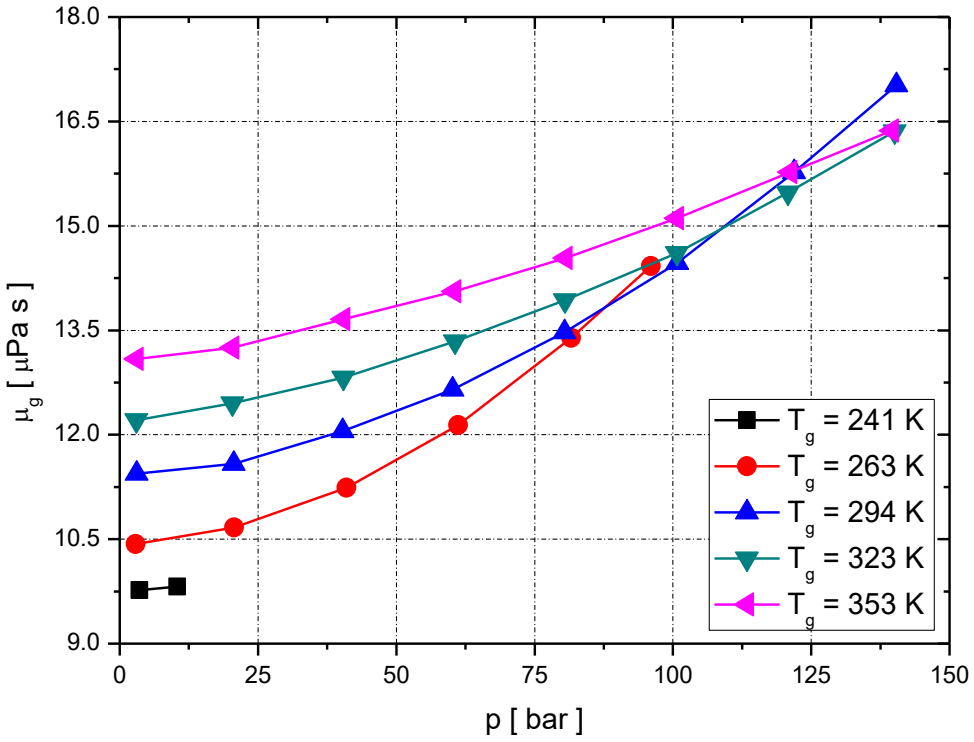

Figure 2.8: Dynamic viscosity for natural gas [2.8].

$$\xi_g = 0.176 \left(\frac{T_c}{M_g^3 \, P_c^4} \right)^{1/6} \tag{14}$$

$$\mu_g = \frac{[\, 0.807 \, T_r^{0.618} - 0.357^{-0.449 \, T_r} + 0.340^{-4.058 \, T_r} + 0.018 \,] \, F_P^o \, F_Q^o}{\xi_g} \tag{15}$$

2.3 Pipe model

Pipes are the elements of the network through which the gas is transported and distributed.
Gas networks and consequently pipes are classified [2.10] according to the working pressure of the gas, as shown in table 2.3. Gas network pipes can also be divided up into high-pressure (1a, 2a, 3a species), medium-pressure (4a, 5a, 6a species) and low-pressure (7a species) pipes. High-pressure pipes are pipelines used for long-range gas transportation. Medium/low-pressure pipes are responsible for distributing gas in urban zones.
Gas standards [2.10] determine a maximum gas flow velocity (v_{max}) for transmission and distribution pipes' species (table 2.4). Velocities into the pipes of the network should be lower than maximum allowed values to minimize pressure drop, impurity dragging and noise phenomena. The overcoming of the velocity limit can produce undesirable high-pressure drops in the network and consequently inadmissible pressure values at demand nodes.

Table 2.3: Working pressure range refereed to the pipes' species [2.10].

	Transportation			Distribution			
	1ª species	2ª species	3ª species	4ª species	5ª species	6ª species	7ª species
$p\ [bar_g]$	> 24	24 ÷ 12	12 ÷ 5	5 ÷ 1.5	1.5 ÷ 0.5	0.5 ÷ 0.04	< 0.04

Table 2.4: Maximum velocity refereed to the pipes' species [2.10].

	Transportation			Distribution			
	1ª species	2ª species	3ª species	4ª species	5ª species	6ª species	7ª species
$v_{max}\ [m/s]$	30	30	30	25	25	15	5

Figures 2.9 and 2.10 shows a real transportation and distribution pipes of a gas network. Pipelines are tubes of large diameter (up to $1.200\ m$) made from unprotected iron and carbon steel. Medium/low-pressure ducts are manufactured by high/medium-density polyethene or polytetrafluoroethylene lined carbon steel or carbon steel (old tubes). Distribution pipe diameter depends on gas pressure and flow rate. Typically, values are included between $80\ mm$ and $300\ mm$.

Figure 2.9: Image of a transportation pipeline.

Figure 2.10: Image of a distribution duct.

For the Gas Network Solver, pipes are linear elements with an inlet and an outlet port (figure 2.11). In particular, they are elements of the network where pressure losses of the gas occur. The modelling of this type of element is fundamental for the network model and the evaluation of its behaviour.

Figure 2.11: Schema of the pipe element.

In the infinitesimal control volume of figure 2.12, the gas flow [2.11] is represented by the fluid dynamics governing equations (16, 17).
Continuity equation (16) represents the conservation of the mass. The algebraic sum of the arriving and leaving mass flow rate is equal to the mass accumulated in the system.
Momentum equation (17) relates the sum of the forces acting on the infinitesimal control volume to its rate of change of momentum. The acceleration of the flow (inertia and convective terms) is due to the pressure, friction and gravity forces present. In gas networks where supply and demand zone can have a different elevation of hundreds of meters, the pipe inclinations are not negligible because of the gravity term effects, significantly, momentum variations.
In the present model, the energy equation is not used because the flow is considered at a constant temperature, and the heat transfer between the flow and the pipe is not modelled. Pipes of gas networks are typically situated under the ground (figures 2.9 and 2.10) and in thermal equilibrium with it. The gas, which flows at a slow velocity, has sufficient time to achieve the temperature of the pipes (ground temperature). Therefore, gas flow through transportation and distribution pipes can be considered in isothermal conditions ($T_g = cost$).

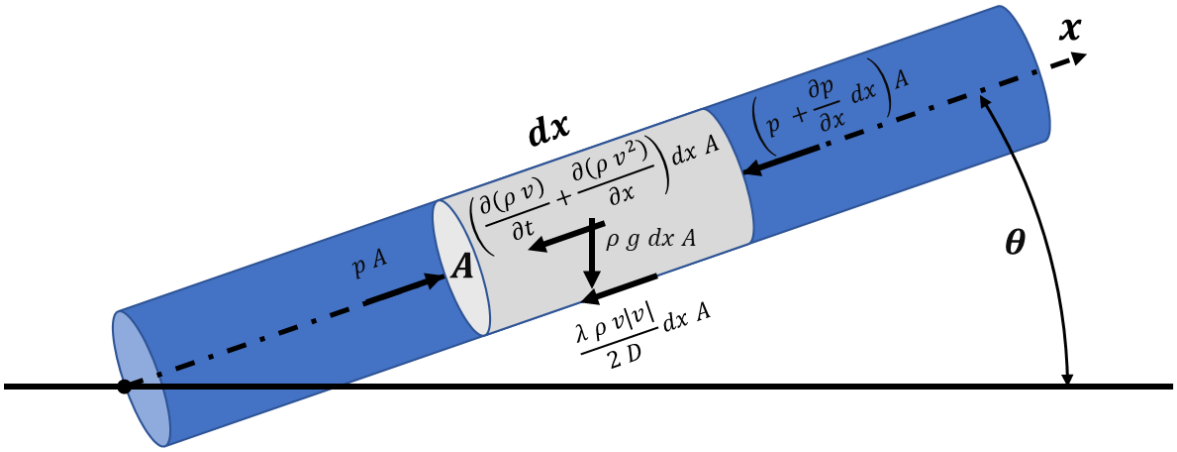

Figure 2.12: Infinitesimal control volume in a pipe.

$$\frac{\partial \rho}{\partial t} + \frac{\partial}{\partial x}(\rho\, v) = 0 \tag{16}$$

$$\frac{\partial(\rho\, v)}{\partial t} + \frac{\partial(\rho\, v^2)}{\partial x} + \frac{\partial p}{\partial x} + \frac{\lambda\, \rho\, v|v|}{2\, D} + \rho\, g \sin\theta = 0 \tag{17}$$

For gas network applications, the velocity (v) of gas flow is up to $25\ m/s$, and the gas speed of sound (c) is about $300\ m/s$. Therefore, the ratio v/c^2 is significantly lower than one, and the convective term in the momentum equation (17) is negligible respect to the pressure variation term, as shown in equation (18).

$$v^2 \frac{\partial\, \rho}{\partial x} = \frac{v^2}{c^2} \frac{\partial\, p}{\partial x} \ll \frac{\partial p}{\partial x} \tag{18}$$

Mass flow rate, through inlet or outlet cross-section of the infinitesimal control volume, is proportional (19) to the gas density (ρ), pipe cross-section area (A) and velocity (v).

$$\dot{m} = \rho\, A\, v \tag{19}$$

Therefore, using (7) and (19), the continuity and momentum equations can be rewritten in the form of equation (20) and (21). Gas pressure (p) and mass flow rate ($\dot{m}$) are the unknown quantities and variables of the problem. The other quantities are parameters of the problem, and they depend on the quality of the gas (Z_g, R_g), boundary conditions (T_g) and characteristics of the pipe (D, A, λ, θ).

$$\frac{\partial p}{\partial t} + \frac{Z_g R_g T_g}{A} \frac{\partial \dot{m}}{\partial x} = 0 \tag{20}$$

$$\frac{1}{A} \frac{\partial \dot{m}}{\partial t} + \frac{\partial p}{\partial x} + \frac{Z_g R_g T_g}{2A^2 D} \lambda \frac{\dot{m}|\dot{m}|}{p} + p\, \frac{g}{Z_g R_g T_g} \sin\theta = 0 \tag{21}$$

2.3.1 Friction factor

Shear stress occurs when the fluid flows within the internal surface of the pipe. Therefore, this friction force produces a loss of pressure from the inlet to the outlet of the pipe. Friction losses increase linearly with the length of the pipe and quadratically with the flow velocity. They also depend on the material and conditions of the internal pipe surface and regime of the flow. The shear stress term in equations (17, 21) is derived from the empirical Darcy-Weisbach equation. This formulation contains a dimensionless coefficient, named Darcy friction factor (λ).

Consider a constant value of λ, as done in several papers [2.12, 2.13], is inaccurate in gas network applications because it produces significant errors in pipes pressure drops estimation. The friction factor (λ) is a function of roughness (ε) and diameter (D) of the pipe and viscosity, velocity and regime of the fluid flow (Re). The Moody diagram [2.14], shown in figure 2.12, relates the friction factor and these parameters. The Reynolds number, which is the ratio between inertial forces and viscous forces, can be calculated by equation (22), where equation (15) is used to estimate the dynamic viscosity of the gas flow. In the laminar region ($Re < 2500$), the friction factor is inversely proportional to the Reynolds number, independent to the pipe roughness and inversely proportional to the Reynold number. After the flow transition, the friction factor is strongly correlated with the surface roughness of the pipe. In the regime of complete turbulence, the friction factor depends only on the roughness, and the effect of the Reynolds number is negligible. The flow, in typical conditions of gas distribution pipes, is in turbulent regime because Reynold number is higher than 4000. In this flow regime, the Colebrook–White [2.15] equation (23) analytically expresses the Moody diagram.

However, when gas flow demand is close to zero (night hours of summer season), the flow velocity in pipes is under $1\ m/s$. Consequently, the gas is in the laminar regime and equation (24) is used to evaluate the friction factor.

The roughness (ε) and diameter (D) of the pipe are characteristics obtained from the geometry of the network and inputs of the problem. Conversely, the Reynolds number depends on the mass flow rate, which is an unknown quantity and a variable of the problem. Therefore, an iterative procedure, which progressively refines the friction factor, is used to solve this implicit equation.

$$Re = \frac{D\,\dot{m}}{\mu_g\,A} \tag{22}$$

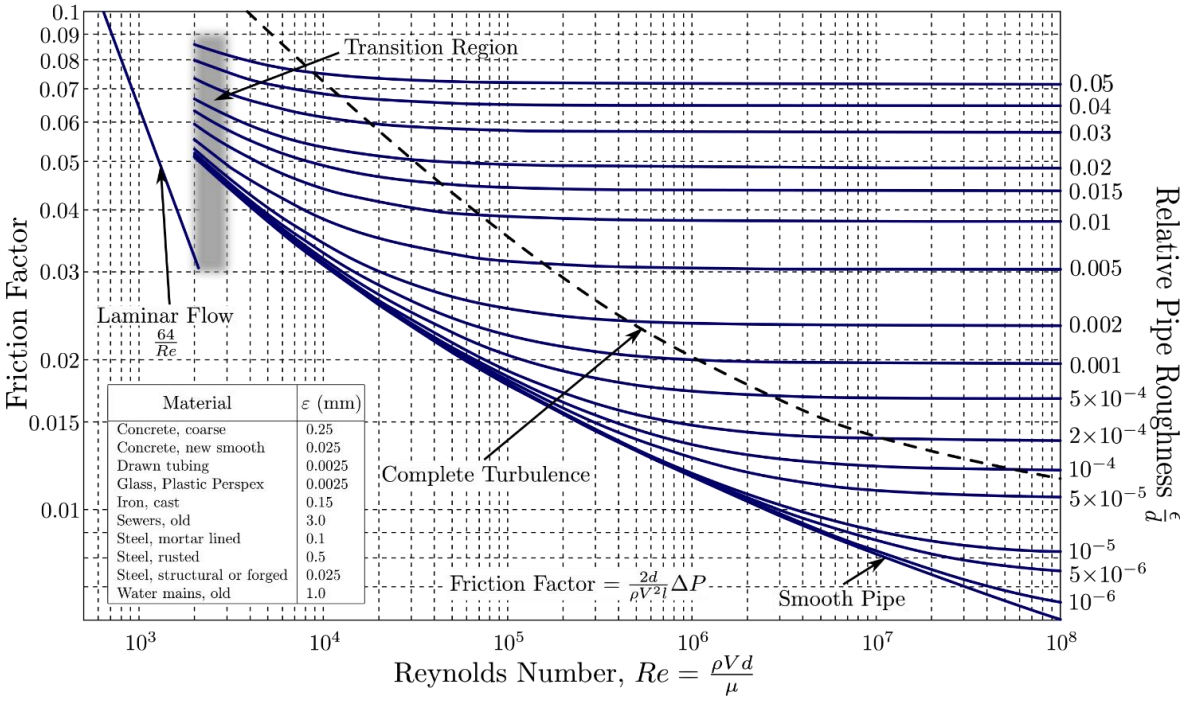

Material	ε (mm)
Concrete, coarse	0.25
Concrete, new smooth	0.025
Drawn tubing	0.0025
Glass, Plastic Perspex	0.0025
Iron, cast	0.15
Sewers, old	3.0
Steel, mortar lined	0.1
Steel, rusted	0.5
Steel, structural or forged	0.025
Water mains, old	1.0

Figure 2.13: Moody diagram [2.12].

Turbulent flow
$$\frac{1}{\sqrt{\lambda}} = -2\,\log\left(\frac{2.51}{Re\,\sqrt{\lambda}} + \frac{1}{3.715}\frac{\varepsilon}{D}\right) \tag{23}$$

Laminar flow
$$\lambda = \frac{64}{Re} \tag{24}$$

2.3.2 Steady-state model

Under steady-state and isothermal conditions, partial derivatives of the time in the governing equations (20, 21) are equal to zero.

In this case, for the Continuity equation (25), the inlet mass flow rate is equal to the outlet mass flow rate. Therefore, pipes do not have inertia because the amount of gas accumulated in the control volume is equal to zero. A change of the outlet flow rate is immediately perceived at the inlet of the pipe.

The Momentum equation turns into the pressure drop equation (26). Pressure value between inlet and outlet cross-section of the control volume is related to the friction loss and gravity if a pipe inclination exists.

$$\frac{Z_g R_g T_g}{A}\frac{\partial \dot{m}}{\partial x} = 0 \tag{25}$$

$$\frac{\partial p}{\partial x} + \frac{Z_g R_g T_g}{2A^2 D}\lambda\frac{\dot{m}|\dot{m}|}{p} + p\,\frac{g}{Z_g R_g T_g}\sin\theta = 0 \tag{26}$$

Considering a straight pipe of length L and constant cross-section A, the governing equations, valid for an infinitesimal control volume, can be integrated along the length to obtain its model equations.

The mass flow rate at the inlet cross-section of the pipe is equal to the mass flow rate at the outlet cross-section of it (27). Therefore, the continuity equation represents the constancy of the mass flow along the pipe.

The difference between quadratic inlet and outlet pressures is related to the quadratic mass flow rate (28). The parabolic pressure drops equation derived takes the name Ferguson equation [2.16]. This integral formulation of the Momentum equation includes the effect of the pipe inclination (θ) neglected by different literature formulations [2.12, 2.13, 2.17].

The equation coefficients (29) are related to friction loss and gravity. When no elevation gain exists, the coefficient c_3 is equal to zero, and the ratio $(1 - c_1)/c_3$ becomes 1. Due to the evolution of the pressure, the compressibility factor (Z_g) along the pipe is not constant. Therefore, the compressibility factor value used in the momentum equation ($\bar{Z}_g$) is calculated, such as the integral mean value of $Z_g(x)$ along the pipe (30).

$$\dot{m}_{in} - \dot{m}_{out} = 0 \tag{27}$$

$$c_1\, p_{in}^2 - p_{out}^2 - c_2\, |\dot{m}|\, \dot{m} = 0 \tag{28}$$

$$c_1 = exp\,(-c_3)\,;\; c_2 = \frac{8\,L}{\pi^2 D^5}\,\lambda\,\bar{Z}_g R_g T_g\,\frac{1-c_1}{c_3};\; c_3 = \frac{2\,g}{\bar{Z}_g R_g T}\,L\,\sin\theta \tag{29}$$

$$\bar{Z}_g = \frac{1}{L}\int_{x=0}^{x=L} Z_g(x)\,dx \tag{30}$$

2.3.3 Dynamic model

Under transient and isothermal conditions, the one-dimensional gas flow through transportation and distribution pipes is modelled by the non-linear partial differential equations (20, 21). Partial derivatives of the time and space are approximated using the finite difference method (FDM) to convert the differential governing equations into non-linear algebraic equations. The domain of the problem should be discretized in time and space to use the finite difference method and correctly evaluate the solution of the problem.

Figure 2.14 shows the numeric schema used for the pipe model. A pipe is discretized in N finite volumes of length Δx. The computational model stores the fluid variables (p, $\dot{m}$) at the borders (i, $i+1$) and evaluates them at the middle (I) for each time step (t_n, t_{n+1}, …) of the simulation and each finite volume. Representing with Y a generic flow variable, the value, partial derivates of the space and time are calculated by equations (31–34).

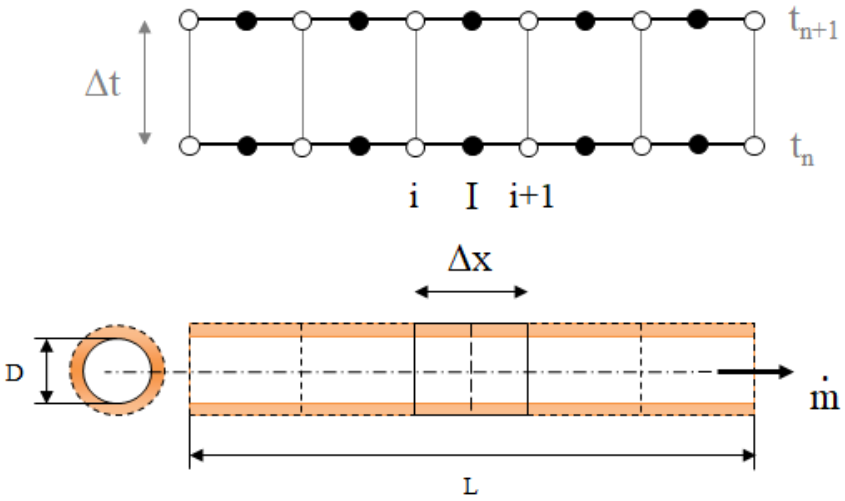

Figure 2.14: Finite difference method scheme.

$$Y_I^n = \frac{Y_{i+1}^n + Y_i^n}{2} + o(\Delta x^2) \tag{31}$$

$$Y_I^{n+1} = \frac{Y_{i+1}^{n+1} + Y_i^{n+1}}{2} + o(\Delta x^2) \tag{32}$$

$$\frac{\partial Y_I^n}{\partial x} = \frac{Y_{i+1}^{n+1} - Y_i^{n+1}}{\Delta x} + o(\Delta x^2) \tag{33}$$

$$\frac{\partial Y_I^{n+1}}{\partial t} = \frac{Y_I^{n+1} - Y_I^n}{\Delta t} + o(\Delta t) \tag{34}$$

The fully implicit method [2.18] used, in the NWG tool, is the first-order forward difference in time and the second-order central difference in space. This approach makes the numeric scheme stable, independently on the time step Δt or the spatial discretization Δx assumed. The non-linear algebraic equations (35, 36), valid in the N finite volumes, are obtained substituting the finite difference equations in the non-linear partial differential equations (20, 21).

The behaviour of each pipe of the network is described by a non-linear system of $2N$ algebraic equations. This system is solved at each time step (t_n, t_{n+1}, …) of the simulation by the iterative algorithm presented in figure 2.15.

$$\frac{p_I^{n+1} - p_I^n}{\Delta t} + \frac{Z_g R_g T_g}{A} \frac{\dot{m}_{i+1}^{n+1} - \dot{m}_i^{n+1}}{\Delta x} = 0 \tag{35}$$

$$\frac{1}{A}\frac{\dot{m}_I^{n+1} - \dot{m}_I^n}{\Delta t} + \frac{p_{i+1}^{n+1} - p_i^{n+1}}{\Delta x} + \frac{Z_g R_g T_g}{2A^2 D}\lambda \frac{\dot{m}_I^{n+1}\left|\dot{m}_I^{n+1}\right|}{p_I^{n+1}} + p_I^{n+1}\frac{g}{Z_g R_g T_g} sin\,\theta = 0 \tag{36}$$

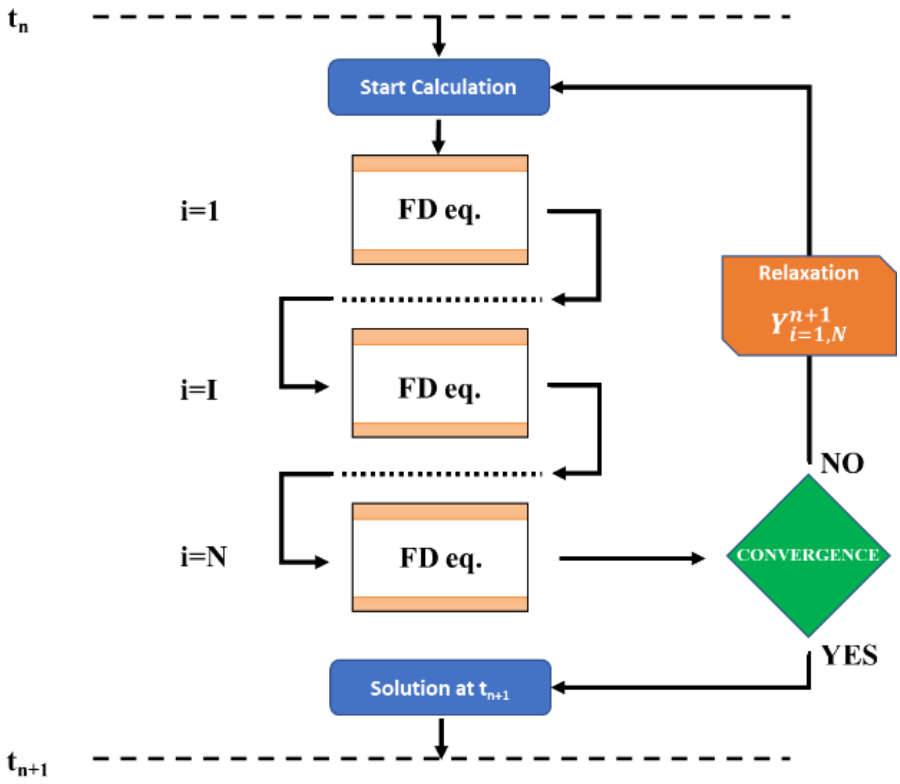

Figure 2.15: Iterative algorithm to solve governing equations.

2.4 Reducing station model

A gas distribution network has the role of delivering the gas into an extensive urban area. Users connected to the grid are small/medium industrial, commercial and domestic customers. The fuel gas required by them is used for several different applications. House and industrial devices work respectively at about $19 \div 21\, mbar_g$ and $0.25 - 0.5 - 1\, bar_g$. Therefore, the gas distributor must be able to supply the gas to all users at the correct pressure.

Reducing stations are used to manage efficiently the different pressure levels of the network, which is a complex structure. The gas is injected into 4a specie pipes of the grid by city gate stations at a pressure between 4 and $7\, bar_g$. A first pressure reduction to $0.2 \div 0.5\, bar_g$ is executed by intermediate reducing stations between pipes of 4a and 5a/6a species. After that, several final reduction stations are installed in specific points of the urban area to reduce the pressure to $22 \div 30\, mbar_g$ and supply the gas to low-pressure pipes (7a species) of a specific downstream district. These systems divide the distribution grid into sections of medium-pressure pipes (4a, 5a, 6a species) and several districts of low-pressure pipes (7a specie).

The stations' shut-off causes the failure to deliver gas at final users. Therefore, more than one reduction stations should supply an isolated area to safeguard the security of gas customer.

Figure 2.16 shows the layout of a gas reducing station, which is formed by gas filters, valves, pressure regulators and pressure gauges. Two flow lines are present to increase the reliability of

the system and have the possibility to replace components or do the maintenance of them. Due to the limited pressure drop, the consequent temperature variation (Joule–Thomson effect) is negligible ($T_g = cost$). Therefore, a gas heater is not necessary for this type of system.

Figure 2.16: Image of a reducing station.

For the gas network model, the gas reducing station is a linear element where the gas flow is subjected to a decompression transformation from the inlet port to the outlet port (figure 2.17).

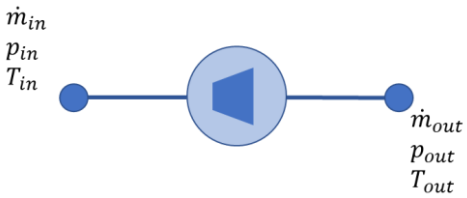

Figure 2.17: Schema of the reducing station element.

The two operative modes of the element are:

- Regulation mode: The gas flows through the element (37), and a manual or electric remote control imposes the pressure of the gas, which leaves the system (38). The position of the pressure regulators is inversely related to the value of the inlet pressure. When the regulator is opened fully, the setpoint value depends on the inlet conditions and the capacity of the system. The gas arrives at the station with low pressure ($p_{in} \leq p_{set}$). Therefore, the minimum pressure drop of the regulator is not sufficient to impose the desired outlet setpoint value.

$$\dot{m}_{in} = \dot{m}_{out} \tag{37}$$

$$\begin{cases} p_{out} = p_{set}\,, & p_{in} > p_{set} + c_{v,100\%}\,\dot{m}^2 \\ p_{in} - p_{out} = c_{v,100\%}\,\dot{m}^2, & p_{in} \leq p_{set} \end{cases} \tag{38}$$

- Anti-reverse flow mode: For the characteristics of the system's components, the gas flow must be unidirectional. Therefore, the station has an anti-reverse flow valve, which prevents the inversion of the gas flow. This event occurs in scenarios where the pressure level of the downstream network is higher than the setpoint value (p_{set}). Under such conditions, the flow through the element is stopped, and inlet and outlet gas flows are set to zero (39).

$$\begin{cases} \dot{m}_{in} = 0 \\ \dot{m}_{out} = 0 \end{cases} \tag{39}$$

2.5 Valve model

Valves are components with the task of intercept, in contingency conditions, the gas flowing into a network (figure 2.18).
They are located every $10 \div 30\ km$ along transportation pipelines and every $2 \div 5\ km$ in medium-pressure networks [2.10]. These elements are also installed in strategic points of the gas network, in order to manage the direction of the flow and isolate specific areas.
Interception valves should work fully open or fully closed. Intermediate positions are not allowed because they may cause significant undesired pressure drops.

Figure 2.18: Image of a valve.

The component is modelled, as a linear element of negligible length and with one inlet port and one outlet port (figure 2.19).

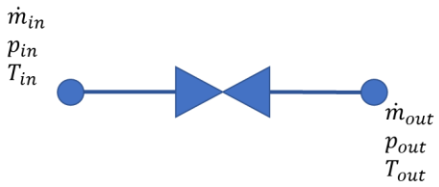

Figure 2.19: Schema of the valve element.

The valve element can work in two operating modes:

- Bypass mode: The valve is fully open, and the gas is free to flow in the downstream pipe (40) and supply users of the corresponding district. The pressure drop through the element (41) is only due to the resistance of the valve (c_v). Therefore, the gas difference temperature is negligible ($T_g = cost$). There are no anti-reverse flow systems. Therefore, the flow can to cross the valve in both directions.

$$\dot{m}_{in} = \dot{m}_{out} \tag{40}$$

$$p_{in} - p_{out} = c_v \dot{m}^2 \tag{41}$$

- Close mode: In this case, the valve stops the gas flow (42), preventing the gas from supplying the downstream area and keeping the gas in the desired upstream zone.

$$\begin{cases} \dot{m}_{in} = 0 \\ \dot{m}_{out} = 0 \end{cases} \tag{42}$$

For the annotation of the previously mentioned modelling equations, the inlet and outlet ports of the valve element are respectively the sections where the gas arrives into the valve and the section where the gas leaves the valve.

2.6 City gate station model

A city gate station represents the interconnection point between transportation and distribution networks. For the high-pressure transportation pipeline, it is an offtake point, where an amount of gas is withdrawn. Conversely, it is the source node which supplies the gas to the downstream medium/low-pressure distribution grid.

The system has the function of measure, odorize and reduce the pressure of the upstream gas. Transportation pipelines of thousands of kilometres require high-pressure to move the gas from production sites to local gas distribution companies. The gas enters into the city gas station at a pressure of $10 \div 30\ bar_g$. A reduction pressure process of $5 \div 25\ bar_g$ is required to guarantee a reasonable level of pressure into the gas distribution grid. The pressure of the gas leaving the station is regulated by a pressure regulator which is opened/closed to achieve the setpoint value.

Due to the significant pressure drop, the Joule–Thomson effect, which decreases the temperature of the gas during the lamination process, is not negligible. Therefore, a boiler heats the gas before the reduction pressure process to maintain approximately constant the temperature of gas leaving the station.

An organosulfur compound odorant, named TetraHydroThiophene $(CH_2)_4$, is added to increase the odour of the mixture. The odorization of the gas is necessary because, in the case of gas leakages,

the gas into the ambient should be easily sensed from the human smell. The amount of $(CH_2)_4$ added is $50 \div 60\, mg/Sm^3$. Therefore, it does not affect the thermodynamic parameters of the gas mixture.

Figure 2.20 shows the layout of a real city gate station. The ground surface occupied by it is remarkable due to the several components (pressure regulators, valves, filters, boilers, odour system, measurement instrument) and an overabundance of gas lines necessary to obtain high reliability of the station.

Figure 2.20: Imagine of a city gate station.

Despite the several components and process, the purpose of the station is to maintain the outlet pressure (p_{out}) and temperature ($T_{out} = T_{set}$) of the gas at the setpoint values independently from the upstream conditions and the gas flow rate demanded by the downstream distribution network. Figure 2.21 shows the schema model of the city gas station element used in the Gas Network Solver. When a gas distribution network is modelled and simulated, the station is a point element (supply node) with a single outlet port.

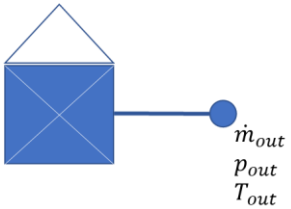

Figure 2.21: Schema of the city gate station element.

The mathematical equations used to describe its behaviour, depend on the operative mode:

- Design mode: The station works, as a gas source which imposes the pressure of the gas injected into the network (43). The gas mass flow rate leaving the station ($\dot{m}_{out}$) depends on the gas flow required by the users connected to the grid.

$$p_{out} = p_{set} \tag{43}$$

- Maximum capacity mode: The pressure regulator of the station is opened/closed according to the pressure set value (p_{set}) and the gas flow rate ($\dot{m}_{out}$). When the maximum position is achieved, the component and the system elaborate the maximum gas flow. Therefore, the outlet mass flow is limited to the maximum capacity of the city gate station (44), and the pressure setpoint value depends on the characteristic curve of the regulator (45).

$$\dot{m}_{out} = \dot{m}_{out,max} \tag{44}$$

$$p_{out} = p_{set}\ (\dot{m}_{out,max}) \tag{45}$$

- Anti-reverse flow mode: In particular conditions of the network, the reverse gas flow can occur if the pressure of the downstream pipe is higher than the pressure set value (p_{set}). This undesired and damaging situation is prevented by a non-return valve, which closes the outlet duct of the station and stops the gas flow (46).

$$\dot{m}_{out} = 0 \tag{46}$$

2.7 Node model

Nodes are point elements where the gas is not subject to a transformation. They are joint of linear elements such as pipes and valves or point where users are connected to the grid. In these elements, the incoming gas is mixed, split and also delivered to users.
According to the different functions, the nodes of a gas distribution network are classified in:

- Junction: It is a point element where two or more different linear elements are connected. For instance, two pipes with different geometrical properties (ε, D, θ, specie) or a split of one pipe into two pipes.
- Intermediate Demand node: Users connected to a pipe of the network are usually attributed to the upstream and downstream nodes connected. For these nodes, a part of the arriving gas is extracted from the network and delivered to the users.
- Final Demand node: It is a final point located at the ends of the network's branches. The total gas flow incoming from the upstream pipe is delivered to the users connected to the node.

Mathematical equations used to model a node of the network are the same independently of its functionality. The node element has $1 \div n$ inlet, $1 \div n$ outlet port and an additional port for the offtake, as shown in figure 2.22.

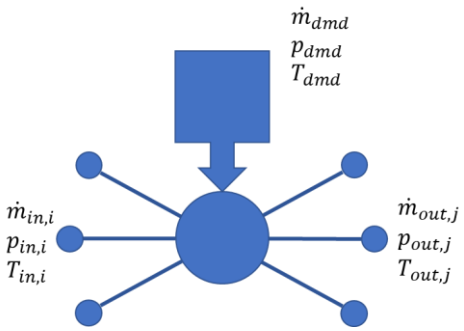

Figure 2.22: Schema of the node element.

For each node of the network, it is valid the first law of Kirchhoff: the algebraic sum of the in/out gas flows is equal to zero (47). In particular, the difference between the inlet and the outlet port flows is equal to the gas extracted ($\dot{m}_{dmd}$) from the node if present.

$$\sum_{i=1}^{n} \dot{m}_{in,i} - \sum_{j=1}^{n} \dot{m}_{out,j} = \dot{m}_{dmd} \tag{47}$$

For the element's characteristics, the process of mixing, splitting and delivery are isochoric and adiabatic. Therefore, the gas leaves the node with the same pressure of the inlet flow (48). Instead, the temperature of the outlet gas flow is the mixing temperature of the incoming flows (49).

$$p_{out,j} = p_{in,i} \tag{48}$$

$$T_{out,j} = \frac{\sum_{i=1}^{n} \dot{m}_{in,i} T_{in,i}}{\sum_{i=1}^{n} \dot{m}_{in,i}} \tag{49}$$

2.7.1 Interchange node

Despite the physical layout, a gas network can be operated and owned by two or more different entities. Therefore, interchange nodes are located at the entities borders to control the flow of gas exchanged by two subnetworks. Secondly, unconventional users, which injects or extracts gas depending on their need, could be connected to the grid.
The schema (figure 2.23) of the interchange node element switches according to its role. For a single gas system model, this element injects (only one outlet port) or extracts (only one outlet port) an amount of gas.
Depending on the network's behaviour and condition, the interchange node works in different operative mode using related modelling equations:

- Injection mode: An amount of gas flow/energy, at a temperature T_{inj}, is injected, from the outlet port, into the gas network (50, 51). The pressure of the leaving gas (p_{out}) is not set but depends on the downstream conditions.

$$\dot{m}_{out} = \dot{m}_{inj} \tag{50}$$

$$T_{out} = T_{inj} \tag{51}$$

- Extract mode: The gas flow arrives from the inlet port, and it is totally extracted from the gas grid (52). In this case, the interchange node is modelled, such as a final demand node with just an inlet port.

$$\dot{m}_{in} = \dot{m}_{dmd} \tag{52}$$

- Balance mode: When the operating mode of the interchange node is not unique, the element imposes its pressure node (53). If the pressure setpoint is higher than the pressure in the connected pipe, the interchange node injects gas into the grid. Otherwise, an amount of gas is extracted according to the pressure of the node.

$$p_{out/in} = p_{set} \tag{53}$$

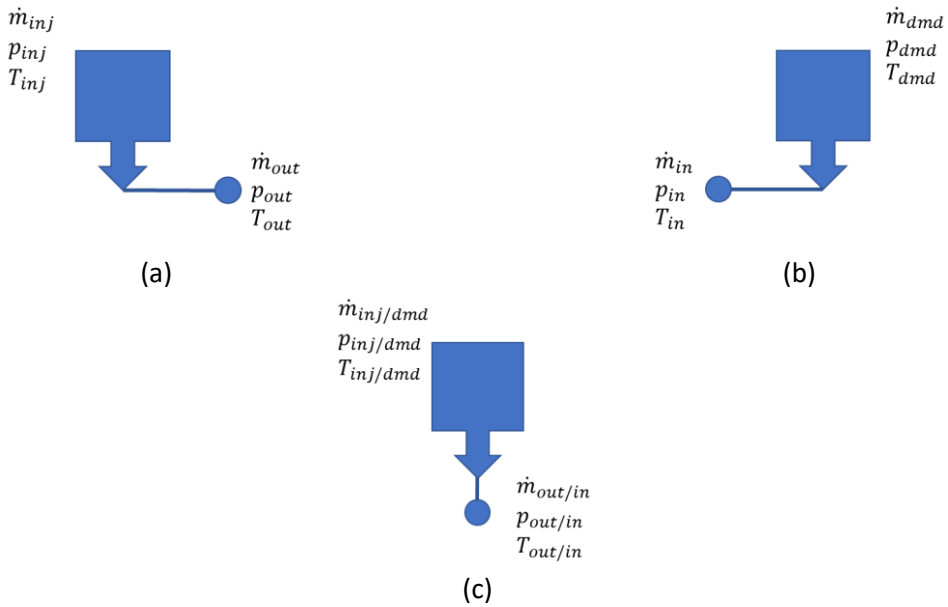

Figure 2.23: Schema of the interchange node element: (a) Injection mode, (b) extracted mode, (c) balance mode.

2.8 Gas quality tracking model

Gas Regulatory Authorities [2.1] determine the allowable ranges for the properties of the gas delivered to industrial, domestic and commercial customers. Generally, city gate stations supply the gas demanded by users connected to gas distribution networks. Nowadays, the increasing production of green gases (biogas, hydrogen and synthetic natural gas) leads towards the use of these gases in the gas networks' decarbonisation. In this new scenario, a gas network can have additional alternative supply nodes which inject biogas, hydrogen or SNG into the grid. Accordingly, a gas quality tracking model is necessary to investigate the effects of unconventional gas injections and evaluate gas composition and properties at each demand node of the network.

In nature, transport of substances in a fluid is due to the combination of advection and diffusion phenomena.

Due to its characteristics, the pipe is the most significant element of the network where the transport phenomena of gas components occur.
In 1-D problems [2.19], there are concentration's gradients just in the x-direction of the pipe. Therefore, the transport of a quantity C, in an infinitesimal control volume, is governed by the advection-diffusion equation (54).

$$\frac{\partial C}{\partial t} + v\,\frac{\partial C}{\partial x} + DD_x\,\frac{\partial^2 C}{\partial x^2} = 0 \tag{54}$$

The general advection-diffusion equation valid for a generic substance can be used for each component (y_k) of the gas mixture (55), where v is the velocity of the flow into the control volume and DD_{kx} is the axial diffusion coefficient of the k component in the other $m - 1$ components of the mixture.

$$\frac{\partial y_k}{\partial t} + v\,\frac{\partial y_k}{\partial x} + DD_{kx}\,\frac{\partial^2 y_k}{\partial x^2} = 0 \tag{55}$$

For gas network applications, the flow velocity (v) is up to $25\ m/s$, the diffusion coefficients of gas components (DD_{kx}) are between 10^{-5} and $10^{-4}\ m^2/s$ [2.20] and pipe length (L) are hundreds or thousands of meters. Therefore, the non-dimensional Peclet number (Pe), calculated by equation (56), is typically significantly greater than one.

$$Pe = \frac{v\,L}{D_x} \tag{56}$$

Consequently, in the gas quality tracking problem [2.21], the equation (55) reduces to the advection transport equation (57) because advection phenomenon is dominant ($Pe \gg 1$) and the diffusion is negligible. In this case, the transportation of a k component of the gas mixture depends only on the velocity of the flow.

$$\frac{\partial y_k}{\partial t} + v\,\frac{\partial y_k}{\partial x} = 0 \tag{57}$$

In steady-state and isothermal condition, the advection transport equation (57) reduces to a differential equation in the space x which can be integrated along the length of the pipe to obtain the mass fraction continuity equation (58).

$$y_k\,\dot{m}_{in} - y_k\,\dot{m}_{out} = 0 \tag{58}$$

For each component y_k, the mass flow rate fraction arriving in the element is equal to the mass flow rate fraction leaving (figure 2.24). These m equations (one for any component of the mixture) represent the transportation of the gas quality in a pipe under steady-state conditions.

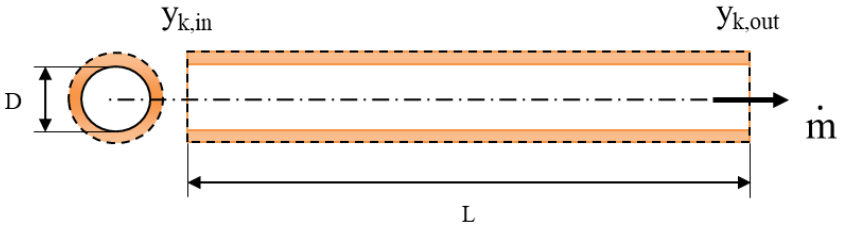

Figure 2.24: Steady-state quality tracking model schema.

In dynamic conditions, the advection transport equation (57) is solved using the batch tracking algorithm [2.22].

The method, implemented in the NWG tool, applies the same numeric schema used to solve the fluid dynamics problem (figure 2.14). Gas quality components (y_k) are stored at the points (1, .., i, .., N), as fluid dynamic variables. Additional finite elements, named batches, with a constant gas composition are defined.

At each time step (t_n, t_{n+1}, ...): a batch of length $v_1^n\,\Delta t$ with a gas composition equal to the boundary value imposed is inserted at the inlet section of the pipe; batches into the pipe move in the direction of the flow; one batch of length $v_N^n\,\Delta t$ leaves the pipe at the outlet section (figure 2.25).

The position of a batch J at the next time step (t_{n+1}) is calculated by equation (31), where v_J^n is the velocity of the batch at the time step t_n.

$$x\,(J, t_{n+1}) \;=\; x\,(J, t_n) + v_J^n\,\Delta t \tag{59}$$

Consequently, at each time step, the gas quality component y_k of each point i is evaluated using the value of the batch J, which is positioned between i and $i+1$ points.

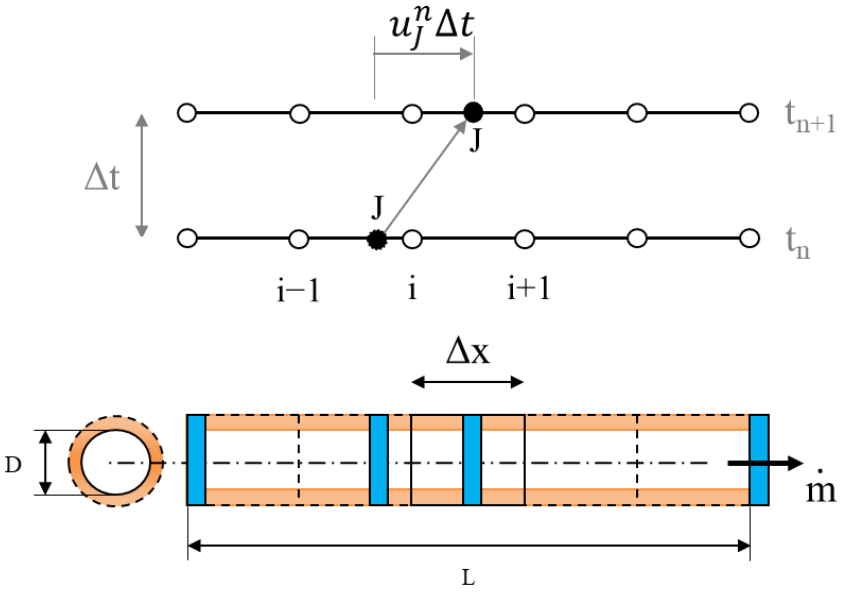

Figure 2.25: Dynamic quality tracking model schema.

For the other linear elements of the gas network (reducing stations, valves), the quality tracking issue is modelled using the same equation (54). Dynamic characteristics of these elements are negligible respect to pipes. Therefore, the quality tracking model is just the mass conservation of each component y_k of the gas (58).

Nodes of the network are point element of negligible volume and dynamic characteristics. In these elements, arriving gas flows, with or without the same composition, are mixed and then split to the outlet ports. Therefore, just the mass conservation equation of each gas component y_k is necessary to model the mixing and split of the quality in a node of the network (60).

$$\sum_{i=1}^{n} y_k \, \dot{m}_{in,i} - \sum_{j=1}^{m} y_k \, \dot{m}_{out,j} = y_k \, \dot{m}_{dmd} \tag{60}$$

Bibliography

[2.1] ARERA, the Italian Regulatory Authority for Energy, Networks and Environment, https://www.arera.it.

[2.2] R. C. Reid, J. M. Prausnitz, B. E. Poling, "The Properties of Gases and Liquids", McGraw-Hill 4° edition (1987).

[2.3] J. Cezar de Almeida, J. A. Velasquez, R. Barbieri, "A Methodology for Calculating the Natural Gas Compressibility Factor for a Distribution Network", Petroleum Science and Technology 32 (2014) 2616–2624.

[2.4] I. Papay, "A termeléstechnológiai paraméterek valtozasa a gaztelepek muvelese soran", OGIL Musz. Tud. Kozl. (1968) 267–273.

[2.5] G. Guandalini, P. Colbertaldo, S. Campanari, "Dynamic modeling of natural gas quality within transport pipelines in presence of hydrogen injections", Applied Energy 185 (2017) 1712–1723.

[2.6] M. Schmidt, M. C. Steinbach, B. M. Willert, "High detail stationary optimization models for gas networks", Optim. Eng. 16 (1) (2015) 131–64.

[2.7] K. A. Pambour, B. Cakir Erdener, R. Bolado-Lavin, and G. P. Dijkema, "SAInt - A novel quasi-dynamic Model for assessing Security of Supply in coupled Gas and Electricity Transmission Networks", Applied Energy 203 (2017) 829–857.

[2.8] M. J. Assael, N. K. Dalaouti, V. Vesovic, "Viscosity of Natural-Gas Mixtures: Measurements and Prediction", International Journal of Thermophysics 22 (2001).

[2.9] K. Lucas, "Phase Equilibria and Fluid Properties in the Chemical Industry", Dechema (1980) 573.

[2.10] UNI 9165, "Condotte con pressione massima di esercizio minore o uguale a 5bar", Milan (2004).

[2.11] H. Daneshyar, "One-dimensional Compressible Flow", Annual Report Pergamon Press. Gassco (2015).

[2.12] M. Abeysekera, J. Wu, N. Jenkins, M. Rees, "Steady state analysis of gas networks with distributed injection of alternative gas", Applied Energy 164 (2016) 991–1002.

[2.13] F. Tabkhi, C. Azzaro-Pantel, L. Pibouleau, S. Domenech, "A mathematical framework for modelling and evaluating natural gas pipeline networks under hydrogen injection", International Journal of hydrogen energy 33 (2008) 6222–6231.

[2.14] L. F. Moody, "Friction factors for pipe flow", Transactions of the ASME 66 (1944) 671–684.

[2.15] C. F. Colebrook, "Turbulent flow in pipes, with particular reference to the transition region between the smooth and rough pipe laws", J. Inst. Civ. Eng. 11 (4) (1939) 133–156.

[2.16] J. A. Ferguson, "Gas flow in long pipelines", Chem. Eng. (2002) 56.

[2.17] S. Pellegrino, A. Lanzini, P. Leone, "Greening the gas network - The need for modelling the distributed injection of alternative fuels", Renewable and Sustainable Energy Reviews 70 (2017) 266–286.

[2.18] M. Abbaspour, K. S. Chapman, "Nonisothermal Transient Flow in Natural Gas Pipeline", J. Appl. Mech 75 (2008).

[2.19] W. Hundsdorfer, J. G. Verwer, "Numerical Solution of Time-Dependent Advection-Diffusion-Reaction Equations", Springer Science & Business Media (2007).

[2.20] R. W. Gallant, C. L. Yaws, "Physical Properties of Hydrocarbons", Gulf Publishing Company (1995).

[2.21] M. J. Ryan, R. L. Mailloux, "Methods for performing composition tracking for pipeline networks", Proceedings of the 18th PSIG Annual Meeting (1986).

[2.22] J. L. Modisette, "Lagrange - a pipeline flow model based on points moving with the fluid", Proceedings of the 36th PSIG Annual Meeting (2004).

Chapter 3

Tool Validation

This chapter focuses on the validation of the Gas Network Solver proposed and developed in chapter 2. The first test case analysed is a single branch network with one source node and one demand node, connected by a single pipe. A looped medium-pressure distribution network, with six pipes, one city gate station and two demand nodes, is used as the second test case. Finally, it is studied as the third test case the triangular high-pressure network available in scientific literature and used in the past by several authors to validate their models. Results of test case 1 and 2 obtained with the tool implemented are compared with data obtained by Scenario Analysis Interface for Energy Systems (SAInt) program. SAInt is a commercial software application for planning, analysing and operating independent or interconnected natural gas and electric power system networks [3.1, 3.2]. Conversely, data available in the literature [3.3, 3.4, 3.5, 3.6] are used to estimate the accuracy of the triangular network's model.

3.1 Test case 1 - Single pipeline

The first network analysed is a single simplified pipeline. The gas is injected at the source node, transported by a single pipe and delivered to the demand node (figure 3.1). Table 3.1 shows the boundary conditions and parameters that should be necessarily set to simulate the network and to evaluate the variables of the problem. Due to the characteristics of source nodes, the pressure, temperature and composition of the gas injected are known and constant values. Usually, the diameter, length, inclination and roughness of the pipe are properties obtained from the geometry and layout of the network. Conversely, the gas withdrawn at demand nodes depends on the energy/flow requested by the users' devices connected to them and it is time-dependent.

Firstly, the test case 1 is analysed in steady-state conditions, setting different values for the boundary conditions and parameters of the model. Secondly, several dynamic scenarios with different source pressures and demand profiles are simulated.

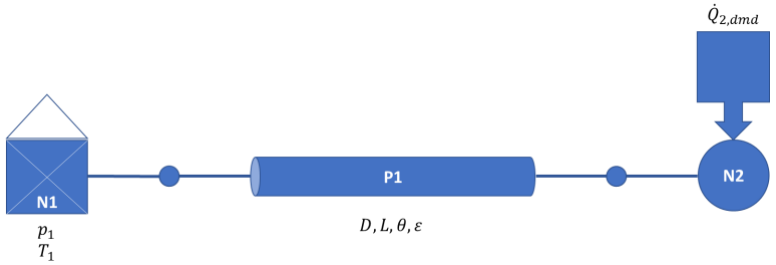

Figure 3.1: Single pipeline schema.

Table 3.1: Boundary conditions and parameters of the single pipeline.

Element	Boundary condition/Parameter			
Supply Node	y_k	p_1	T_1	
Demand Node	$\dot{Q}_{2,dmd}$			
Pipe	D	L	θ	ε

3.1.1 Steady-state validation

The single pipeline is, firstly, simulated in steady-state conditions to benchmark the steady-state gas network model, which is the initial state for dynamic simulations. The source node injects methane gas (CH_4) at a pressure p_1 and a temperature T_1. The demand node withdraws $\dot{Q}_{2,dmd}$ standard metro cubic per hour necessary to provide the energy requested by users' combustion devices connected to it. Boundary conditions imposed in this scenario are shown in table 3.2. Different values of supply pressure in the range of $1.00 \div 50.00\ bar_g$ and volumetric gas flow rate demand in the range of $100 \div 1'000\ Sm^3/h$ are simulated to evaluate the accuracy and adequacy of the tool developed.

Table 3.2: Boundary conditions imposed for the steady-state validation.

Boundary Condition	Value			
y_{CH4} [%]	100			
p_1 [bar_g]	1.00	5.00	10.00	50.00
T_1 [°C]	15.00			
$\dot{Q}_{2,dmd}$ [Sm^3/h]	100	200	500	1'000

Table 3.3 shows the characteristics of the pipe used to model the branch which connects supply and demand nodes. These nodes are located at the same altitude. Therefore, no inclination of the pipe is considered in these simulations.

Table 3.3: Pipe parameters imposed for the steady-state validation.

Parameter	$D\ [mm]$	$L\ [m]$	$\theta\ [°]$	$\varepsilon\ [mm]$
Value	100	100	0.00	0.010

For the source pressures simulated, pressure differences between the supply node and demand node as a function of the standard volumetric gas flow demand are shown in figure 3.2. Pressure losses across the pipe increase quadratically with the flow velocity and consequently with the gas flow rate. Increasing pressure of the source (p_1), pressure drops of the pipe decrease because a higher density of the gas flow reduces friction forces and losses. Differences between the model proposed (NWG) and the commercial software (SAInt) increase with the gas flow rate and reducing the pressure of the gas. Deviations shown are a consequence of the different pressure drop and viscosity equations used to model the pipe. However, relative differences evaluated are lower than 5% for the all $p_1$and $\dot{Q}_{2,dmd}$ values simulated.

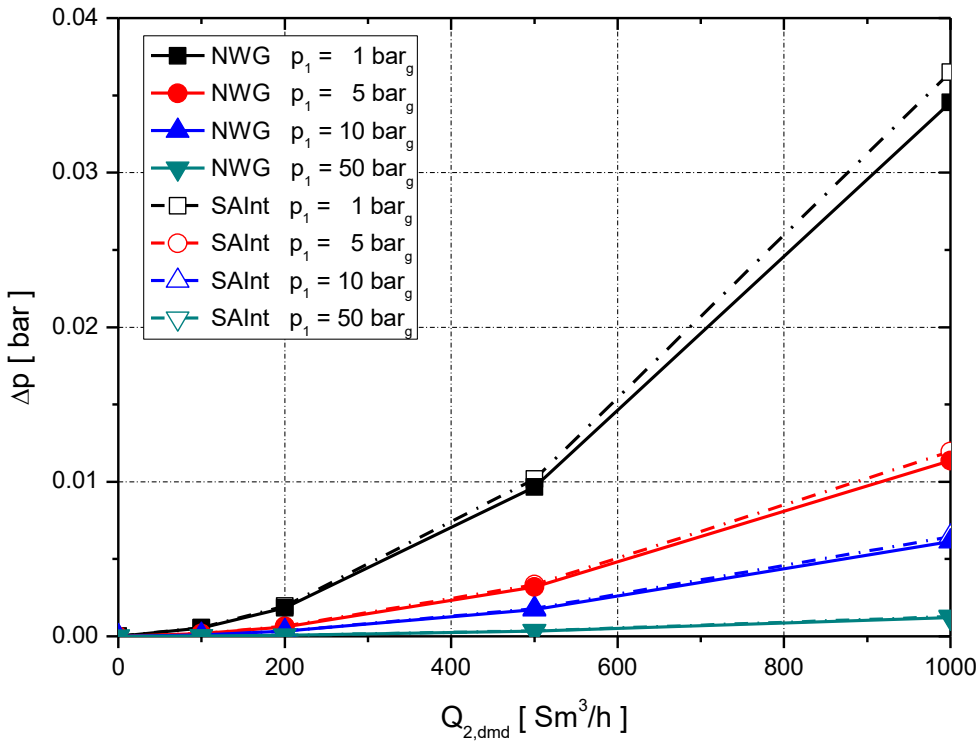

Figure 3.2: Pressure drop versus demand gas flow.

3.1.1.1 Effect of pipe parameters

Pressure losses across the pipe and consequently pressure at the demand node depend on the pressure of the gas at the source node, and the gas flow rate into the pipe. However, also pipe properties have a high effect on the pressure profile along the pipe.
Several diameters, lengths and inclinations of the pipe which connects demand and supply nodes are analysed to benchmark the gas network model with different geometries of the network (table 3.4).

Table 3.4: Values of pipe parameters used for the steady-state validation.

Parameter	Value			
$D\ [mm]$	100	200	300	
$L\ [m]$	100	1'000	10'000	50'000
$\theta\ [°]$	0.00	0.30	0.60	1.00

Under the same conditions ($p_1$and $\dot{Q}_{2,dmd}$), increasing the pipe diameter, the velocity of the gas flow decreases. Therefore, pressure losses across the pipe decrease too. Figure 3.3 shows pressure drops obtained for the cases simulated. Deviations between the two tools are marginal (about 5%) and comparable for the different pipe diameters analysed.

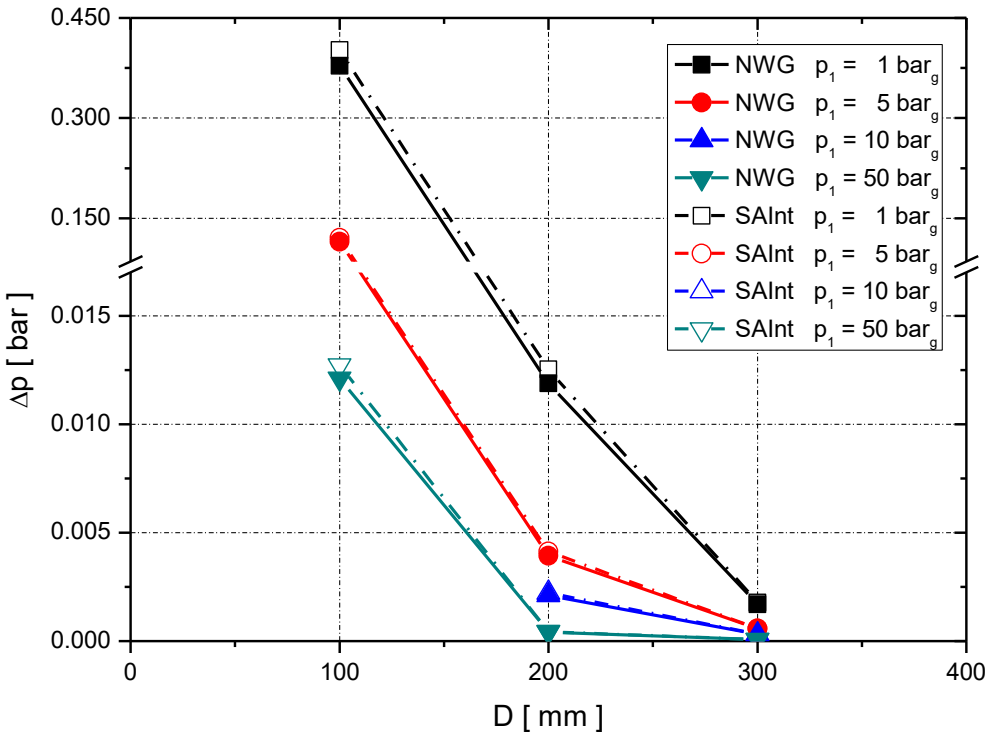

Figure 3.3: Pressure drop versus pipe diameter for L = 10'000 m.

Pressure drops across a pipe are proportional to the length of it. As shown in figure 3.2, friction losses are inversely related to the pressure of the gas. In this case, the deviations between the two models accumulate with the pipe length (figure 3.4). Maximum differences (6.5%) are evaluated for an inlet pressure of $1.00\ bar_g$ and a pipe of $50'000\ m$.

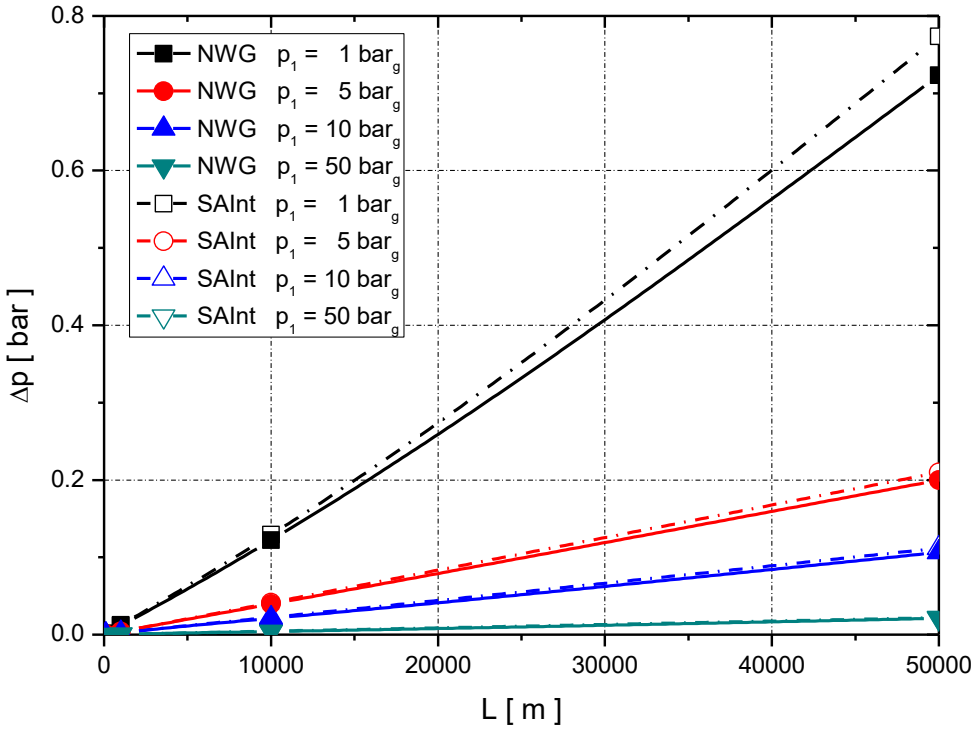

Figure 3.4: Pressure drop versus pipe length for D = 200 mm.

For a source pressure of $50.00\ bar_g$, pressure drop across the pipe increases with the inclination of the pipe (figure 3.5). However, decreasing the pressure of the source node, the density of the gas flow decreases. As a consequence, the gravity term, which is proportional to the gas density, decreases too. When the source pressure is low ($1.00 - 5.00\ bar_g$), the inclination of the pipe does not affect the pressure at the demand node because differences are lower than $1\ Pa$. Deviations between values evaluated by the SAInt software and the Gas Network Solver (NWG) are maximum (7%) for an inlet pressure of $50.00\ bar_g$ and an inclination of $1.00\ °$. Therefore, the comparison between the two tools shows that there are marginal differences in the evaluation of the gravity term.

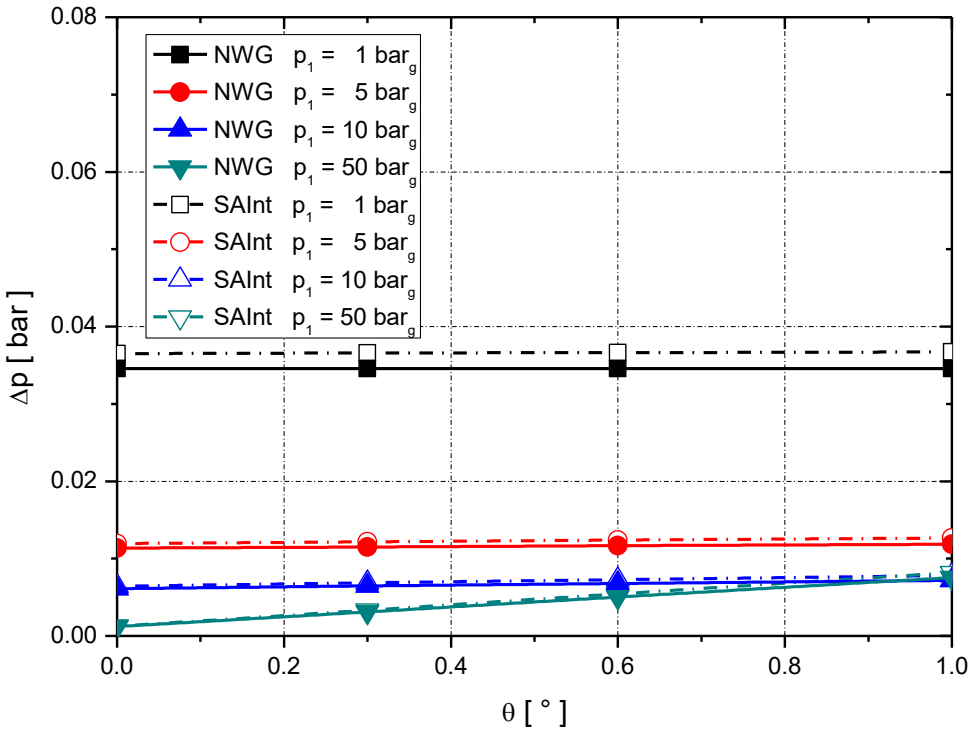

Figure 3.5: Pressure drop versus pipe inclination for D = 100 mm and L = 100 m.

3.1.1.2 Effect of gas composition

Fluid dynamics properties of a gas flow, which has a high impact on the network behaviour, depends on the composition of it. Therefore, it is essential to benchmark the model proposed with different gas qualities. The standard natural gas mixture [3.7] and pure hydrogen gas (table 3.5) are also analysed to evaluate the effects of gas composition on pressure losses and accuracy and adequacy of the tool developed.

Table 3.5: Gas compositions used for the steady-state validation.

	y_k [%]									
Source	CH_4	C_2H_6	C_3H_8	C_4H_{10}	C_5H_{12}	C_6H_{14}	CO_2	N_2	He	H_2
CH_4	100	-	-	-	-	-	-	-	-	-
Standard NG	97.201	1.862	0.393	-	-	-	-	0.544	-	-
H_2	-	-	-	-	-	-	-	-	-	100

Figure 3.6 shows pressure differences between supply and demand nodes for the different gas compositions and inlet pressures simulated. The standard natural gas is a mixture composed by a

large part of methane (about 97%) and a smaller fraction (about 3%) of other hydrocarbons (C_2H_6, C_3H_8) and contaminant (N_2). Therefore, pressure losses difference between a source of pure methane and a source of standard natural gas are marginal (2.5%).
As shown in chapter 2, the hydrogen is a fuel gas with low specific gravity. For the same standard volumetric gas flow demand, the velocity of the gas flow is about the same. However, pressure drops are considerably lower due to the smaller density of the hydrogen. Comparison between the NWG tool and the SAInt software shows that relative deviations are acceptable for the three gas compositions analysed. Maximum differences (11%) are evaluated in the case of a gas source of pure hydrogen. The SAInt software uses a specific correlation for the natural gas to evaluate the viscosity of the flow. Therefore, in this case, the viscosity of pure hydrogen gas is not evaluated correctly.

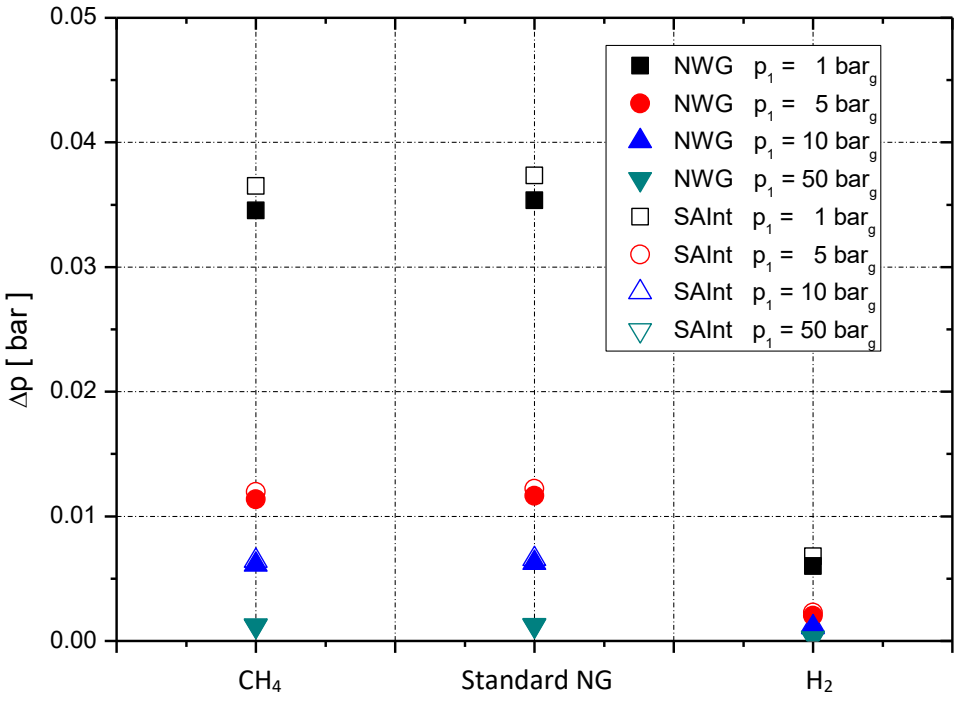

Figure 3.6: Pressure drop versus gas composition for D = 100 mm and L = 100 m.

3.1.2 Dynamic validation

Gas flow withdrawn at demand nodes is not usually constant in time, but it depends on the energy/flow requested by devices of users connected to these nodes. Therefore, the dynamic validation of the tool developed is essential to evaluate the accuracy and adequacy of gas network simulations. Table 3.6 shows the boundary conditions set for dynamic simulations of the test case 1. Two different pressures of the source (5.00 and 10.00 bar_g), in the typical pressure range of city gate stations, are simulated. A horizontal pipe with a diameter of 200 mm, length of $10'000$ m and roughness of 0.010 mm connects supply and demand nodes (table 3.7).

Table 3.6: Boundary conditions imposed for the dynamic validation.

Boundary Condition	Value	
y_{CH4} [%]	100.00	
p_1 [bar_g]	5.00	10.00
T_1 [°C]	15.00	
$\dot{Q}_{2,dmd,nom}$ [Sm^3/h]	1'000	

Table 3.7: Pipe parameters imposed for the dynamic validation.

Parameter	D [mm]	L [m]	θ [°]	ε [mm]
Value	200	10'000	0.00	0.010

Two scenarios with different standard volumetric gas flow demand during the day (figure 3.7 and 3.8) are analysed. The first one imposes a gas flow profile which is characteristic of industrial users. Gas demand by industrial users is typically constant and maximum during the day when factories work at full load. Instead, a gas flow trend requested by residential users is set at the demand node in the second scenario. Generally, for residential customers, there are three peaks of demand (morning, lunchtime and evening) when all people use gas for cooking and heating their homes. In the other hours of the day, the natural gas is used, not simultaneously, by only some users. Therefore, the gas demand is smaller than the nominal demand.

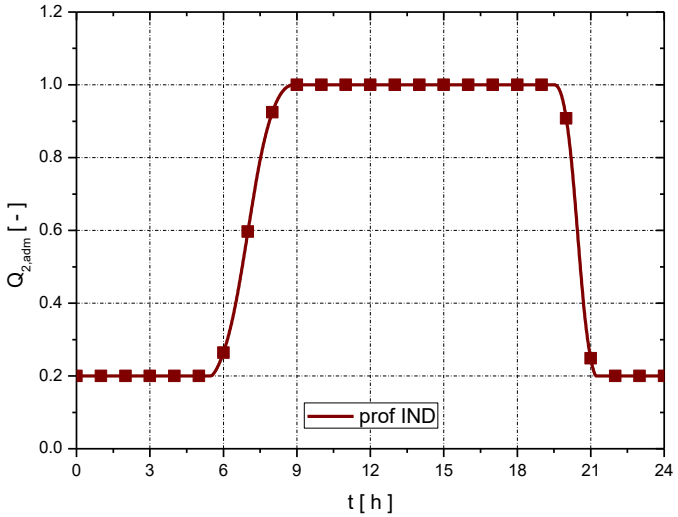

Figure 3.7: Industrial gas flow demand profile.

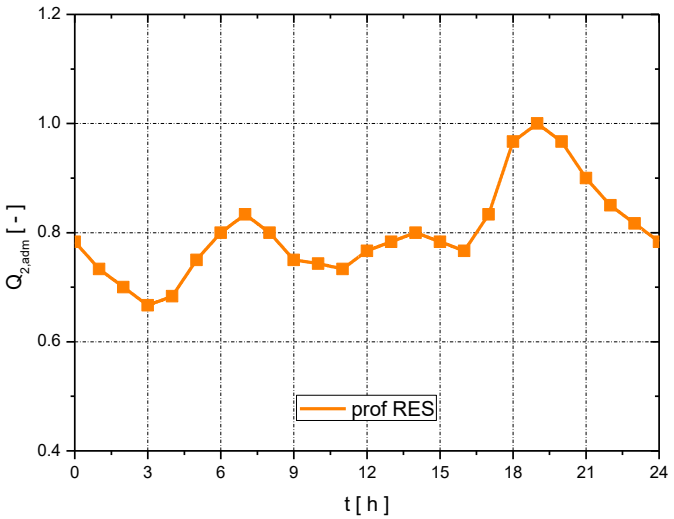

Figure 3.8: Residential gas flow demand profile.

Figure 3.9 shows the pressure difference between source node and demand node as a function of the hours of the day, in the case of industrial users. During the periods of increment/reduction of demand, values calculated by the Gas Network Solver are in good agreement with results of the SAInt software. However, due to the marginal difference of steady-state models, relative deviations of 4.7% are evaluated during maximum and minimum gas flow demand. As previously shown in section 3.1.1, differences decrease if the pressure of the gas is high ($10.00\ bar_g$).

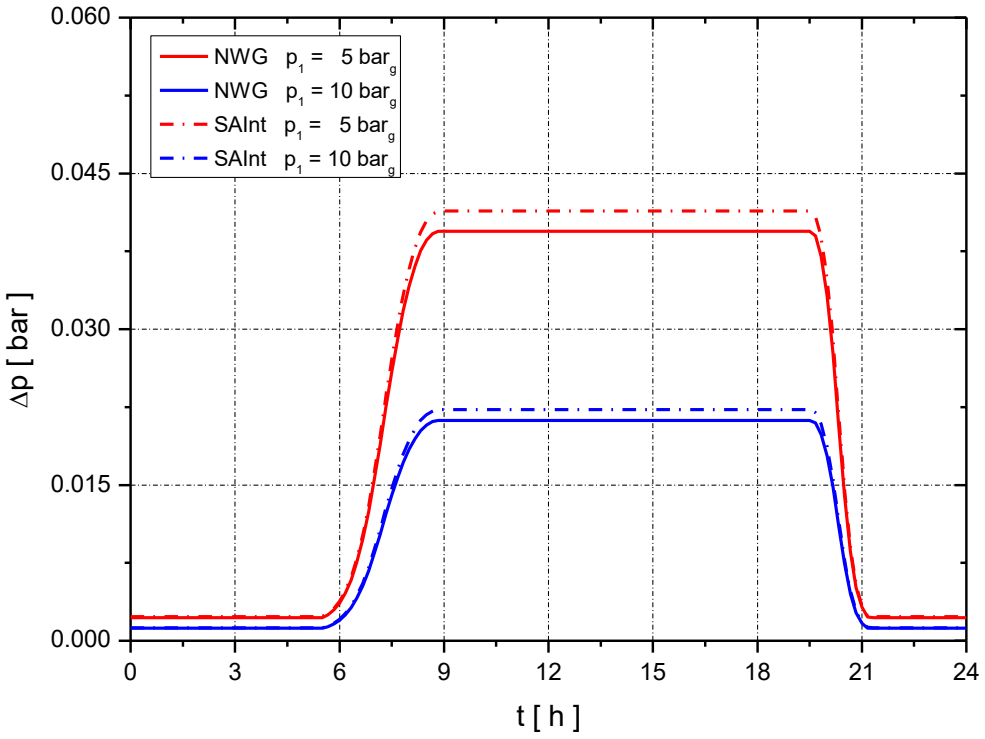

Figure 3.9: Pressure drop versus time for the industrial gas flow demand.

Due to the large variability of the residential gas demand, the steady-state regime is not achieved during the day (figure 3.10). Evolutions of pressure drops are predicted correctly in time. However, values evaluated by the NWG model are lower (4.5%) than the reference data (SAInt). The different initial pressure drop ($t = 0\ h$) is kept for all subsequent time steps of the simulations. Even then, deviations of pressure losses values are lower in the case of an inlet gas pressure of $10.00\ bar_g$.

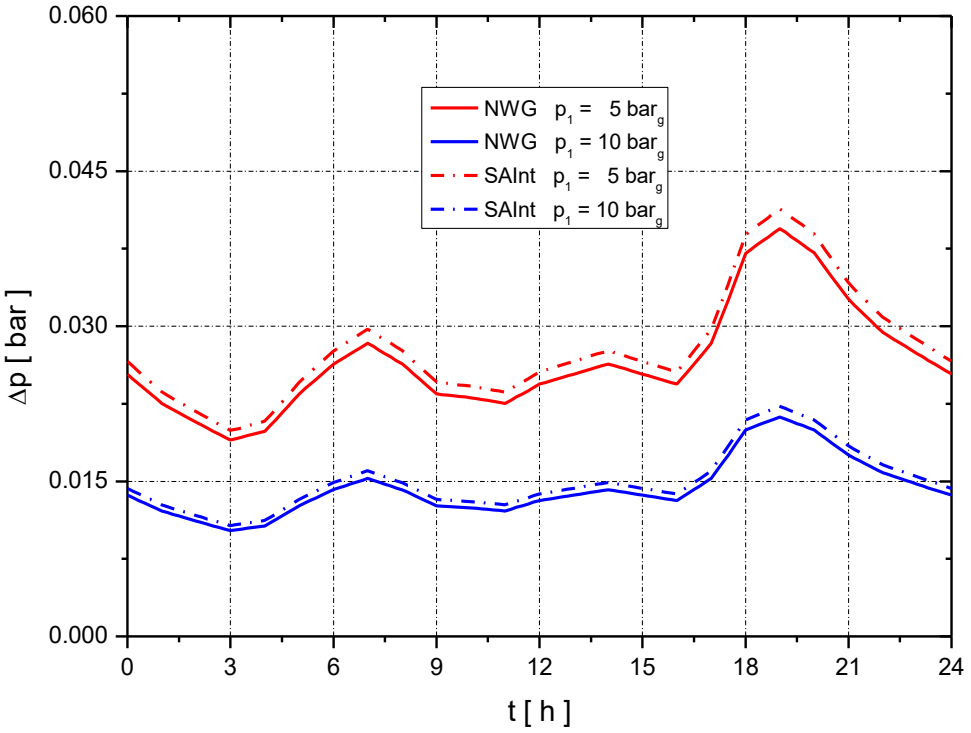

Figure 3.10: Pressure drop versus time for the residential gas flow demand.

3.2 Test case 2 - Looped distribution network

A looped medium-pressure distribution network is studied as a second test case (figure 3.11). The gas is supplied by a city gate station (N1) located at an altitude of $100\ m$. Six pipes of different lengths and diameters distribute the gas to residential and industrial users connected to the grid (N2, N3). Demand nodes are respectively located at an altitude of $70\ m$ and $115\ m$. Due to the different elevation of the nodes and junctions of the network, pipes have inclinations between $-2.29\ °$ and $+0.40\ °$. Tables 3.8 and 3.9 show, detailed characteristics and geometry of the distribution network analysed.

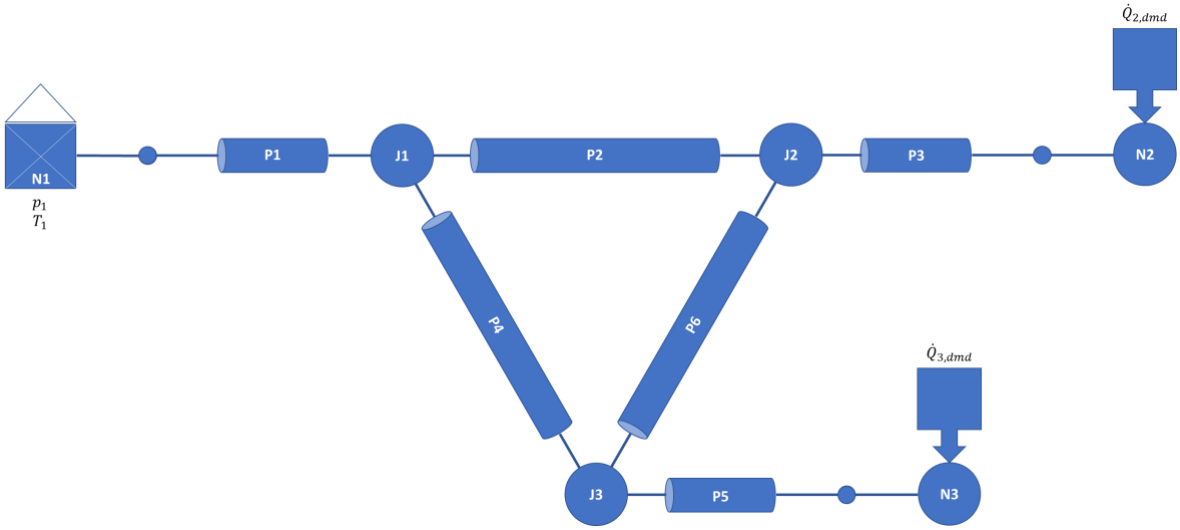

Figure 3.11: Looped distribution network schema.

Table 3.8: Characteristics of the nodes of the Looped distribution network.

Node	N1	J1	J2	J3	N2	N3
$H\ [m]$	100	80	70	115	70	115
N° Inlet Port	0	1	2	1	1	1
N° Outlet Port	1	2	1	2	0	0

Table 3.9: Characteristics of the pipes of the Looped distribution network.

Pipe	P1	P2	P3	P4	P5	P6
Inlet Node	N1	J1	J2	J1	J3	J3
Outlet Node	J1	J2	N2	J3	N3	J2
$D\ [mm]$	250	180	150	180	150	180
$L\ [m]$	500	5’000	300	5’000	300	5’000
$\varepsilon[mm]$	0.012	0.012	0.012	0.012	0.012	0.012

The standard natural gas, which characteristics are shown in table 3.10, is used as the quality of the source. Table 3.11 shows the boundary conditions imposed for the simulation of the network. The city gate station supplies gas at a pressure of $5.00\ bar_g$ and a temperature of $15\ °C$. Gas flows of $2'500\ Sm^3/h$ with a residential profile and $800\ Sm^3/h$ with an industrial profile are withdrawn at demand nodes.

Table 3.10: Properties of the gas used for the looped network validation.

Source	$M\ [kg/kmol]$	$SG\ [-]$	$HHV_g\ [MJ/Sm^3]$	$WI\ [MJ/Sm^3]$
Standard NG	16.4790	0.5690	38.28	50.74

Table 3.11: Boundary condition for the looped network validation.

Boundary Condition	Value	Profile
$p_1\ [bar_g]$	5.00	-
$T_1\ [°C]$	15.00	-
$\dot{Q}_{2,dmd,nom}\ [Sm^3/h]$	2500.00	RES
$\dot{Q}_{3,dmd,nom}\ [Sm^3/h]$	800.00	IND

The looped medium-pressure distribution network is firstly, simulated and validated in steady-state conditions with the gas flow demand at the time $t = 0\ h$. Secondly, the steady-state values are used as the initial condition to simulate and validate the dynamic scenario that performs the network behaviour during the day.

3.2.1 Steady-state validation

The validation of the test case 3, in steady-state conditions, is done by simulating the network with gas demands at the first hour of the day ($t = 0\ h$), when residential and industrial gas flow demand are respectively the 78.33% ($1'958.25\ Sm^3/h$) and 20% ($160\ Sm^3/h$) of the nominal value.

Figure 3.12 shows pressure at nodes and junctions of the network. Due to the negative inclinations of pipes P1, P2 and P6 pressure losses across them are partially compensated by the gravity effect. For pipe P1, which has a standard volumetric gas flow of $2'118.25\ Sm^3/h$, a length of $500\ m$ and a negative inclination, the outlet pressure ($5.003\ bar_g$) is higher than the inlet pressure ($5.00\ bar_g$). Deviations evaluated (up to 10%) are a consequence of the different model used for the calculation of the ambient conditions. In SAInt, a correlation that estimates the ambient pressure as a function of the altitude is not implemented. The software uses a constant value previously set. However,

NWG pressure values corrected using a constant ambient pressure of $100'056\ Pa$, agree with data of SAInt.

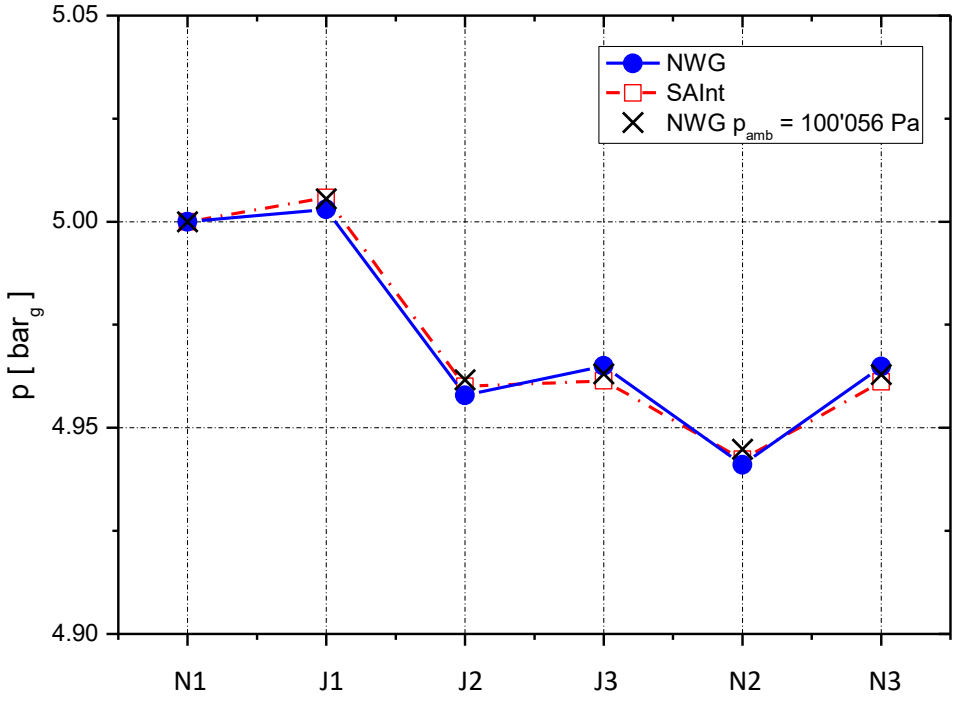

Figure 3.12: Pressure at nodes of the network.

3.2.2 Dynamic validation

The steady-state simulation previously done at $t = 0$ is set as the initial condition for the analysis of the dynamic behaviour and pressures of the network. After that, the dynamic scenario is created setting as boundary conditions residential and industrial gas demand profiles.
Figure 3.13 shows pressure evolution at demand nodes during the day. Minimum pressure values of $4.881\ bar_g$ and $4.910\ bar_g$ are achieved for demand nodes at about the 19 h when gas demand by residential users is maximum. For node N3 pressure values calculated by NWG are about 4.5% lower than SAInt data during all day. Instead, deviations of node N2 are between –1% and + 5%. However, as shown in section 3.1.2, pressures evolution in the time are predicted correctly by the Gas Network Solver.

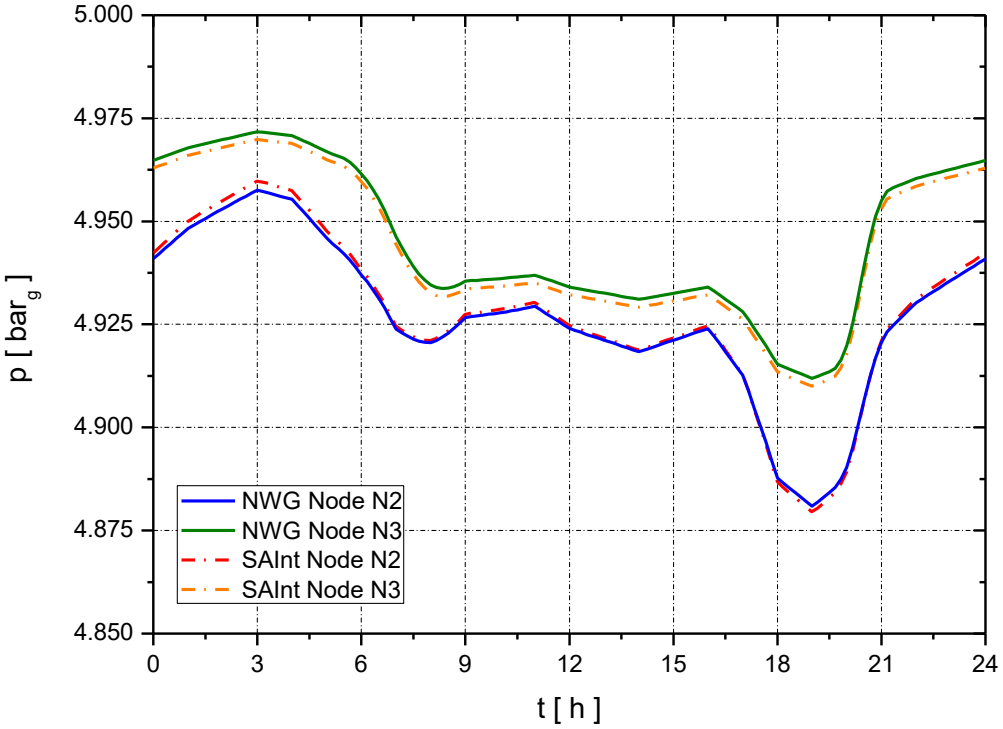

Figure 3.13: Pressures at demand nodes versus time.

3.3 Test case 3 - Triangular high-pressure network

The test case 3 is the triangular high-pressure network (figure 3.14) analysed in previous literature works. In this case, the Gas Network Solver is validated using data of the published articles [3.3, 3.4, 3.5, 3.6].

The network is composed of one source and two demand nodes which are located at the same altitude and connected by three pipes with the same diameter and different length. Table 3.12 resumes geometrical data and layout used to model the network.

The gas, which is injected at a temperature of $5\ °C$ and a pressure of $50.00\ bar_g$, is considered in isothermal condition. The gas is withdrawn at node 2 and 3 with the trends shown in figure 3.15. Node 3, which is the furthest from the source, reaches a maximum of $180\ kSm^3/h$ and a minimum of $108\ kSm^3/h$ during the day. Values of node 2 are $72\ kSm^3/h$ less for each hour in comparison with node 3. Boundary conditions of table 3.13 are imposed to create a dynamic scenario of the network.

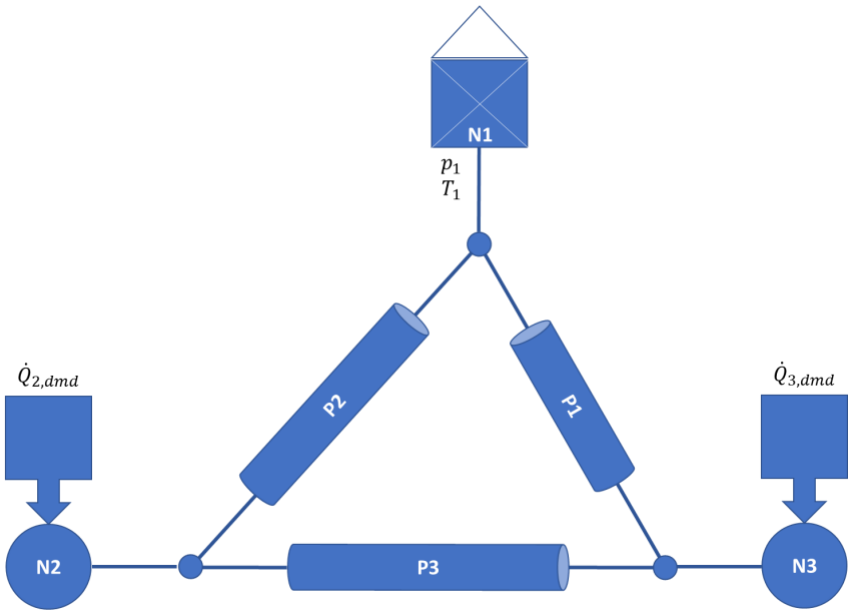

Figure 3.14: Triangular high-pressure network schema.

Table 3.12: Characteristics of pipes of the triangular high-pressure network.

Pipe	P1	P2	P3
Inlet Node	N1	N1	N2
Outlet Node	N3	N2	N3
$D\ [mm]$	600	600	600
$L\ [m]$	80’000	90’000	100’000

Table 3.13: Boundary condition for the triangular network validation.

Boundary Condition	Value	Profile
$p_1\ [bar_g]$	50.00	-
$T_1\ [°C]$	5.00	-
$\dot{Q}_{2,dmd,max}\ [Sm^3/h]$	180’000	N2
$\dot{Q}_{3,dmd,max}\ [Sm^3/h]$	108’000	N3

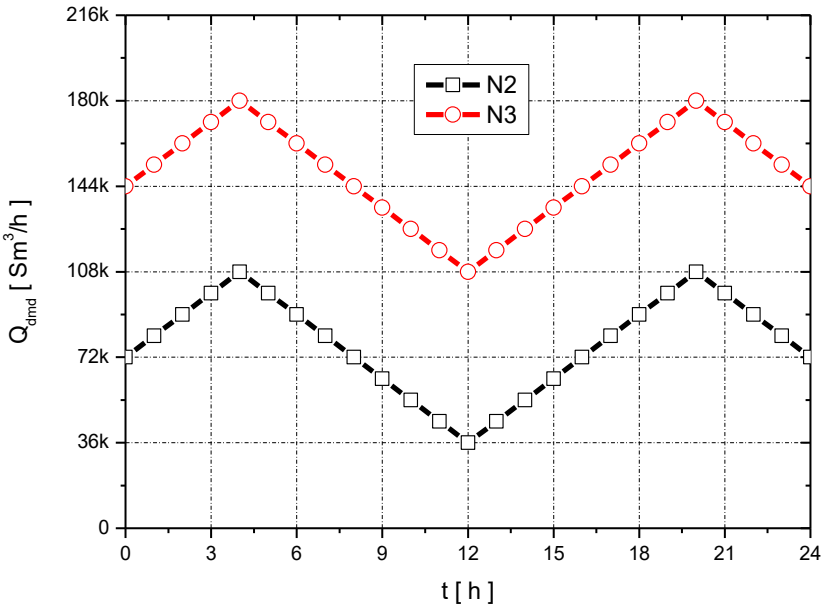

Figure 3.15: Volumetric gas flow demand during the day.

Several cases are simulated due to the different surface roughness value used in the previous works. Osiadacz [3.4] and Ke & Ti [3.5] consider a constant friction factor of 0.003. Otherwise, Taherinejad [3.3] uses a pipe surface roughness of $0.015\ mm$. The proprieties of the gas used in the simulations are shown in table 3.14.

Table 3.14: Gas composition used for the triangular high-pressure network validation.

Source	$M\ [kg/kmol]$	$SG\ [-]$	$HHV_g\ [MJ/Sm^3]$	$WI\ [MJ/Sm^3]$
NG [3.6]	17.1535	0.5850	38.85	50.80

Figures 3.16 and 3.17 show the pressures at node 2 and 3 as function of the time for different values of friction factor ($0.030 \div 0.012$) used. Results of simulation show a good agreement of values evaluated with data of Elaoud [3.6] when a friction factor of 0.010 is assumed. Otherwise, the correct value of the pipe surface roughness is $0.01\ mm$ if the Colebrook–White equation is turned on to calculate the value of λ. Therefore, the Gas Network Solver predicts, correctly, time and value of pressure peaks at demand nodes.

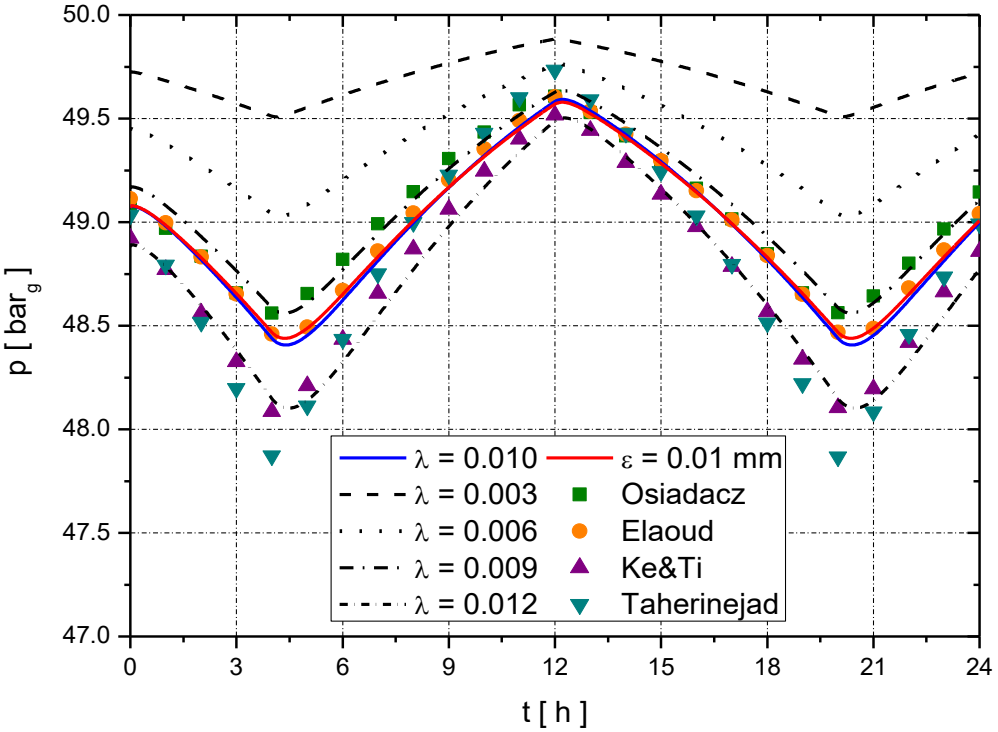

Figure 3.16: Predicted relative pressure versus time at node 2.

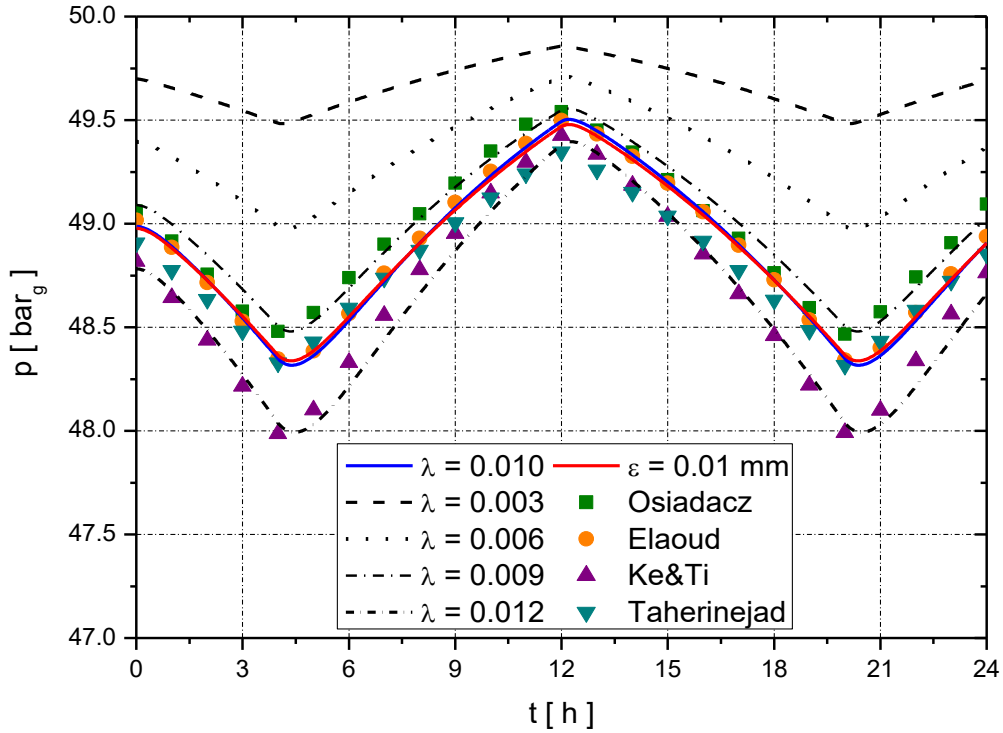

Figure 3.17: Predicted relative pressure versus time at node 3.

Bibliography

[3.1] K. A. Pambour, B. Cakir Erdener, R. Bolado-Lavin, and G. P. Dijkema, "SAInt - A novel quasi-dynamic Model for assessing Security of Supply in coupled Gas and Electricity Transmission Networks", Applied Energy 203 (2017) 829–857.

[3.2] K. A. Pambour, R. Bolado-Lavin, G. P. Dijkema, "An integrated transient model for simulating the operation of natural gas transport systems", Journal of Natural Gas Science and Engineering 28 (2016) 672–690.

[3.3] M. Taherinejad, S. M. Hosseinalipour, R Madoliat, "Dynamic simulation of gas pipeline networks with electrical analogy", J Braz. Soc. Mech. Sci. Eng. 39 (2017) 4431–4441.

[3.4] A. J. Osiadacz, "Simulation of transient gas flows in networks", Int. J. Numer. Methods Fluids 4.1 (1984) 13–24.

[3.5] S.L. Ke, H.C. Ti, "Transient analysis of isothermal gas flow in pipeline network", Journal of Natural Gas Science and Engineering 9 (2000) 51–59.

[3.6] S. Elaoud, Z. Hafsi, L. Hadj-Taieb, "Numerical modelling of hydrogen-natural gas mixtures flows in looped networks", Journal of Petroleum Science and Engineering 159 (2017) 532–541.

[3.7] ARERA, the Italian Regulatory Authority for Energy, Networks and Environment, https://www.arera.it.

Chapter 4

Case Study

In this chapter, the Gas Network Solver is applied to analyse a case study on a gas distribution network located in a hilly area of central Italy. Two city gate stations supply the natural gas to the network. Medium-pressure pipes transport gas from the source area to the small industrialises and the urban zones. Several final reduction stations are installed in specific points of the urban areas to reduce the pressure and supply the gas to low-pressure pipes, which are responsible for distributing the natural gas to residential customers. Firstly, the network is simulated in steady-state and dynamic conditions to evaluate pressures at demand nodes, velocity in pipes and gas flow rate processed by the two city gate stations and reducing stations. Secondly, an additional source of hydrogen is added to analyse the impact of the injection of alternative zero-carbon fuels on the network's thermodynamic parameters and quality of gas delivered to customers. Several steady-state simulations are done to study different locations and amount of hydrogen injected by the alternative source. The medium-pressure network is simulated during the hours of the day to analyse the effects of variable gas demand on the pipe velocities, gas quality and pressure of demand nodes.

4.1 Distribution network

The gas distribution network analysed is a real medium/low-pressure network located in a hilly area of Tuscany (figure 4.1). Small industries are located along main suburban roads which connect the small and medium villages in a total area of interest is about $50\ km^2$. The network (figure 4.2) supplies gas to industrial users connected to the medium-pressure pipes and residential users connected to the pipes of different low-pressure subnetworks located in the urban areas.

Figure 4.1: Geographical map of the area of interest of the distribution network.

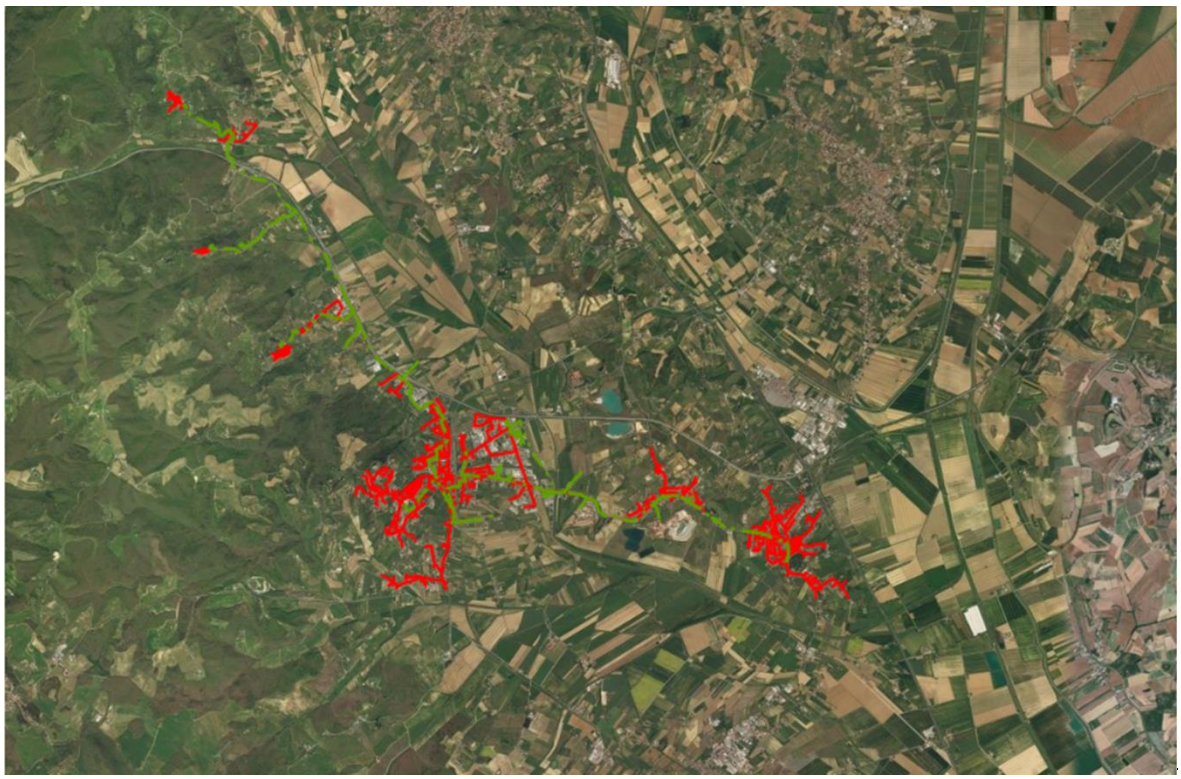

Figure 4.2: Distribution network map.

Figure 4.3 shows the detailed schema of the gas distribution network. The natural gas is injected at a relative pressure of $4\ bar_g$ and a temperature of $15\ °C$ into the network by two city gate stations (CGS) situated in suburban areas near the largest village. Reducing stations (RS), located in urban areas, connect the medium-pressure network (MP) with the several low-pressure subnetworks (LP). The pressure of the gas arriving in these stations is reduced to $20 \div 27.5\ bar_g$ to manage efficiently the operation of gas distribution to residential users. In nominal conditions, a total amount of natural gas of $1527.53\ Sm^3/h$, which corresponds to about $16.24\ MW$ of energy, is requested by the 949 industrial and residential users connected along the $78.65\ km$ of the network. The main characteristics of the distribution network analysed are summarized in table 4.1.

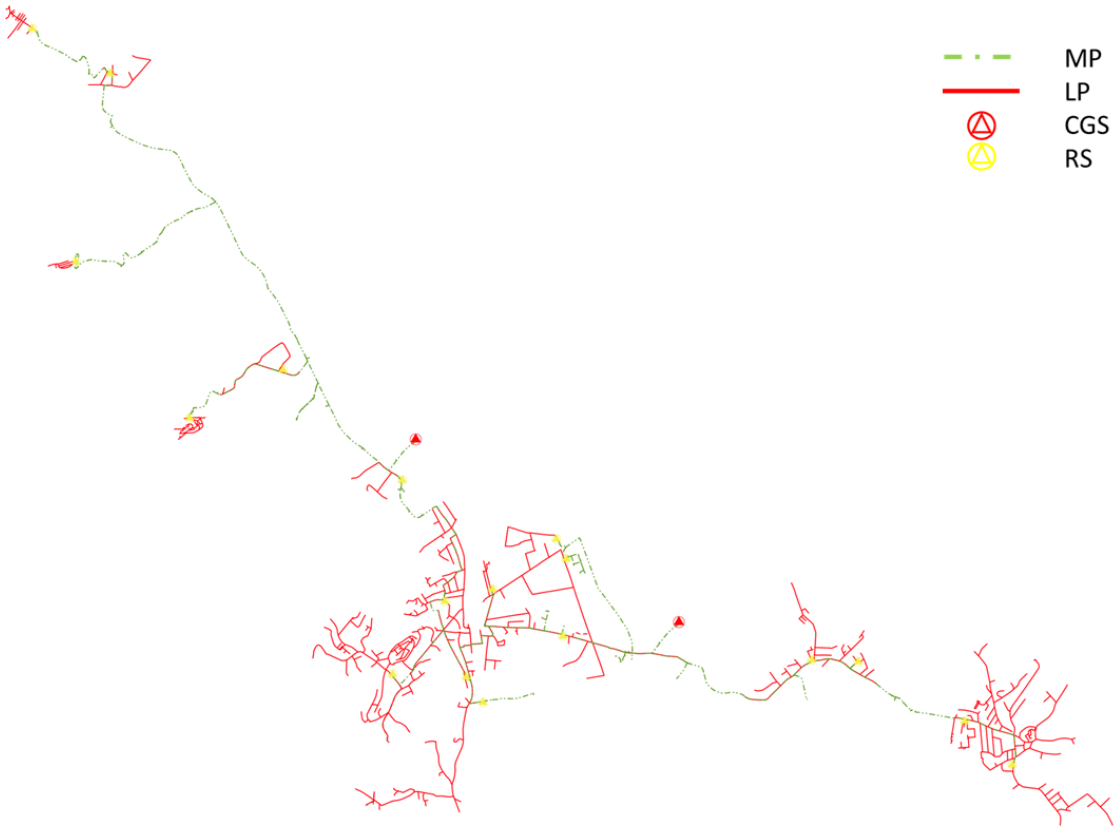

Figure 4.3: Distribution network schema.

Table 4.2 shows the elements that compose the full network. There are necessary 1089 medium/low-pressure pipes, 65 valves and 166 junctions to connect the 2 city gate stations with the 18 reducing stations and the 949 demand nodes. A total number of 2289 linear and point elements are used to model the gas distribution network studied.

The medium-pressure network is responsible to transport the gas from the two city gate stations to small industrial users located in suburban areas and reducing stations situated in the proximity of the villages (figure 4.4). This network has a branched-structure: sources supply the gas to a main "line" which crosses the area of interest from north-west to south-east; additional branches, connected to the main "line", transport the gas in zones where MP customers are located. Industrial

users are attributed to the upstream and downstream nodes connected to intermediate pipes. Conversely, reducing stations are connected at the ends of the MP network's branches.

Table 4.1: Characteristics of the distribution network.

Parameter	Value
$p_{CGS}\ [bar_g]$	4.00
$T_{CGS}\ [°C]$	15.00
$p_{RS}\ [mbar_g]$	20.0 ÷ 27.5
$\dot{Q}_{tot,nom,dmd}\ [Sm^3/h]$	1527.53
$L_{tot}\ [km]$	78.65

Table 4.2: Elements of the distribution network.

Total	CGS	JUNC	NODE	VALV	RS	PIPE
2289	2	166	949	65	18	1089

The gas flowing in medium-pressure pipes is characterized by pressure between 4 and $3.5\ bar_g$ and a medium density of about $3.44\ kg/m^3$. In nominal conditions, industrial users connected along the $24.30\ km$ of this network withdraw $304.80\ Sm^3/h$ of natural gas. The remain gas flow ($1222.73\ Sm^3/h$) is delivered to the 18 reducing stations. Table 4.3 summarizes the main characteristics of the medium-pressure network studied.

Table 4.3: Characteristics of the medium-distribution network.

Parameter	Value
$p_{CGS}\ [bar_g]$	4.00
$T_{CGS}\ [°C]$	15.00
$\dot{Q}_{ind,nom,dmd}\ [Sm^3/h]$	304.80
$\dot{Q}_{res,nom,dmd}\ [Sm^3/h]$	1222.73
$L_{MP}\ [km]$	24.30

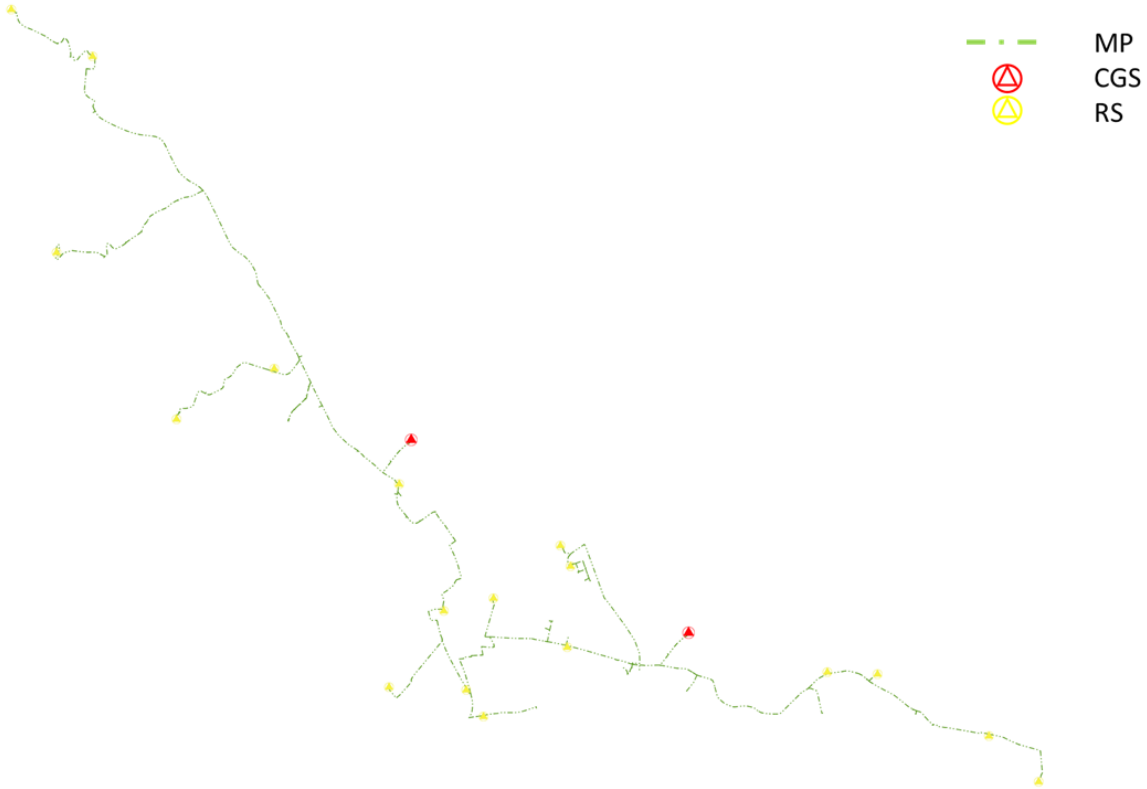

Figure 4.4: Medium-pressure distribution network schema.

Due to the branch structure, medium-pressure networks are composed of a low number of elements. In particular, the MP network analysed has a total number of elements of 762, divided as shown in table 4.4. Many valves (61) of the total 65 are installed in the medium-pressure network to intercept/manage the direction of the flow and isolate specific areas in contingency conditions. There are necessary 311 pipes and 140 junctions to transport the gas from the city gate stations (2) to the industrial demand nodes (230) and the reducing stations (18) located in the area of interest.

Table 4.4: Elements of the medium-pressure distribution network.

Total	CGS	JUNC	NODE	VALV	RS	PIPE
762	2	140	230	61	18	311

Figure 4.5 shows the diameter values of the 311 medium-pressure pipes. Minimum and maximum values are respectively $27.9\ mm$ and $211.1\ mm$. The main "line", which transports the largest amount of gas flow, is composed of pipes with the biggest diameters ($160 \div 211.1\ mm$). Moving away from the sources to the final nodes, the gas flowing into pipes decreases due to the intermediate withdrawals. Consequently, diameters of primary, secondary and final branches are

smaller. Most of the pipes have a diameter between 80 and 120 mm. In particular, 72 pipes with a diameter of 82.5 mm and 95 pipes with a diameter of 107.1 mm.

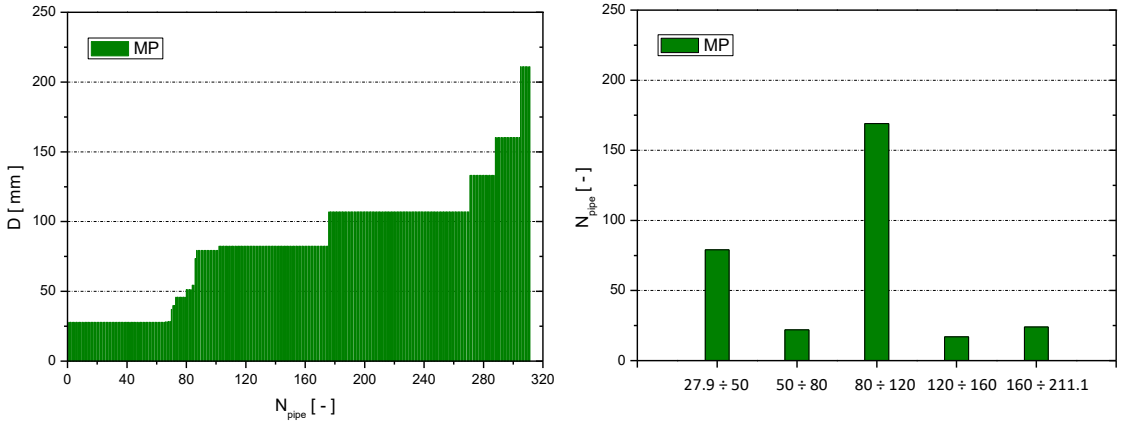

Figure 4.5: Diameter of medium-pressure pipes.

Due to the hilly territory where the distribution network studied is situated, sources and MP nodes of the network are located at different altitudes, as shown in figure 4.6. The gas is injected into the network at two city gate stations, which are respectively at 264.4 and 276.08 meters above sea level. Conversely, demand nodes are at different altitudes between 256.33 and 393.59 m. Therefore, the gas flowing into the network must overcome pressure drops due to friction losses and even in some cases positive elevation gain of hundreds of meters. However, most of the demand nodes have an altitude close to the city gate stations values ($250 \div 280\ m$).

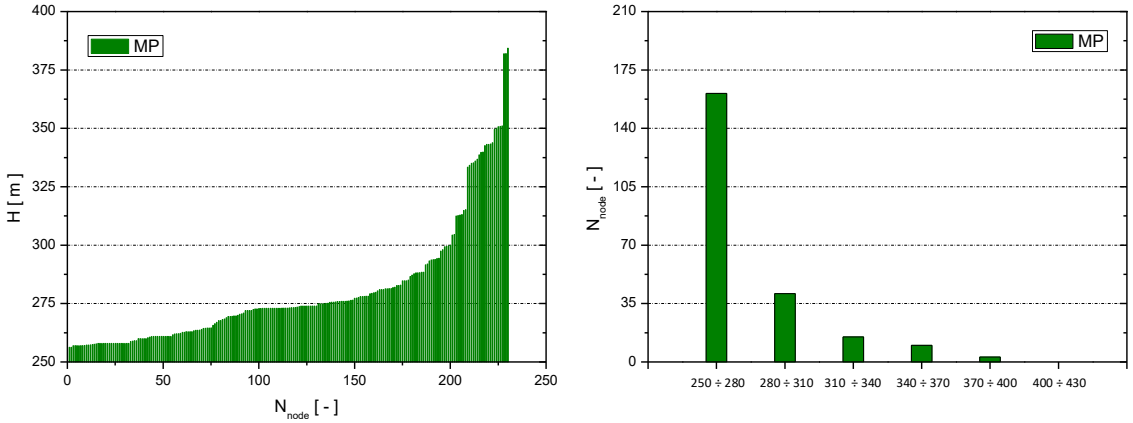

Figure 4.6: Altitude of medium-pressure junctions and demand nodes.

Low-pressure subnetworks of the distribution network analysed are shown in figure 4.7. These networks are responsible for distributing gas to residential users connected to them. The gas, arriving from the reducing stations, is uniformly distributed in urban areas by looped pipes. This type of structure is requested due to the complexity and constraints of cities and villages. Looped pipes need to provide the desired pressure at demand nodes, improve the reliability of the subnetwork and increase the possibility of maintenance operations. The present distribution

network has 11 low-pressure subnetworks located in the small, medium and large villages of the area of interest.
Two of them (SCS00055 and CBS0011) deliver the gas to the largest village situated in the middle of the area of interest. Subnetworks SCS00059 and SCS00060 distribute the gas into two medium villages located in the south-east of the map. The remaining subnetworks provide the gas to customers in smaller urban zones.

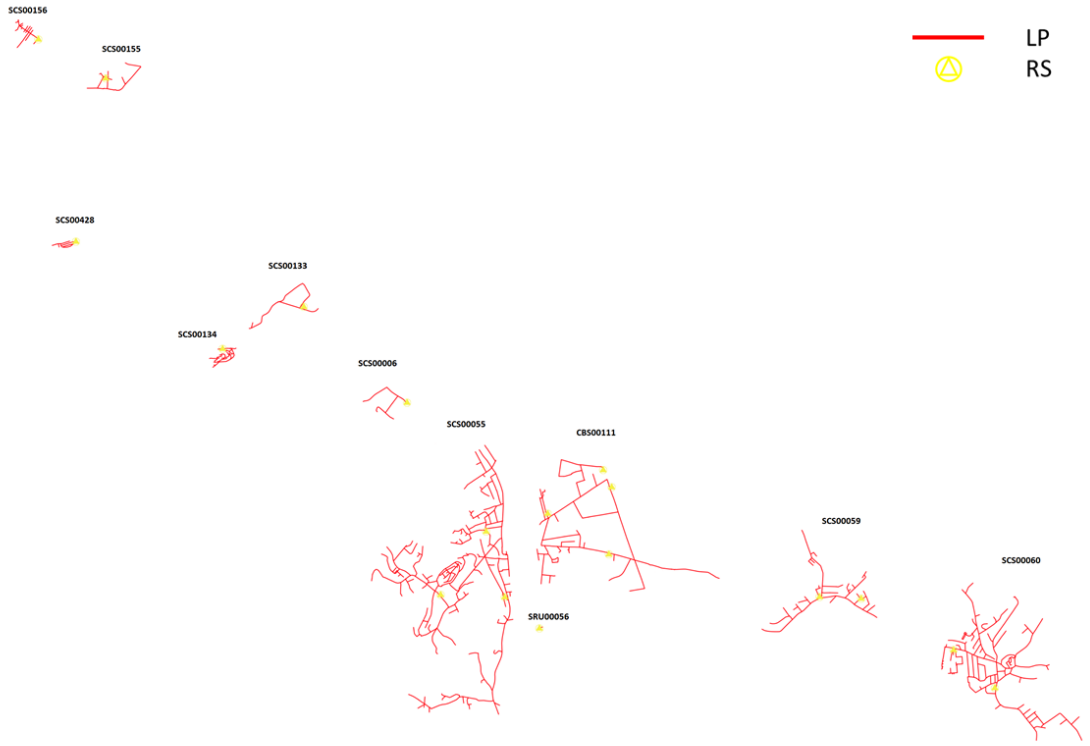

Figure 4.7: Low-pressure distribution network schema.

The main characteristics of the low-pressure subnetworks are shown in table 4.5. Reducing stations inject 1222.73 Sm^3/h of natural gas into LP subgrids at a pressure between 20 and 27.5 $mbar_g$. Different supply pressures are set due to the different altitude of the RS, pipe characteristics and gas flow demand by the specific subnetwork.

Table 4.5: Characteristics of the medium-distribution network.

Parameter	Value
p_{RS} $[bar_g]$	20.0 ÷ 27.5
$\dot{Q}_{res,nom,dmd}$ $[Sm^3/h]$	1222.73
$L_{LP,total}$ $[km]$	54.35

Table 4.6 shows the elements of the low-pressure subnetworks. Due to the complex structure, these subnetworks are composed of a large number of elements. In particular, the 11 LP subnetwork studied has a total number of elements of 1545. Point elements (26 junctions, 719 demand nodes and 18 reducing stations) of the subnetworks are connected by 778 pipes.

Table 4.6: Elements of the 11 low-pressure distribution subnetworks.

Total	CGS	JUNC	NODE	VALV	RS	PIPE
1545	0	26	719	4	18	778

Diameters of 778 LP pipes of the network are shown in figure 4.8. Values are between 27.9 and 211.1 mm, as previously shown for the MP pipes. As a consequence of a large number of parallel pipes and the subnetworks structure, the amount of gas flowing into each low-pressure pipe is lower respect to medium-pressure pipes. However, due to the lower density of the gas (0.69 kg/m^3), pipes with medium diameters are necessary to maintain gas velocities lower than the maximum allowed values [4.1]. Nearly 90% of the pipes have a diameter greater than 80 mm. The diameters lower than 80 mm are used only for final branches, which provide the gas to final demand nodes.

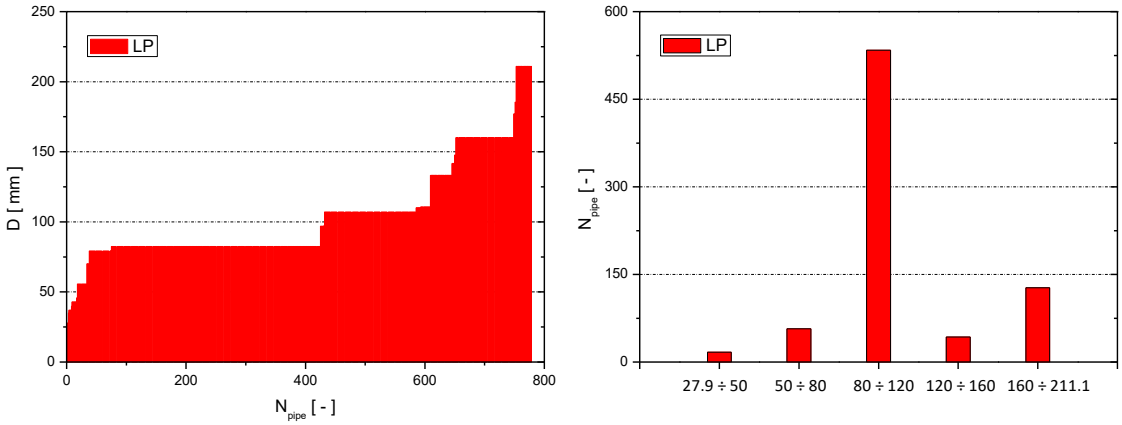

Figure 4.8: Diameter of low-pressure pipes.

As mentioned above, for medium-pressure demand nodes, users connected to low-pressure pipes are located at different altitudes (figure 4.9). 4 of the 18 reducing stations are situated at an altitude between 342.64 and 393.59 m. The remain RS have an altitude lower than 288.51 m. There are 10 demand nodes at an altitude greater than 400 meters above the sea level. In this case, due to the low gas pressure (27 ÷ 19 $mbar_g$), the gas density is lower than the density of the ambient air. Therefore, in a low-pressure subnetwork, a positive elevation gain produces an increase of the relative pressure. However, about the 73% of the demand nodes have an altitude lower than 310 m.

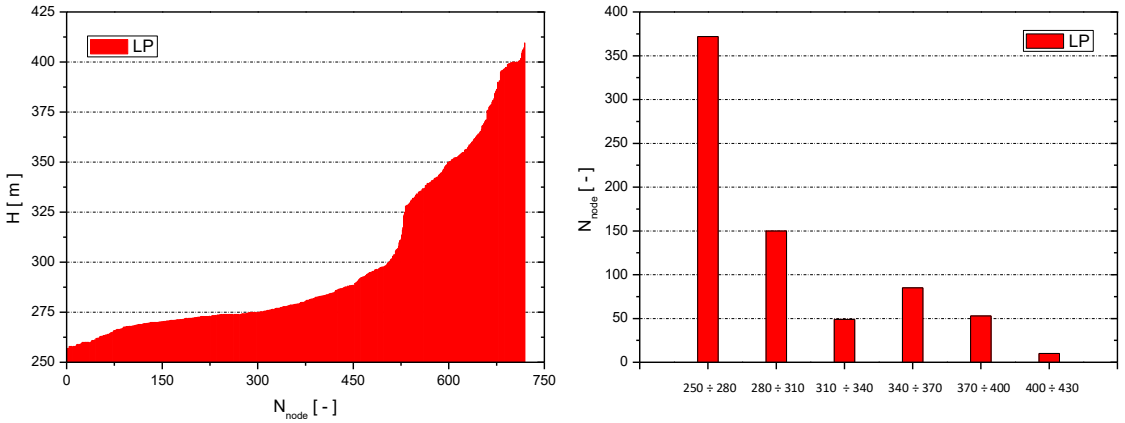

Figure 4.9: Altitude of low-pressure junctions and demand nodes.

Figures 4.10 and 4.11 show the characteristics of each low-pressure subnetwork. CBS0011, SCS00055, SCS00006 and SCS00059 are the 4 subnetworks with the greatest number of elements and gas demand by users connected to them. The subnetwork CBS0011 has 4 reducing stations even if it is not the one with the greatest gas flow supply. Therefore, it is the network with the highest level of customer safeguard. Conversely, SCS00055, SCS00006 and SCS00059 subnetworks have 2 or 3 reducing stations and a lower level of safeguard due to the higher number of users per RS. The remaining 7 subnetworks have only 1 reducing station, a nominal gas demand lower than 50 Sm^3/h and less than 100 elements.

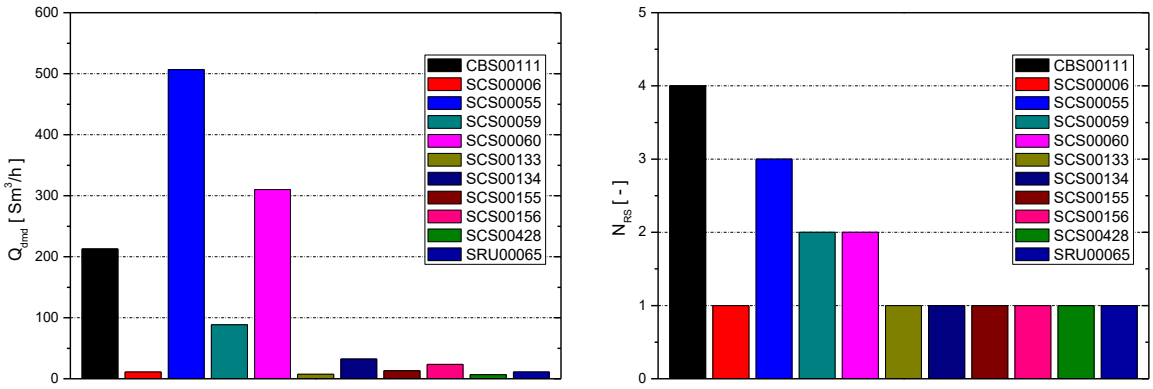

Figure 4.10: Low-pressure subnetworks: flow demand and reducing stations.

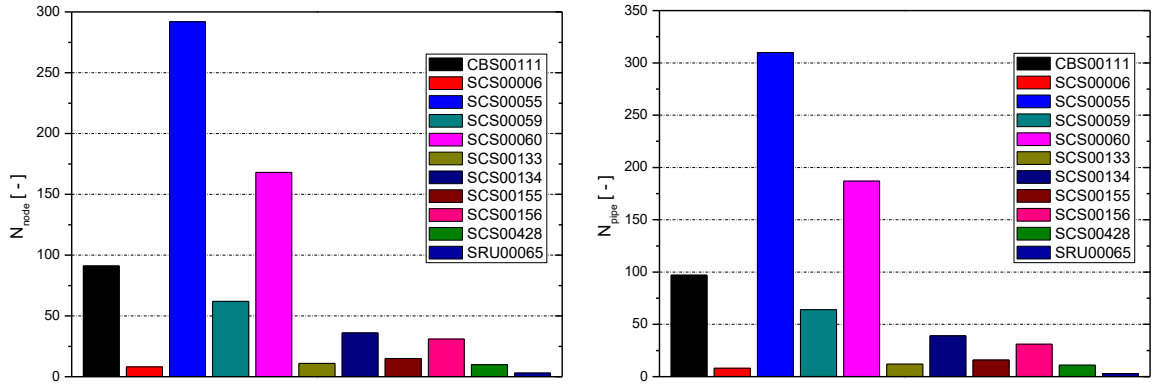

Figure 4.11: Low-pressure subnetworks: demand nodes and pipes.

4.1.1 Steady-state simulation

The main problem of a gas network is to evaluate: gas pressure (p) at demand nodes; velocity (v) and pressure drop (Δp) of pipes. These values must be checked to satisfy the gas demand by users and respect gas Standards [4.1] in any condition of the network. For gas distribution networks, where there are several stations which supply the gas or reduce the pressure of the gas, it is also important to evaluate the flow elaborated by them to guarantee the correct operation of the network. Due to a large number of elements and complex structure of gas distribution networks, steady-state simulations are the main method used to monitor and predict the performances of them in specific scenarios.
In the present case study, a steady-state simulation of the entire distribution network is carried out to analyse its behaviour and identify critical elements. Table 4.7 shows the gas composition used for modelling and simulating the network studied. The reference standard natural gas mixture provided by the Italian Regulatory Authority for Energy, Networks and Environment is chosen because of the lack of accurate real data and the high dependence of the composition on the period of the year. This quality is composed of a high percentage of methane (CH_4) and a low percentage of ethane (C_2H_6), propane (C_3H_8) and nitrogen (N_2). Main parameters which characterise the gas mixture are shown in table 4.8. The Wobbe index of the gas selected is significantly higher than the minimum allowed value ($47.2\ MJ/Sm^3$) defined by the Italian gas safety management regulations [4.1].

Table 4.7: Compositions of the gas supplied by the city gate stations.

	y_k [%]									
Source	CH_4	C_2H_6	C_3H_8	C_4H_{10}	C_5H_{12}	C_6H_{14}	CO_2	N_2	He	H_2
Standard NG	97.201	1.862	0.393	-	-	-	-	0.544	-	-

Table 4.8: Properties of the gas supplied by the city gate stations

Source	$M\ [kg/kmol]$	$SG\ [-]$	$HHV_g\ [MJ/Sm^3]$	$WI\ [MJ/Sm^3]$
Standard NG	16.4790	0.5690	38.28	50.74

The natural gas injected into the network is delivered to industrial and residential users connected respectively at 230 medium-pressure and 719 low-pressure demand nodes, as previously shown in tables 4.4 and 4.6. Figure 4.12 shows the amount of gas withdrawn at each demand node of the grid. For MP demand nodes, minimum and maximum values are respectively $0.2\ Sm^3/h$ and $5.7\ Sm^3/h$. Due to the characteristics of the network and its modelling at each medium-pressure demand node is assigned only one industrial user. Conversely, LP demand nodes have usually more than one residential user connected as a result of the high population and so many residential gas

users of urban areas. Gas demand by these nodes achieves up to $12.8\ Sm^3/h$. However, most of the MP and LP demand nodes have a gas flow demand between 0.2 and $1\ Sm^3/h$.
These values are set as boundary conditions to simulate the steady-state behaviour of the gas distribution network in the nominal scenario.

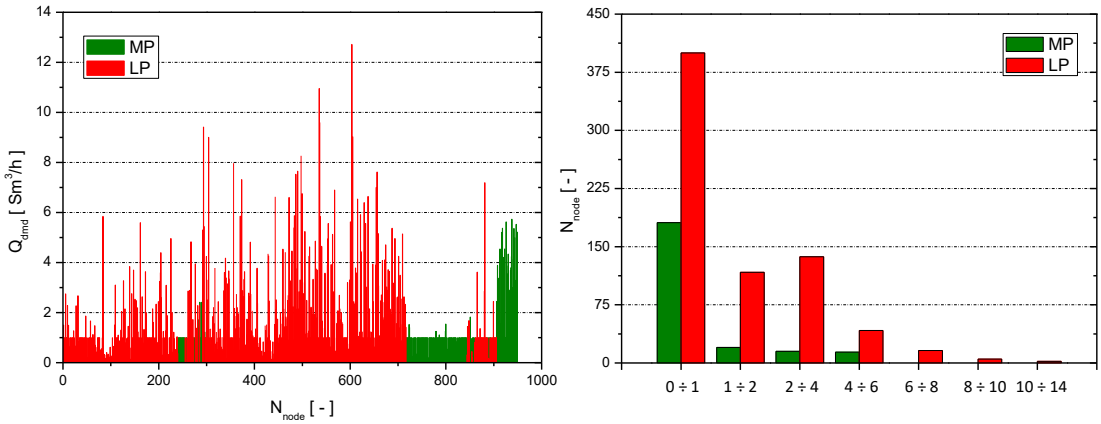

Figure 4.12: Gas flow imposed at demand nodes.

The complex structure of a gas distribution network requires reducing stations to divide it into different isolate subgrids and to supply the correct working pressure level of users' devices. Figure 4.13 shows the pressure imposed by the reducing stations of the network investigated. The gas entering the station with a medium-pressure ($3.9 \div 3.7\ bar_g$) is laminated to achieve an outlet pressure between 20 and $27.5\ mbar_g$. The set value depends on characteristics of the downstream subnetwork, altitude and gas flow supplied by the station. The highest outlet pressures are imposed for subnetworks where pressure drops are significant or final demand nodes are very distant from the reducing stations.

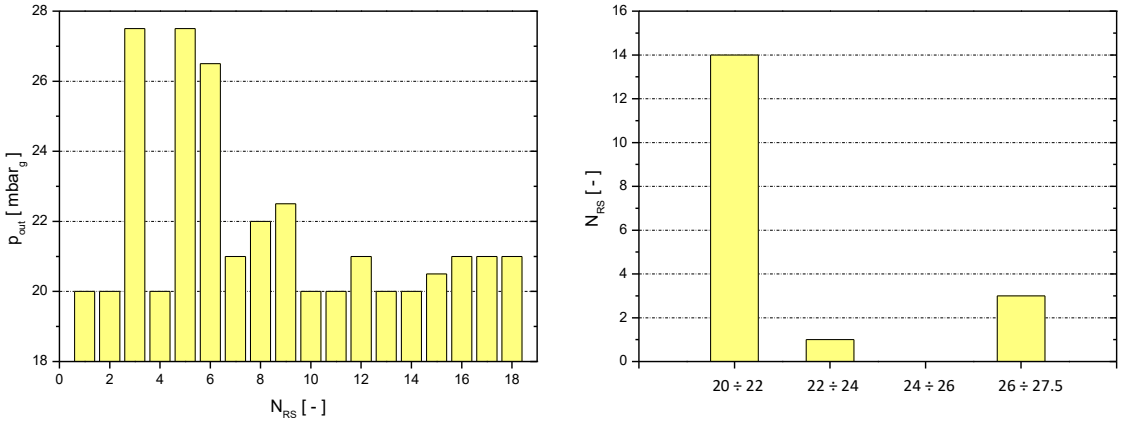

Figure 4.13: Pressure imposed at reducing stations.

Main results of the steady-state simulation of the gas distribution network studied are velocities in pipes, pressures at demand nodes and loads of reducing stations.
Maximum values of velocity are defined by gas standards [4.1] to guarantee the correct operation and safety of gas networks, as previously mentioned in section 2.3. The overcoming of the velocity

limit in some pipe would results in possible sanction by the gas regulators. Figure 4.14 shows velocities into medium-pressure and low-pressure pipes. The maximum allowed velocity for MP pipes (4ª specie) is $25\ m/s$. The computed values for these pipes are considerably lower than the maximum. Conversely, the gas in the low-pressure pipe (7ª specie) must flow slower than $5\ m/s$. Nevertheless, for the scenario simulated, the gas flow velocity is lower than $4.8\ m/s$ into each LP pipe. In particular, the gas flowing in the 75% of medium-pressure and 85% of low-pressure pipe has a velocity between 0.1 and $1\ m/s$.

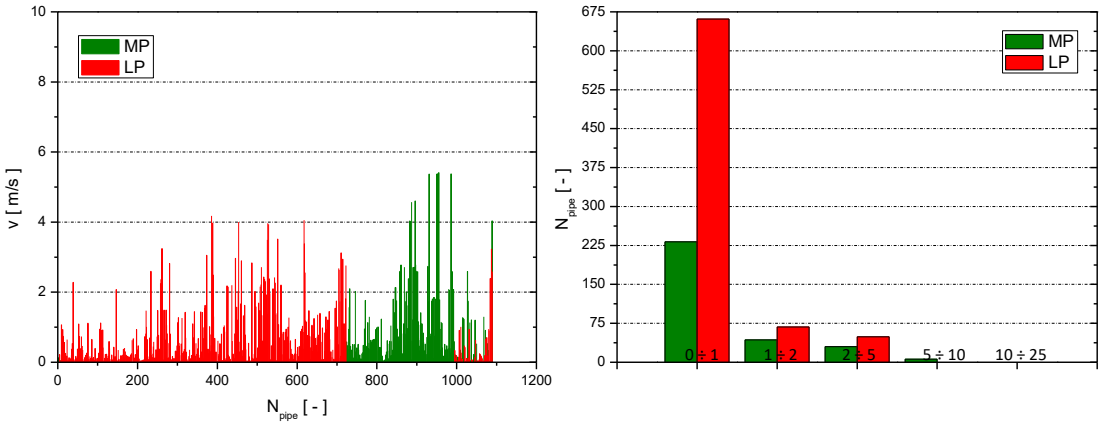

Figure 4.14: Pipe velocities.

Resulting pressures of the gas delivered at medium-pressure nodes are shown in figure 4.15. The gas is injected into the network at a pressure of $4\ bar_g$. Maximum and minimum pressure drops calculated between source and demand nodes are respectively $0.12\ bar_g$ and $0.02\ bar_g$. There are no particular criticalities because the pressure required by the reducing stations is significantly lower and the maximum pressure required by industries connected to the MP network is up to $3.8\ bar_g$.

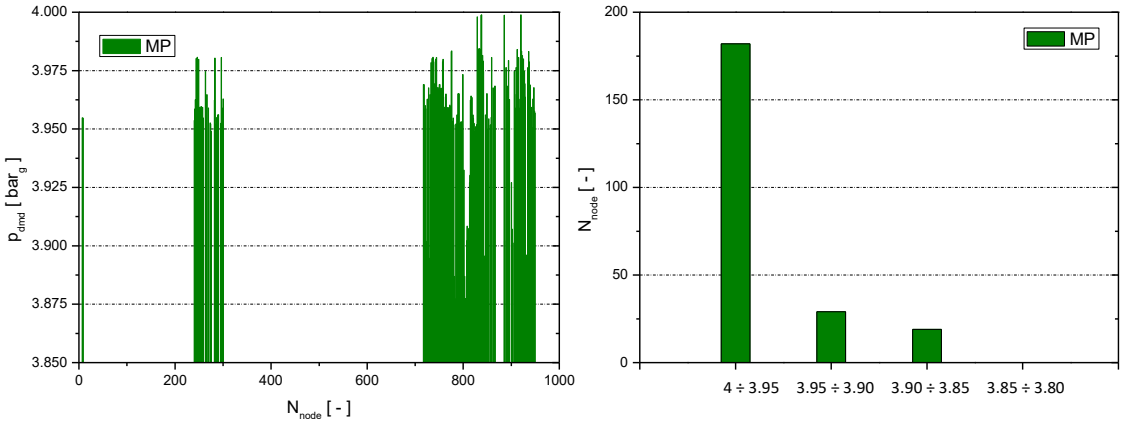

Figure 4.15: Pressure at medium-pressure demand nodes.

Figure 4.16 shows pressures evaluated at the 719 residential demand nodes. The minimum value achieved is $19.27\ mbar_g$, adequately higher than the limit value ($19\ mbar_g$) defined by the gas regulators [4.1]. The gas is delivered to about 45% of the nodes at the optimal pressure level

$(21 \div 19\ mbar_g)$. However, due to the structure and characteristics of the low-pressure subnetworks studied, the gas arrives at about 30% of the nodes at a pressure between 28.24 and $25\ mbar_g$. Pressure drops between low-pressure sources (RS) and demand nodes are very low because users are located near the corresponding reducing station. If the pressures imposed by the stations were reduced, the minimum pressure of the subnetworks would be lower than the allowed values defined by the gas standards.

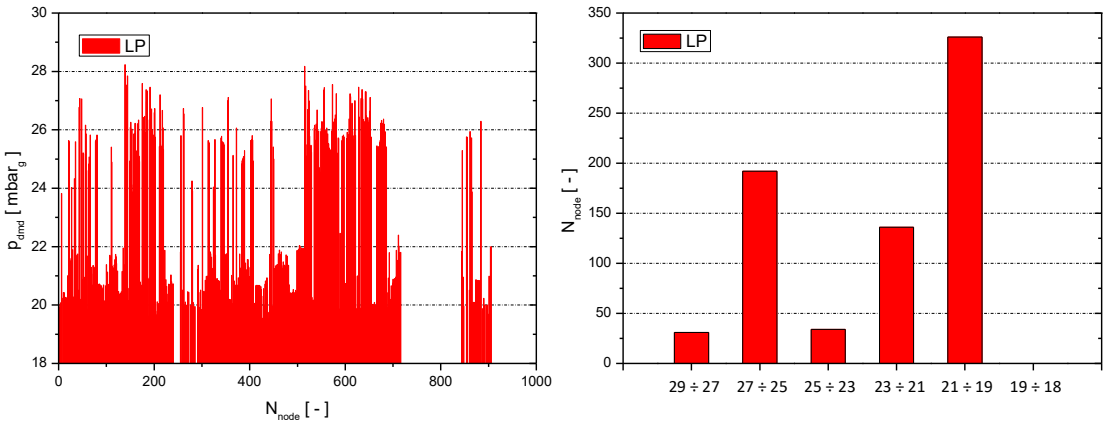

Figure 4.16: Pressure at low-pressure demand nodes.

Reducing stations, installed at interconnection points between the medium-pressure network and the low-pressure subnetworks, are critical elements of the network. They are source points of the isolated areas where residential users are connected. Therefore, it is important the monitoring of the loads and pressure drops performed by the regulator of the stations. A high level of stress of the station's components could cause shut-off of the system and consequently the failure to deliver gas at users.

The gas flow supplied by the 18 reducing stations is between 6.6 and $203\ Sm^3/h$ (figure 4.17). The high stress of some of the stations is compensated by the greater number of sources in the belonging subnetwork. However, most of the stations (about 60%) elaborate an amount of gas up to $50\ Sm^3/h$.

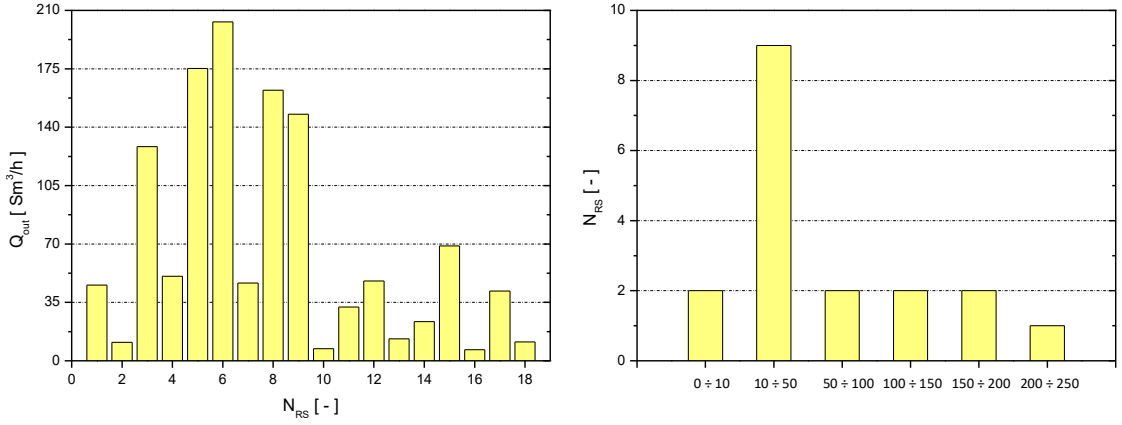

Figure 4.17: Load of reducing stations.

Figure 4.18 shows the pressure drop performed by valves installed in the reducing stations. Minimum and maximum pressure differences between inlet and outlet ports of stations are respectively 3.85 and 3.96 bar_g. The resulting high-pressure drops are due to the large difference in pressure level required by users of the medium-pressure network (industries) and residential customers connected the low-pressure subnetworks.

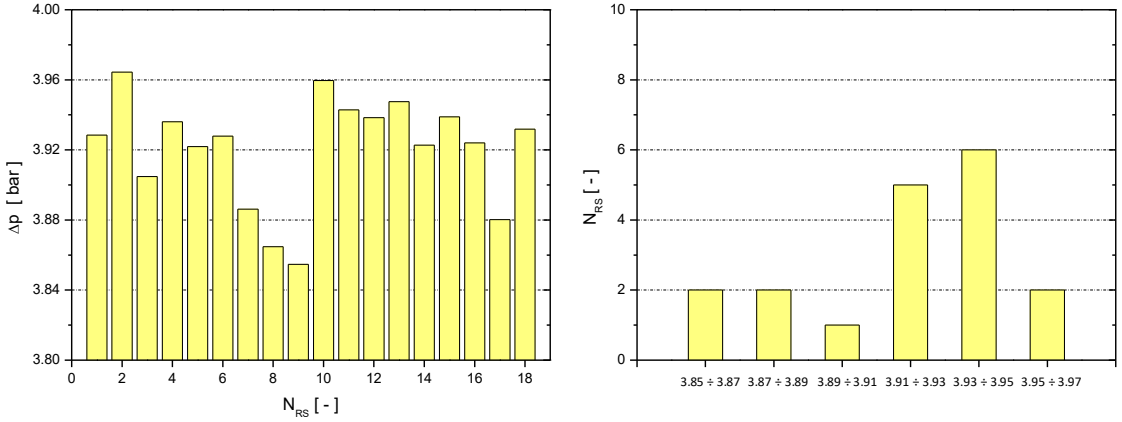

Figure 4.18: Pressure drops performed by reducing stations.

4.1.2 Dynamic simulation

Gas flow withdrawn at demand nodes is not usually constant in time, but it depends on the energy/flow requested by devices of users connected to these nodes. Therefore, the nominal scenario is not sufficient to predict the behaviour of the network. Due to a large number of elements and complex structure of the gas distribution network studied, the dynamic simulation is performed only for the medium-pressure network (figure 4.4) which is composed of 311 pipes, 61 valves, 140 junctions and 230 demand nodes. The 18 reducing stations are converted into 18 demand nodes which withdrawn the gas flow necessary to satisfy the demand of low-pressure users.

Table 4.9 shows the boundary conditions imposed for the simulation of the network. The city gate stations supply gas at a constant pressure of 4.00 bar_g and a constant temperature of 15 $°C$, as in the steady-state scenario. For the gas consumptions required by the medium-pressure demand nodes and reducing stations are used three profiles (RES, IND1 and IND2) because the real profiles of each demand node are not available/accessible. It is assumed that each low-pressure demand node has the same gas consumption profile during the day. Instead, MP demand nodes are divided into nodes with a gas demand lower and higher than 1.5 Sm^3.

Figure 4.19 shows the unidimensional profiles used to calculate gas consumption of demand nodes. Industries usually work at full load during the entire day or only for the central hour of the day. Therefore, two different realistic profiles are created to model these two types of operation. Instead, in urban areas, the gas is mostly used by people for cooking and heating their homes. There are usually three peaks of demand during the morning, lunchtime and evening when people are at their homes. Each residential user and so LP demand node has in the reality its profile which depends on its gas consuming. However, as a simplification, it is assumed that all residential

demand nodes and so reducing station have the same unidimensional gas consumption during the day.

Table 4.9: Boundary conditions imposed for the dynamic validation.

Boundary Condition	Value	Profile
$p_{CGS}\ [bar_g]$	4.00	-
$T_{CGS}\ [°C]$	15.00	-
$\dot{Q}_{RS,dmd}\ [Sm^3/h]$	$6.6 \div 203.08$	RES
$\dot{Q}_{MP,dmd}\ [Sm^3/h]$	$1.6 \div 5.85$	IND1
$\dot{Q}_{MP,dmd}\ [Sm^3/h]$	$1 \div 1.5$	IND2

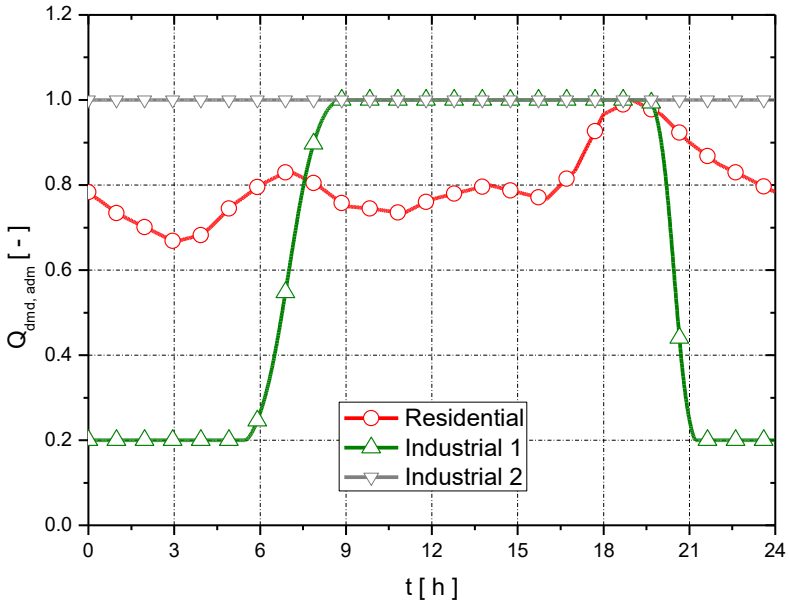

Figure 4.19: Gas flow demand profiles.

Firstly, the medium-pressure network is simulated imposing the gas flow demand by users of the network at the time $t = 0$. This simulation is necessary to initialize the dynamic simulation. Secondly, the dynamic scenario is created setting as boundary conditions residential and industrial gas demand profiles, previously illustrated.

Figure 4.20 shows the gas flow supplied by the 2 city gate stations during the day. The city gate station CGS1, located at south-east (figure 4.4), supplies a variable amount of gas in the range $586.90 \div 881.70\ Sm^3/h$. Conversely, the amount of gas provided by the second city gate station CGS2 is up to $646.30\ Sm^3/h$ and has a smaller variation during the day respect to the other source

node. As a consequence of the dynamic characteristics of the pipes that compose the network, an amount of gas is stored into the network during the hours of the day (figure 4.21). However, due to the typical slower gas flow variation during the day and especially because of the characteristics of the distribution network studied, the gas stored is limited. For positive values, the gas is stored (up to $+3\ Sm^3/h$) and for negative values, it is thrown out (up to $-1\ Sm^3/h$).

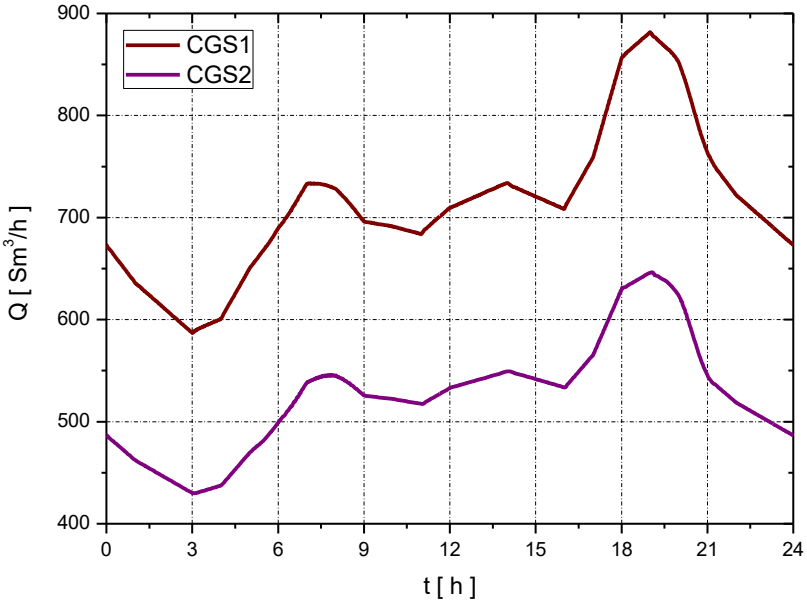

Figure 4.20: Gas supplied by the 2 city gate stations.

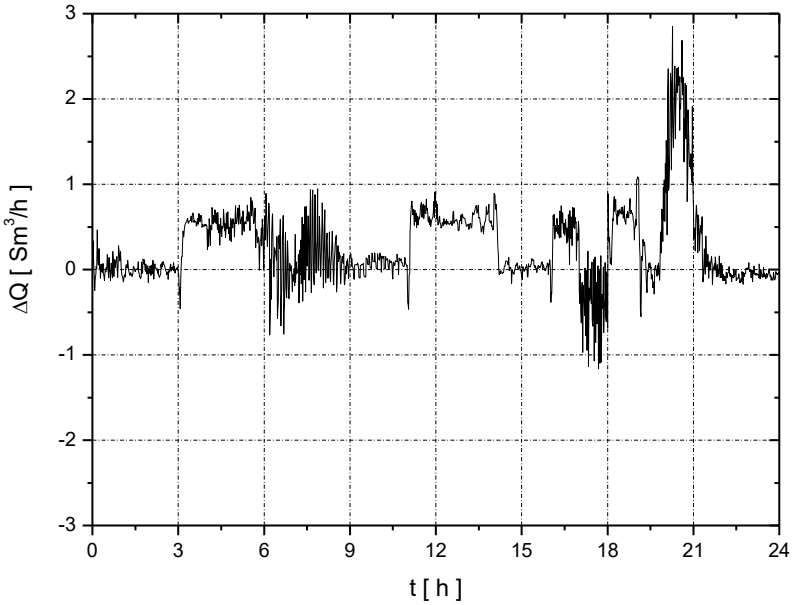

Figure 4.21: Difference between gas flow withdrawn and supplied.

The maximum flow velocity into pipes and the minimum pressure at demand nodes as a function of the hours of the day are shown in figure 4.22. Minimum pressure ($3.897\ bar_g$) and maximum

flow velocity ($5.46\ m/s$) are achieved at about the $19\ h$ when gas demand by users connected to the network is maximum. At the $3\ h$, where gas demand is minimum, the gas flows into pipes at low velocity and so pressure drops are very low. If the gas arrives at demand nodes with too high pressure, there could be problems in the reducing stations or reducing systems of industries because of increased pressure drop performed by them. For the other hours of the day, pressure and velocity values fluctuate due to the variable gas demand.

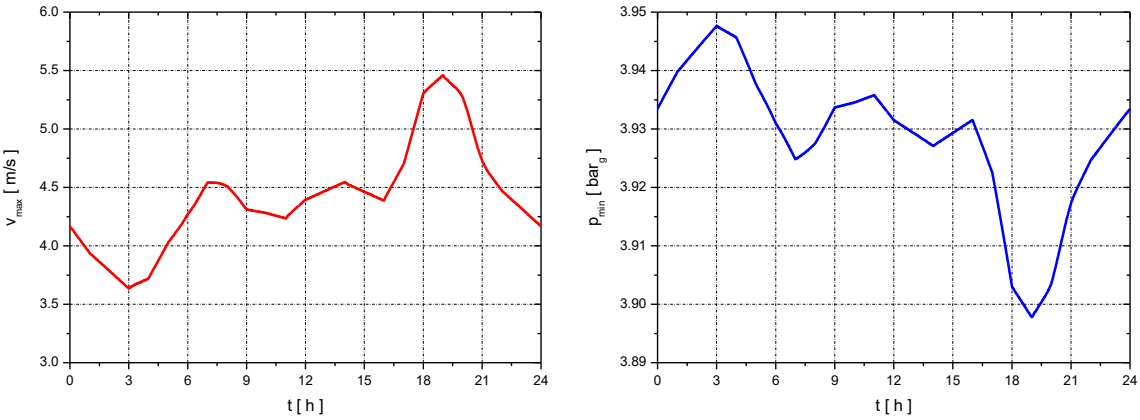

Figure 4.22: Maximum flow velocity and minimum pressure during the day.

As previously illustrated, reducing stations are critical elements used to manage efficiently the different pressure levels of the network. The stress level of these elements is correlated to the pressure drop performed by them. Therefore, it is important to check this parameter with the purpose of preventing shut-offs and failures of these systems. The pressure reductions performed by the 18 reducing stations as a function of the hours of the day are shown in figures 4.23 and 42.4. Due to the different positions of the reducing stations in the network and the flow elaborated, the gas arrives with different pressure and so unequal pressure drops are performed by them. Maximum pressure drop variations are evaluated for SCS00059, SCS00060, SCS00061 and SCS00439 stations which are located at south-east of the map (figure 4.7). These stations are forced to operate in highly variable mode. For the other RS, pressure reduction fluctuations are limited.

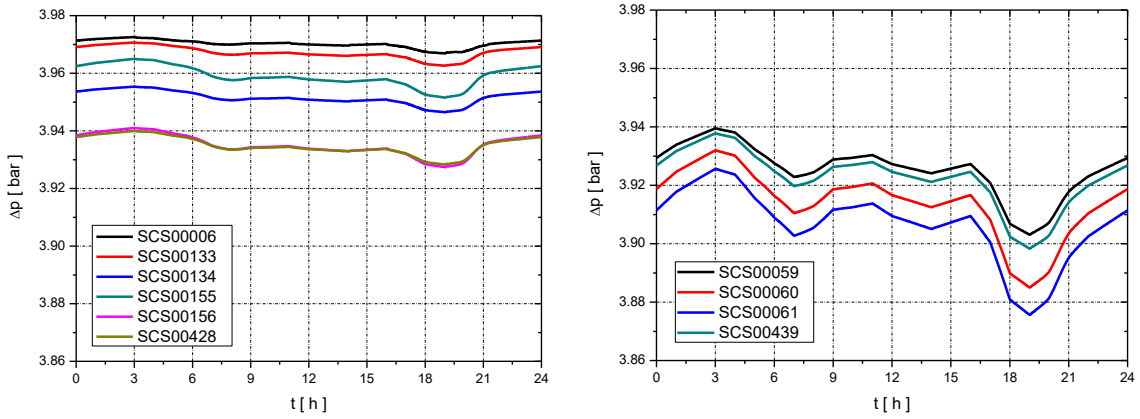

Figure 4.23: Pressure drops performed by north-west and south-east reducing stations during the day.

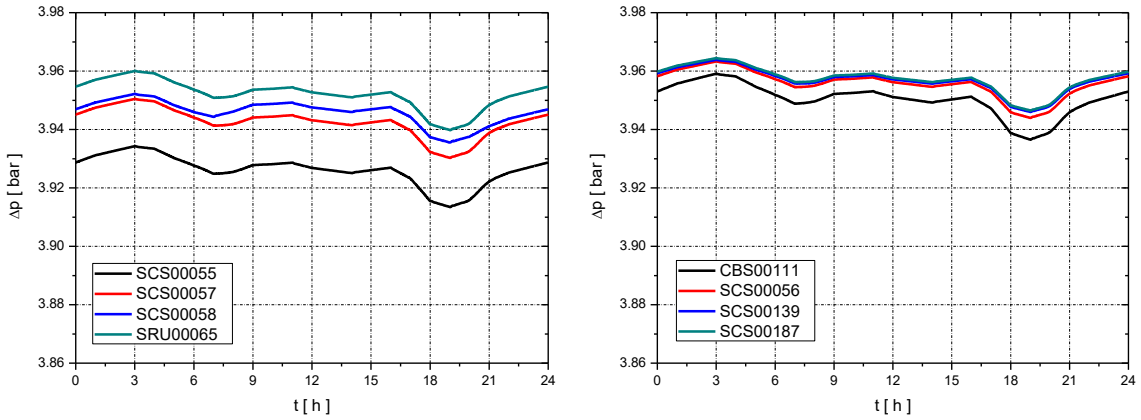

Figure 4.24: Pressure drops performed by centre-left and centre-right reducing stations during the day.

4.2 Distribution network with H2 localized injections

Power-to-gas technology is a potential solution to support and accelerate the penetration of renewable sources and the decarbonisation of the energy sector. The excess of power generated by renewable energy sources is used by power-to-gas systems to produce alternative fuels. The resulting gas (hydrogen or synthetic natural gas) can be injected and stored into the existing gas grid.

In the case study, one power-to-gas facility, which produces H_2 is connected to the medium-pressure network. Properties of the green hydrogen gas used for the analysis are shown in table 4.10. Compared with the characteristics of the standard natural gas supplied by the 2 city gate stations (table 4.8), the hydrogen is a fuel gas with very low mass density and specific energy that is about one-third of it. Therefore, as shown in section 2.2, specific gravity, higher heating value and Wobbe index of a natural gas and hydrogen mixture can be significantly different respect to reference values.

Table 4.10: Properties of the green gas injected into the distribution network.

Source	$M\ [kg/kmol]$	$SG\ [-]$	$HHV_g\ [MJ/Sm^3]$	$WI\ [MJ/Sm^3]$
H_2	2.0159	0.0696	12.08	45.79

The NWG solver is used to simulate different amounts of hydrogen injected and positions of the alternative source. The analysis aims to evaluate the impact of green gas injection (in this case H_2) on network behaviour and quality of the gas delivered to users connected to the grid.

4.2.1 Steady-state simulation with gas quality tracking

The gas distribution network with localized hydrogen injection is simulated using the steady-state method of the Gas Network Solver. Due to a large number of elements and complex structure of

the network studied, steady-state simulations are more appropriate, in comparison with dynamic simulation, to analyse different amounts of hydrogen injected and different injection positions. Figure 4.25 shows the 4 different location (A, B, C and D) for the installation of the power-to-gas facility (P2G). The hypothesized places for the installation of the system are suburban areas with a large surface available for the construction of a P2G plant (figure 4.26). The green hydrogen produced is carried into a pipe which is directly connected to the medium-pressure network.
The steady-state analyses aim to evaluate the impact of hydrogen injection to determine the most favourable and unfavourable position for the alternative source and estimate the maximum amount of hydrogen injectable respecting gas standards.

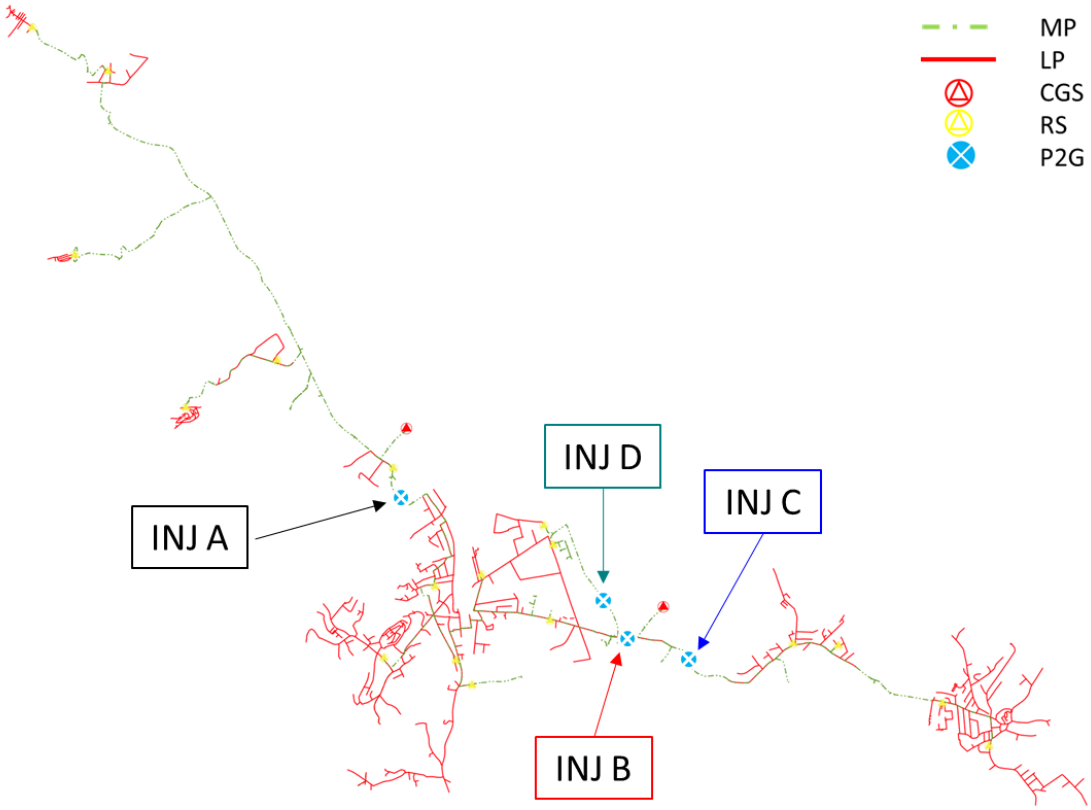

Figure 4.25: Distribution network schema with localized hydrogen injections.

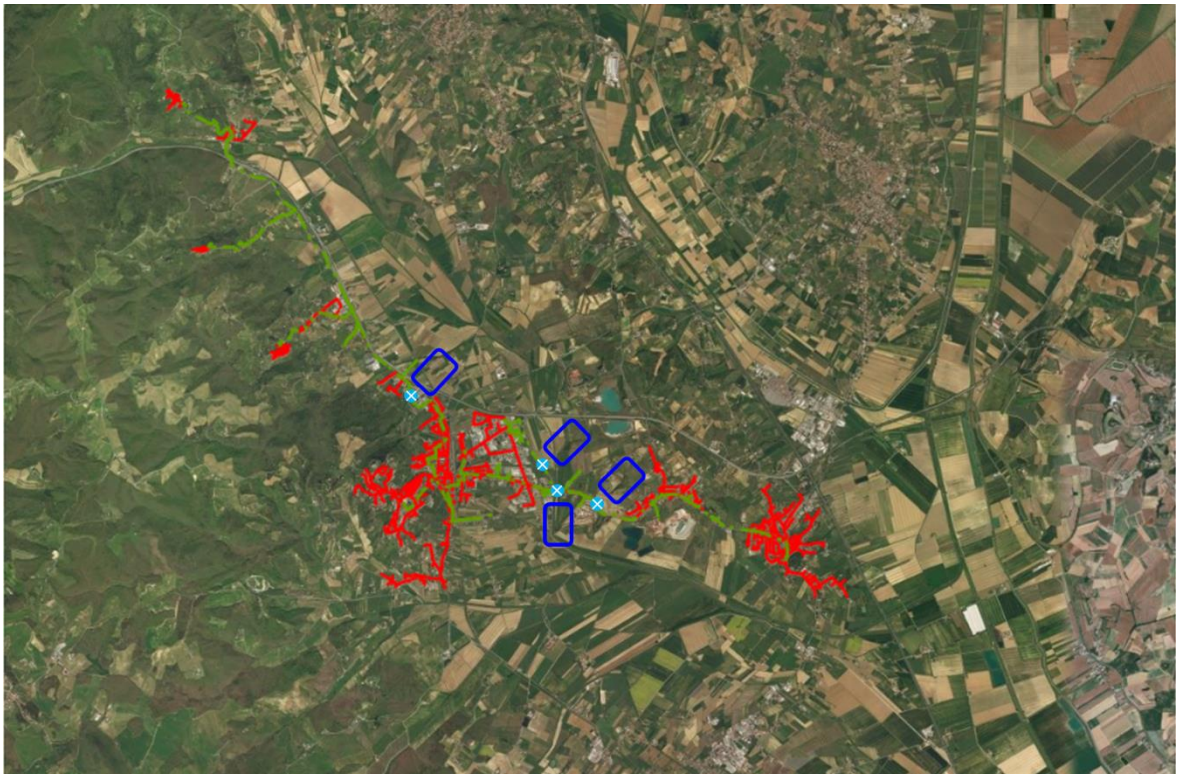

Figure 4.26: Geographical map of the hypothesized places for the power-to-gas facility.

4.2.1.1 Injection at Node A

The first analysis illustrates results for the scenario where the power-to-gas facility is built in the suburban area A. From the Hydrogen source, it is injected into the node A an amount of energy between 100 and $1000\ kJ/s$. The outlet pressure of the alternative source is regulated, according to network conditions, with the purpose of guarantee the injection of the quantity of hydrogen set.

4.2.1.1.1 Energy method versus flow method

The energy required by users is proportional to the gas flow and the higher heating value of the gas quality. However, as previously shown in section 2.2, the HHV depends on the composition of the NG and H_2 mixture. Therefore, the traditional flow method, which imposes the volumetric gas flow, does not satisfy the energy requested by users (figure 4.27). The energy undelivered increases with the amount of hydrogen injected. For $1000\ kJ/s$, due to the different quality of the gas, about 13.4% of the total energy demand by users is not supplied by the network.
The energy formulation, proposed and developed in chapter 2, can satisfy the energy requested by users' devices independently of the composition of the gas delivered at demand nodes. Figure 4.27 shows how to deliver the right amount of energy demand by users, the volumetric flow of gas withdrawn increases with the amount of hydrogen injected into the grid. Due to the lower higher heating value of the natural gas and hydrogen mixture, the total volumetric gas flow supplied by the network is up to 11.8% more than in the scenario without H_2 injection.

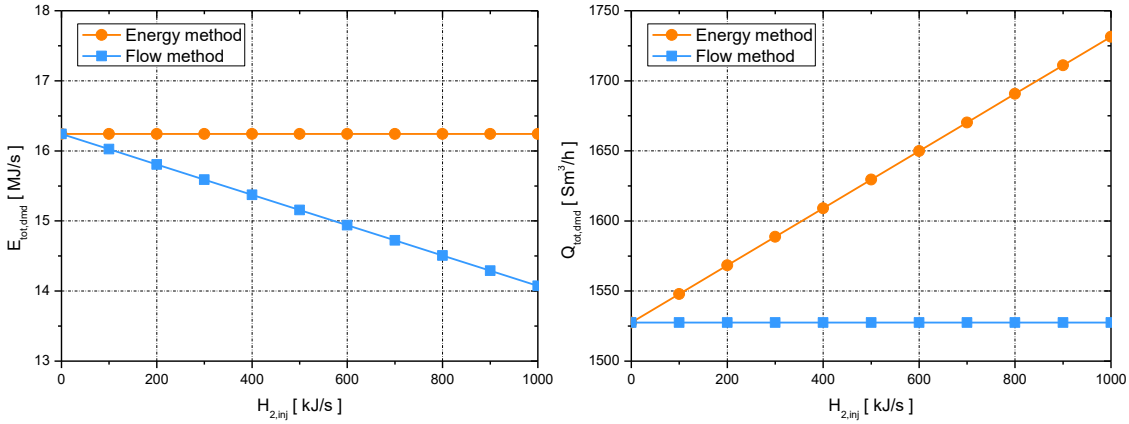

Figure 4.27: Energy and volumetric flow demand for the two methods proposed.

When Hydrogen is injected, the mixture of the gas flowing into the network changes. Figure 4.28 shows how the maximum fraction of hydrogen evaluated at demand nodes increases with the amount of H_2 energy injected. The impact on the demand nodes depends on the type of boundary condition method used. When the energy method is used, the maximum hydrogen fraction achieved for $1000\ kJ/s$ is 9.78%. Conversely, setting as boundary conditions the volumetric gas flow, the network delivers gas to users with a hydrogen mass fraction up to 13.49%. As a consequence of the different gas quality, the higher heating value of the gas delivered changes as shown in figure 4.28. Minimum HHV of about 26 and $23.6\ MJ/Sm^3$ are achieved respectively for the energy and flow methods. Very low values compared to the reference values of standard natural gas ($38.28\ MJ/Sm^3$).

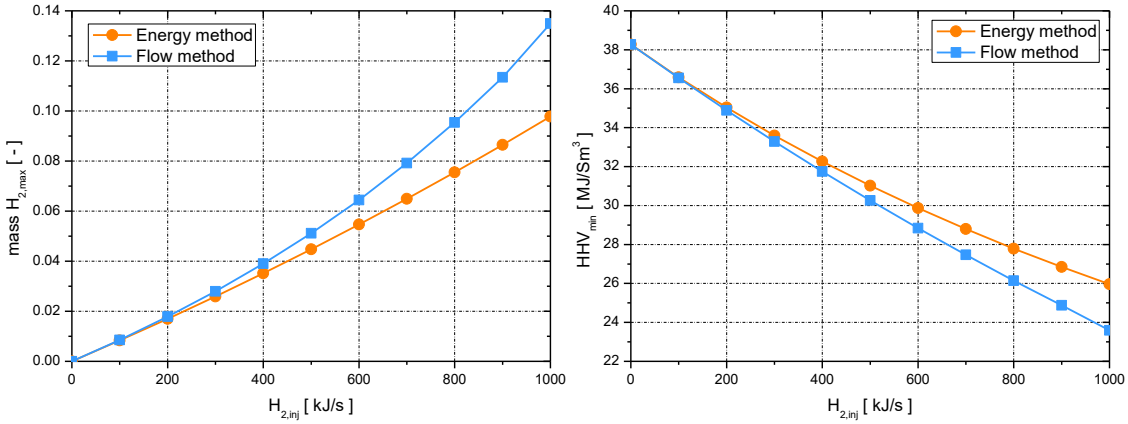

Figure 4.28: Maximum H_2 mass fraction and minimum higher heating value of demand nodes.

The Wobbe index is highly influenced by the composition of the gas mixture, as previously shown in sections 2.2. Figure 4.29 shows the trend of WI as a function of the total H_2 flowing into the network. When hydrogen is not injected, the Wobbe index is $50.75\ MJ/Sm^3$. Increasing hydrogen fraction, the WI of the gas mixture delivered at demand nodes decreases. For the flow demand method, an injection of $500\ kJ/s$ does not guarantee the respect of the minimum allowable Wobbe index. On the contrary, imposing the energy consumption at demand nodes, values, lower than the

minimum allowed Wobbe index, are not achieved. Only for an amount of hydrogen greater than $600\ MJ/Sm^3$, some nodes of the network withdrawn gas with a WI lower than $47.2\ MJ/Sm^3$. Injecting the maximum value of H_2, the network supplies gas not conform to standards [4.1] to 308 demand nodes (flow method) and 225 demand nodes (energy method).

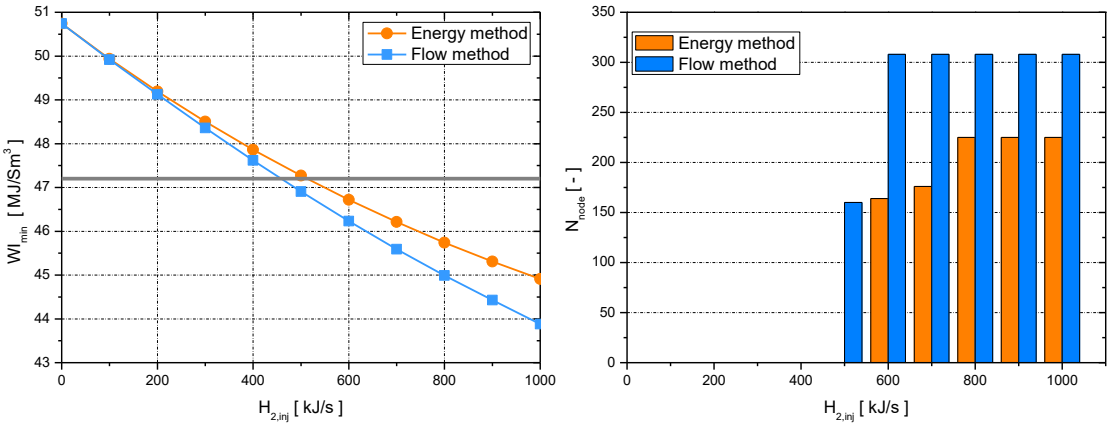

Figure 4.29: Minimum Wobbe index of demand nodes.

The velocity of the gas flowing into pipes increases with the mass fraction of hydrogen of the mixture and so with the amount of hydrogen injected by the alternative source. Due to the lower higher heating value of the natural gas and hydrogen mixture, using the energy approach, the gas supplied, transported and delivered by the network increases too. Therefore, velocity in low-pressure pipes achieves a value higher than the maximum allowed value for a lower amount of hydrogen injected respect to the flow method, as shown in figure 4.30. Maximum velocities of 6.24 and $5.28\ m/s$ are evaluated respectively for the energy and flow method when $1000\ MJ/Sm^3$ of H_2 is injected into the network. Figure 4.31 shows that hydrogen injection has an impact on most of the pipes of the network. Velocities increase also in pipes where less gas is flowing.

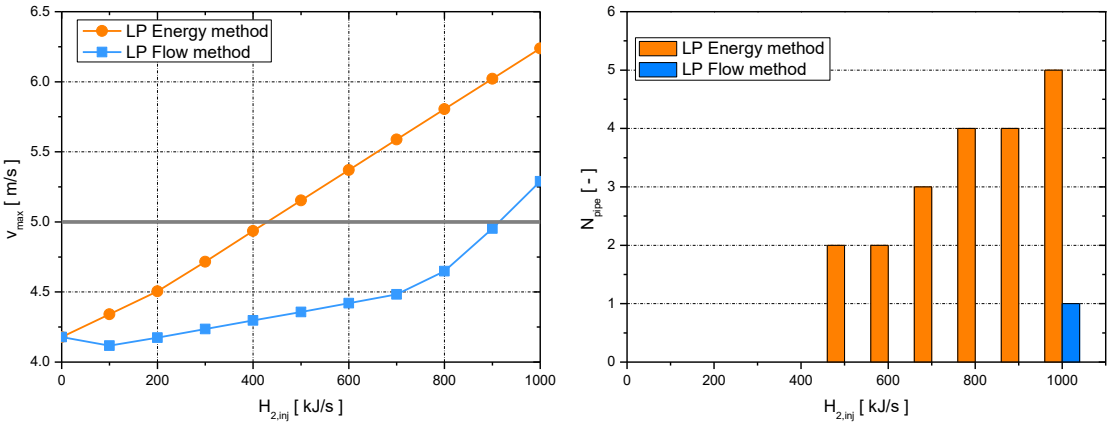

Figure 4.30: Maximum velocity of low-pressure pipes.

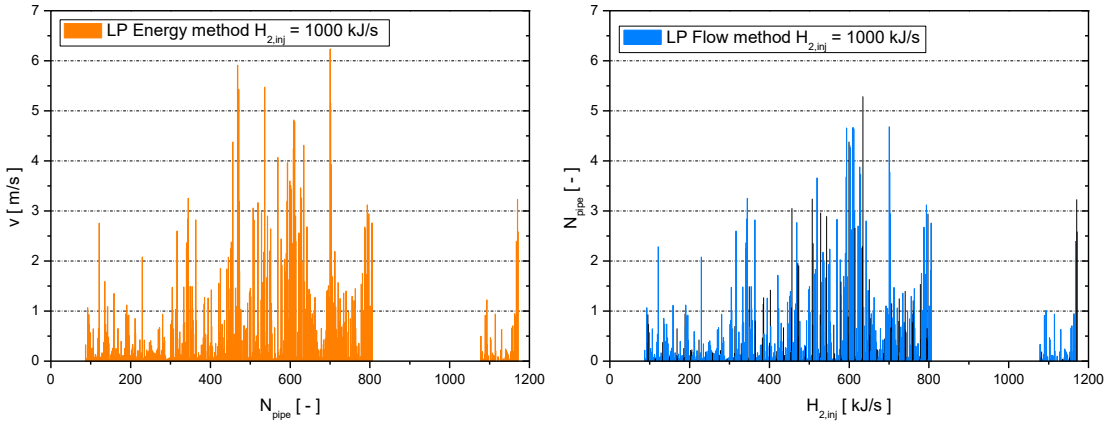

Figure 4.31: Velocity at low-pressure pipes.

As shown above, with a higher fraction of H_2, the HHV of the gas mixture delivered is lower. Therefore, a higher gas flow, which produces more significant pressure drops, is required to satisfy the same energy demand by customers. Figure 4.32 shows the minimum pressure at LP demand nodes as a function of the amount of hydrogen injected. Using the flow method, the minimum value is independent of the total amount of H_2 into the network. Conversely, imposing the energy demand, hydrogen injection influences the minimum pressure. Value achieved in some demand nodes of the low-pressure subnetworks is lower than the minimum allowed pressure ($19\ mbar_g$) defined by gas standards with an H_2 mass fraction higher than $900\ kJ/s$. Injecting the maximum amount of hydrogen, the gas delivered at 9 LP demand nodes does not respect the pressure level required by combustion users' devices connected to the network.

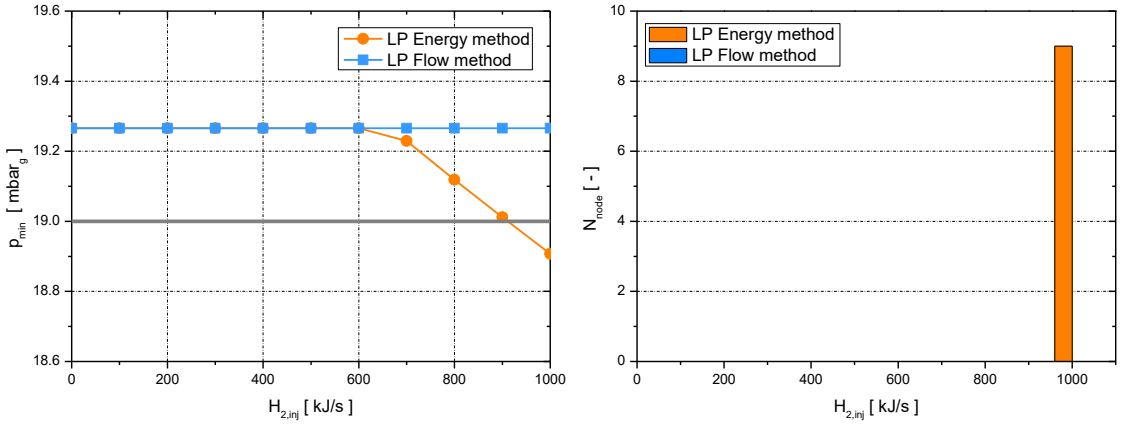

Figure 4.32: Minimum pressure at low-pressure demand nodes.

Results show that there are significant differences between the traditional method and the energy method. In the case of an NG and H_2 mixture, the first approach does not satisfy the energy requested by users. The comparison of the two methods also indicates that the impact of hydrogen injection on Wobbe index, velocity and pressure values of the network's elements is different.
Therefore, for the other simulations, the network is modelled setting as boundary conditions the amount of energy demand by users' devices connected to the grid.

4.2.1.1.2 Injection of 500 kJ/s at Node A

The scenario with a hydrogen injection of $500\ kJ/s$ is compared with the standard case without alternative sources. As shown in the results of the previous paragraph, $500\ kJ/s$ is the maximum amount of H_2 injectable respecting the Wobbe Index limit imposed by gas standards [4.1].
Figure 4.33 shows hydrogen mass fraction evaluated at the 949 demand nodes of the network. Hydrogen injected by the alternative sources does not reach all users connected to the grid. It is delivered to demand nodes a mixture with 4.47% of H_2 at the latest. For the medium-pressure network, about 90% of demand nodes are not affected by the injection at node A. Just 3 and 17 nodes achieved a percentage of hydrogen respectively in the range $2 \div 3\%$ and $4 \div 5\%$. Instead, a lot of nodes of low-pressure subnetworks withdraw gas with a different quality from the standard one. A hydrogen mass fraction higher than 2% is achieved by 288 LP demand nodes.

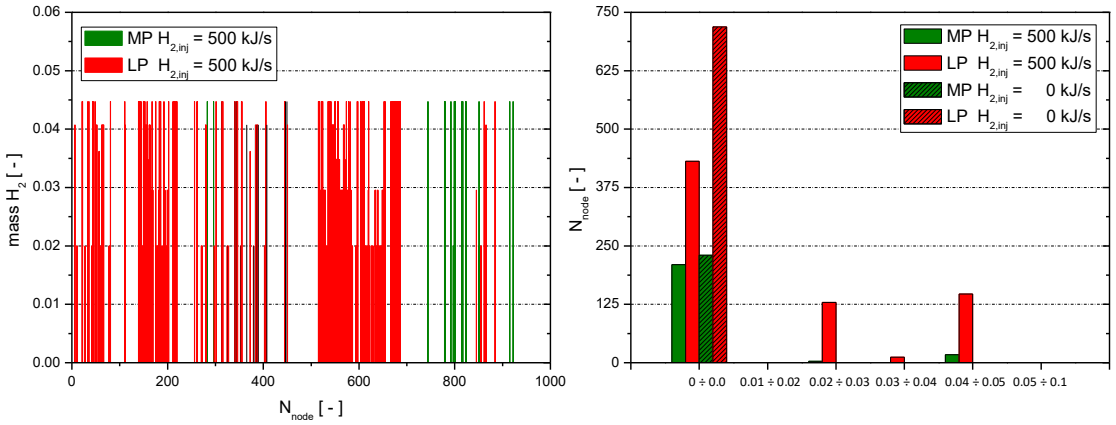

Figure 4.33: Hydrogen mass fraction at demand nodes.

As a consequence of the several gas qualities flowing in pipes of the network, properties of the gas delivered to users differ from those of standard natural gas (table 4.10). Wobbe index values achieved by demand nodes of the network are shown in figure 4.34. There are 20 MP and 288 LP demand nodes which supply gas to users' devices with a Wobbe index lower than the value of the standard NG ($50.74\ MJ/Sm^3$). If the alternative source injects $500\ kJ/s$, the minimum Wobbe index allowed of $47.20\ MJ/Sm^3$ is not achieved. However, values very close to the limit ($47.27\ MJ/Sm^3$) are evaluated at 125 medium-pressure and low-pressure demand nodes.

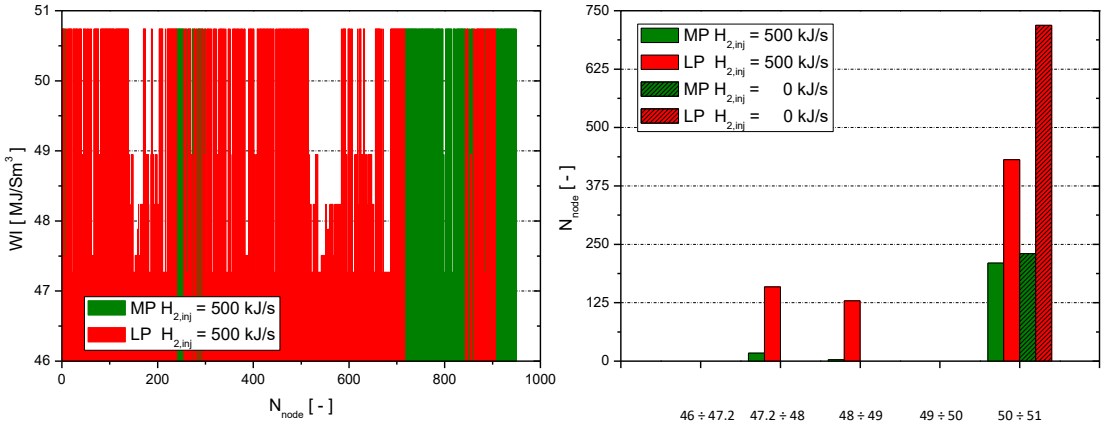

Figure 4.34: Wobbe index at demand nodes.

As shown in the previous paragraph (4.2.1.1.1), the presence of hydrogen in the gas mixture has also a not negligible impact on gas velocities and pressures.
Figure 4.35 shows velocity values evaluated into pipes of the network. Due to the different natural gas and hydrogen mixture and mass balances, the gas flow in pipes changes. For low-pressure pipes, velocity in some pipes decreases and in others increases. The number of pipes with a velocity in the range $0 \div 1$ increases. However, there are 2 LP pipes that achieve a value higher than the maximum velocity allowed by gas standards [4.1]. Instead, the structure of the medium-pressure network mitigates flow changes. Velocities in all MP pipes increase slightly because of the higher volumetric gas flow required by users connected to the grid.

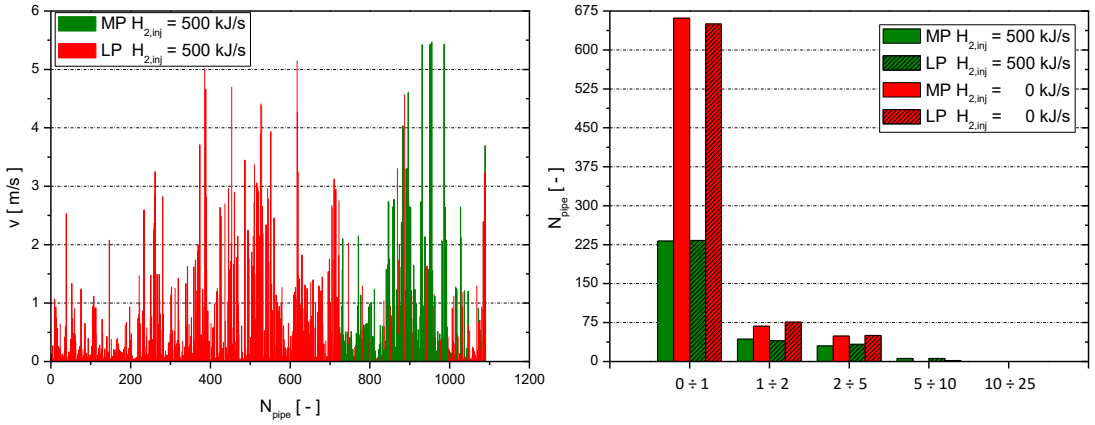

Figure 4.35: Flow velocity into pipes.

Pressures of the gas withdrawn by medium-pressure and low-pressure demand nodes are respectively shown in figure 4.36 and 4.36. Minimum pressures achieved for MP and LP demand nodes are respectively 3.87 and $19.27\ mbar_g$. Compared to the scenario without H_2 injection, pressure values change only for nodes of the gas network in areas where an amount of hydrogen arrives. For MP demand nodes, there are only 3 nodes which change the pressure level from $3.95 \div 3.90\ mbar_g$ to $4 \div 3.95\ bar_g$. The number of LP demand nodes in the range $27 \div 25\ mbar_g$ and $23 \div 21\ mbar_g$ increases. Conversely, nodes in the other pressure range

decrease. However, for a hydrogen injection of $500\ kJ/s$, all low-pressure demand nodes have a pressure level higher than the minimum value required by users' devices connected to the grid.

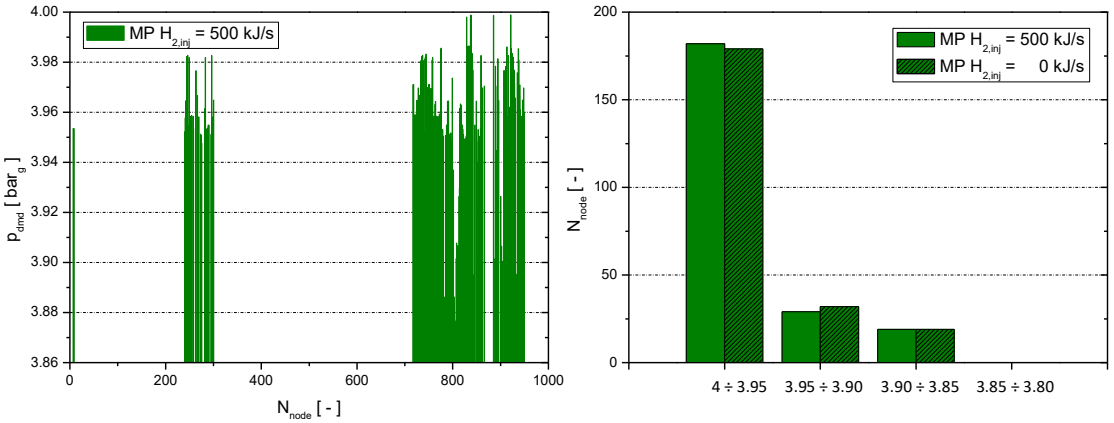

Figure 4.36: Pressure at medium-pressure demand nodes.

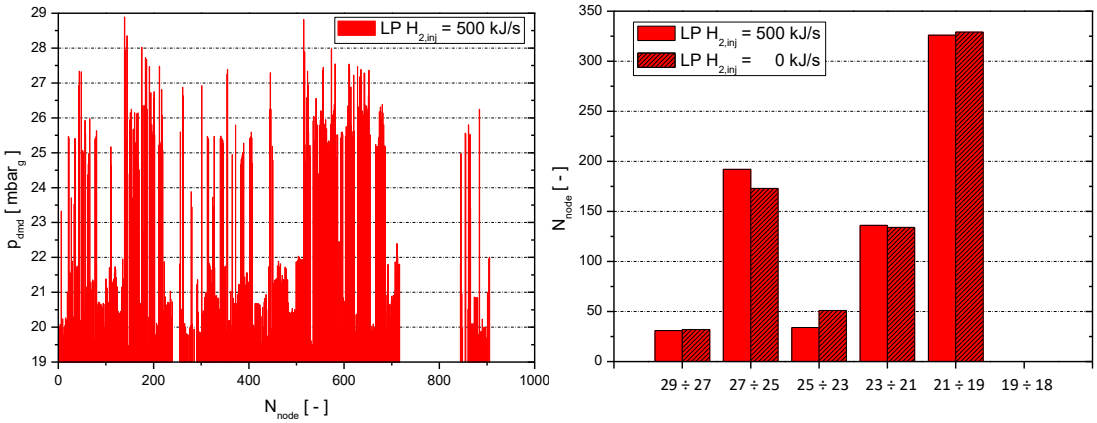

Figure 4.37: Pressure at low-pressure demand nodes.

4.2.1.2 Influence of the Injection position

The present analysis aims to determine the influence of the green hydrogen source on the parameters and behaviour of the distribution network studied. Table 4.11 summarizes the 4 positions analysed for the construction of the power-to-gas facility. As previously shown in figure 4.25 and 4.26, there are selected different location close to a medium-pressure pipe and with large surface available for the installation of the H_2 production plant.

Table 4.11: P2G facility's positions analysed.

Injection Node	A	B	C	D
Map position	West	North-Central	South-Central	East

Figure 4.38 shows maximum hydrogen evaluated at demand nodes as a function of the total amount of energy supplied by the alternative source for the different positions studied. Considering the same total H_2 injected, the maximum percentage of it into the mixture greatly depends on the source position. Maximum hydrogen values achieved in the A, B and C scenarios are quite similar. For $500\ kJ/s$ and $1000\ kJ/s$ of H2 injected, it is delivered to users a gas quality with a mass fraction of hydrogen respectively up to about 4.6 and 9.8%. Instead, when hydrogen is injected at the node D, maximum H_2 fractions achieved are three and four times more than values evaluated for the other cases. Increasing the total amount of hydrogen injected, differences are considerably higher. It is possible to inject only about $18\ kJ/s$ at the location D to achieve an H_2 percentage lower than 4.6%.

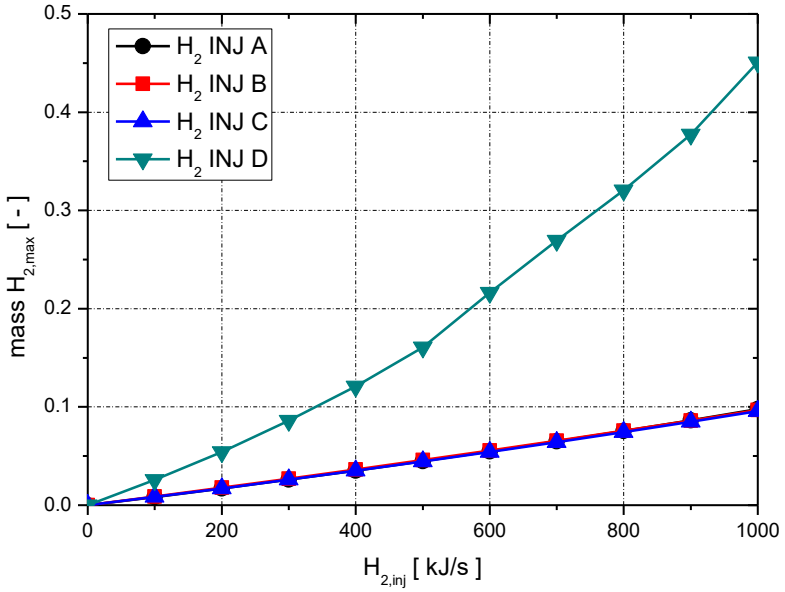

Figure 4.38: Maximum hydrogen mass fraction at demand nodes.

Figure 4.39 shows mass H_2 fraction evaluated at demand nodes for the injection of $500\ kJ/s$ in the 4 different locations of the alternative source. Pure hydrogen, injected into a point of the network, is mixed with the natural gas flowing into the network. However, a gas mixture with H_2 does not reach all nodes of the network because of the gas flows direction. Despite the comparable maximum fraction evaluated for the A, B and C scenarios, demand nodes affected by the H_2 injection are different, as shown in figure 4.39.

For the A and C positions, several H_2 percentages into the mixture respectively in the range $2.00 \div 4.47\%$ and $0.09 \div 4.59\%$ are achieved. Instead, injecting H_2 at node C, all demand nodes affected have a hydrogen mass fraction of 4.45%. When the alternative source is at location D, some nodes achieve a mixture with an H_2 percentage between 2.5 and 4.0%. However, a lot of the nodes with a composition that differs from the standard, have a hydrogen mass fraction of 14.5%.

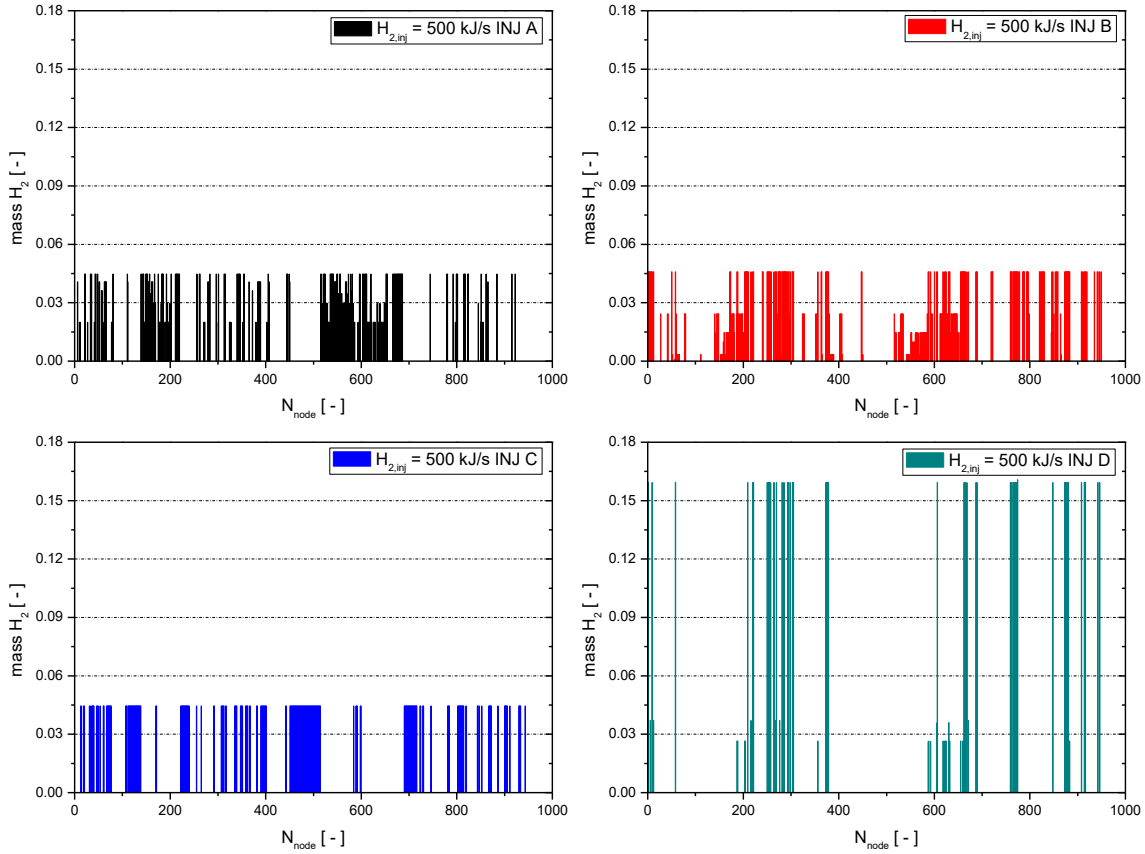

Figure 4.39: Hydrogen mass fraction values at demand nodes for 500 kJ/s of H_2 injected.

As a consequence of the hydrogen in the mixture, properties of the gas delivered and so, Wobbe index differ from values of the standard natural gas. Increasing the total amount of energy supplied by the alternative source, the minimum Wobbe index evaluated at demand nodes decreases. Figure 4.40 shows that the trend of minimum WI versus total H_2 injected depends on the location of the injection point. Values of WI_{min} evaluated in the A, B and C scenarios are comparable. Wobbe index values higher than $47.20\ MJ/Sm^3$ are achieved only if more than $500\ kJ/s$ of hydrogen are injected into the network. Instead, significantly lower Wobbe index values are obtained when H_2 is injected at node D. In this case, it is possible to inject only about $180\ kJ/s$ respecting limit WI values defined by gas standards.

Figure 4.41 shows the number of medium-pressure and low-pressure demand nodes that achieve a Wobbe index value lower than $47.20\ MJ/Sm^3$ as a function of the total amount of H_2 injected by the alternative source. The impact on MP and LP demand node network is different. The highest impact is for hydrogen injected at node B. Conversely, for low-pressure nodes, the maximum number of nodes with a WI lower than the limit is evaluated in case C. It is important to note that even if minimum Wobbe index values are evaluated in scenario D, the impact on the network is highly localized. Choosing this position, there are only 26 MP and 39 LP demand nodes with a WI lower than the limit value. Increasing the total amount of H_2 injected, the number of demand nodes with a WI lower than the minimum allowed value is practically the same for the all alternative

source positions. Instead, a higher total amount of hydrogen into the network corresponds to a greater number of demand nodes which do not respect WI gas standard.

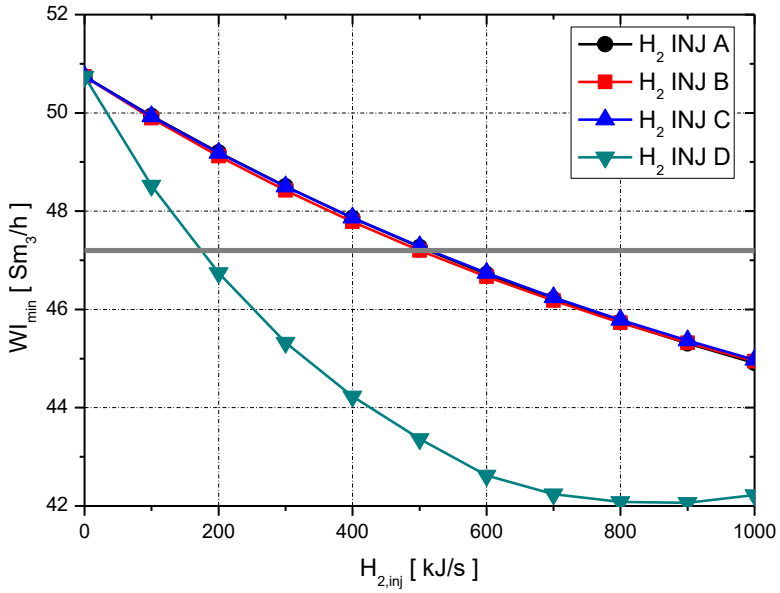

Figure 4.40: Minimum Wobbe index at demand nodes for 500 kJ/s of H_2 injected.

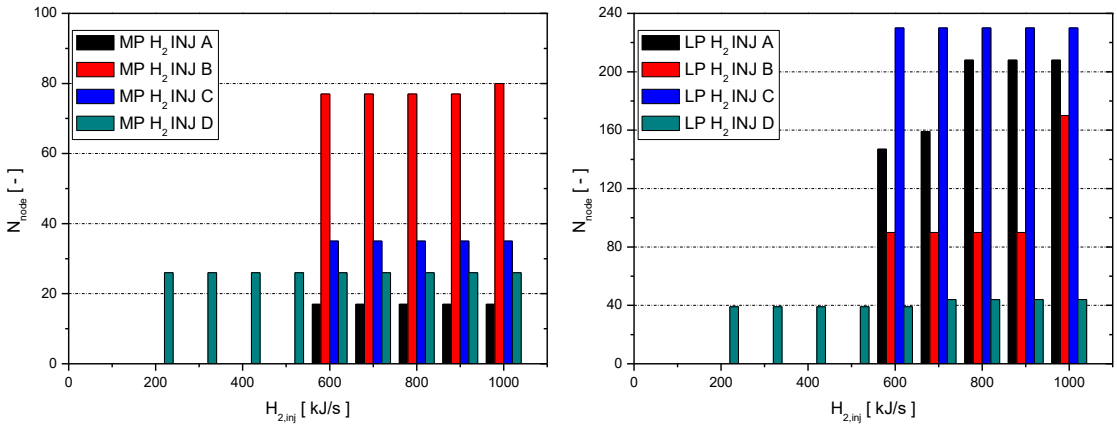

Figure 4.41: Demand nodes with a Wobbe index lower than the minimum allowed value.

Increasing the amount of H_2 supplied by the alternative source, the higher heating value of the gas delivered to users decreases. As a consequence of the use of the energy method, demand nodes withdraw a greater amount of gas. Consequently, mass flow balance and flow velocities in the network are greater too. Figure 4.42 shows maximum velocity achieves by medium-pressure and low-pressure pipes as a function of the total amount of hydrogen injected. For the MP network, in some cases, maximum velocity decreases (B and D), in other is quite similar (case A) and in other firstly decreases and then increases (case C). However, gas flows into the network at a velocity significantly lower than the limit, even for scenario C which achives maximum velocity values ($6.75\ m/s$). Maximum velocity achieved in LP pipes almost increases with the amount of H_2 injected into the network. Different maximum values are achieved for the 4 locations of the alternative

source studied. When hydrogen is injected at node A, it is not possible to inject more than about $420\ kJ/s$ without the gas velocities exceeding the value of $5\ m/s$. For the other alternative source positions, there are no appreciable problems. Values higher than the limit are achieved for case B only if $1000\ kJ/s$ of hydrogen are injected into the network. The number of low-pressure pipes which exceeds the maximum velocity defined by the gas standard is shown in figure 4.43. The gas flow achieves a velocity higher than $5\ m/s$ only into 5 and 2 LP pipes for scenario A and B.

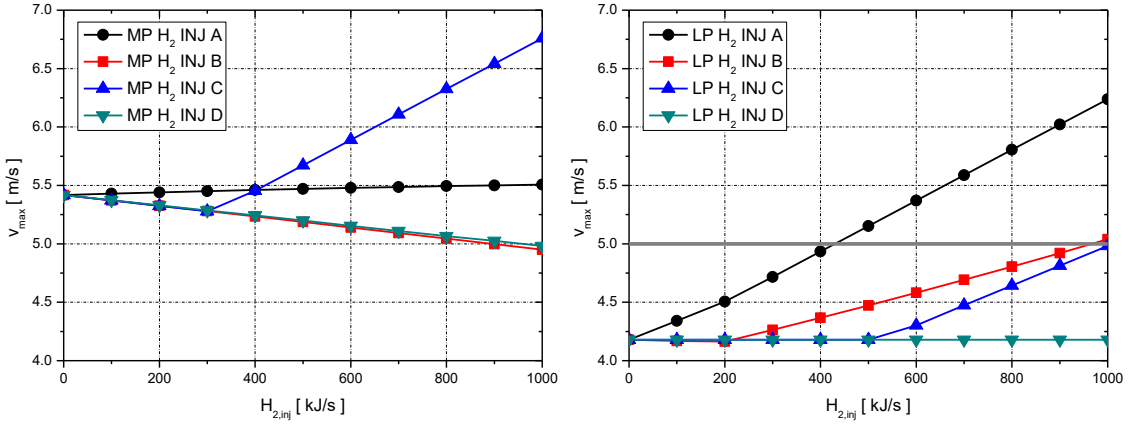

Figure 4.42: Maximum pipe velocity for 500 kJ/s of H_2 injected.

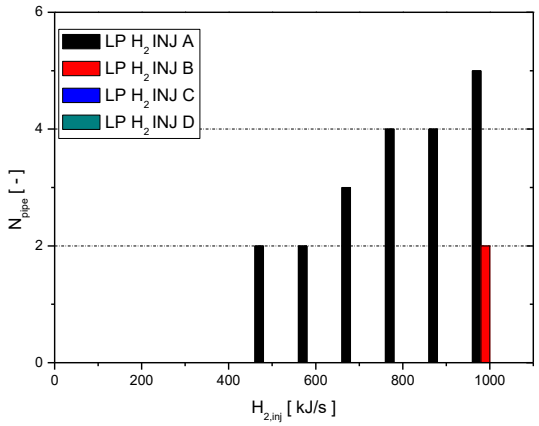

Figure 4.43: Low-pressure pipe with a velocity higher than the maximum allowed value.

Figure 4.44 shows the minimum pressure value of medium-pressure and low-pressure demand nodes of the network. For scenario B and D, minimum pressure values achieved by MP demand nodes increase with the hydrogen injected. Conversely, the trend is opposite when the alternative source is located at the position A or C. Increasing the total of H_2 supplied, pressure values at LP demand decrease. The maximum amount of hydrogen injectable without achieving an undesired pressure level depends on the injection position. For the injection at node C, no more than $490\ kJ/s$ of hydrogen can be injected. Instead, case D is the only position in which it is possible to inject $1000\ kJ/s$ respecting minimum pressure value defined by gas standards. The number of nodes that do not respect pressure level required by users' devices are shown in figure 4.45. The position C has a minimum impact on pressure value of LP demand nodes, but just with only $500\ kJ/s$ of H_2 injected

there are some nodes with a pressure lower than $19\ mbar_g$. Instead, for case A only 10 LP demand nodes do not respect minimum pressure value if $1000\ kJ/s$ are injected. The largest number of LP demand node that has a pressure not allowed is achieved when the maximum amount of hydrogen is injected at node B.

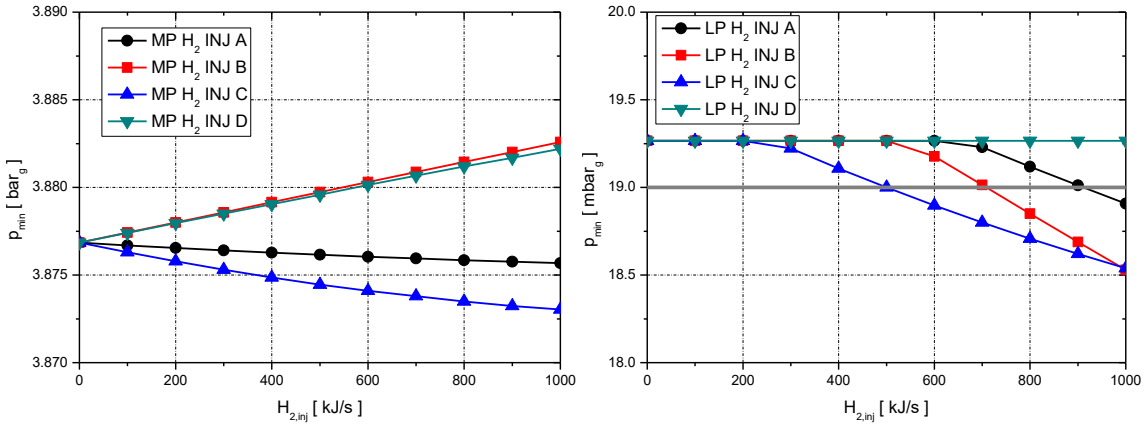

Figure 4.44: Minimum pressure at demand nodes for 500 kJ/s of H_2 injected.

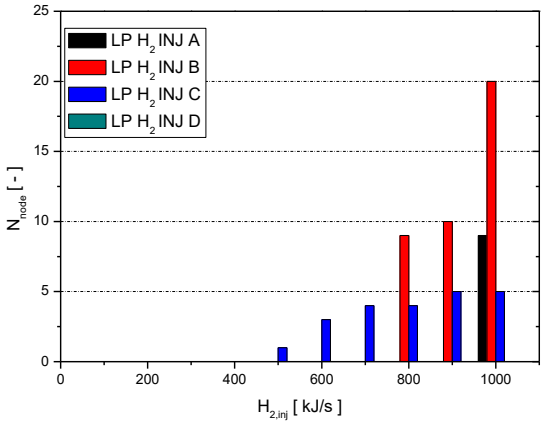

Figure 4.45: LP demand nodes with a pressure lower than the maximum allowed value.

4.2.2 Dynamic simulation with gas quality tracking

The nominal scenario of the network allows to evaluate pressures, velocities and the other parameters of the network during the hour of maximum gas consumption. However, during the other hours of the day, gas demand by the users is variable and so performances of the network changes. Furthermore, in the case of localized alternative fuel injection, it is important to simulate the transport of the different gases in the elements of the network during the hours of the day and its impact on the gas delivered to users. Therefore, dynamic simulations are necessary to predict correctly the behaviour of the network and respect gas standards during all the day.

The medium-pressure network is simulated in the presence of a hydrogen injection at node A (figure 4.24). A constant amount of $500\ kJ/s$ is injected by the alternative source during all hours of the day. The other 2 traditional sources (city gate stations) inject natural gas at a pressure of

$4.00\ bar_g$ and a temperature of $15\ °C$. Gas demand by MP demand nodes and reducing stations are the same as the dynamic simulation of section 4.1.2.

Figures 4.46 4.47 show the gas flow supplied by the 2 city gate stations and demanded by the 3 reducing stations which are affected by the hydrogen injection. Due to the gas flow velocities ($3 \div 5\ m/s$) and the reduced distances between the hydrogen source and the 3 reducing stations ($1.23 \div 1.85\ km$), the time necessary to transport an amount of hydrogen is significantly lower than an hour ($3 \div 8\ min$). Therefore, the time delays are limited and negligible for a simulation of 24 hours. Due to the lower higher heating value of the NG and H_2 mixture, the gas required by medium-pressure and low-pressure subnetworks and so elaborated by reducing stations is higher than in the scenario without hydrogen injection. As a consequence of the use of alternative gas into the network, the gas supplied by the city gate station CGS2 decreases. However, a limited increment of the gas provided by CGS1 is necessary to balance pressures and gas flows of the network.

The maximum hydrogen mass fraction of the gas delivered to users during the hours of the day is shown in figure 4.48. During night hours (minimum gas demand), the percentage of hydrogen injected increases compared to the total energy injected into the network and so the H_2 fraction at demand nodes increases too. The maximum mass hydrogen concentration achieved is 7.1%. For the other hours of the day, the fraction of hydrogen is almost lower than 6%.

As a consequence of the different hydrogen fractions into the network during the day, the Wobbe Index at demand nodes changes, as shown in figure 4.49. For the scenario studied, if $500\ kJ/s$ of hydrogen is injected, the minimum allowed WI is respected only for the hours of maximum demand ($19,\ 20\ h$). A minimum value of $45.9\ MJ/Sm^3$, significantly lower than the limit value of $47.2\ MJ/Sm^3$, is evaluated at about $t = 3.05\ h$.

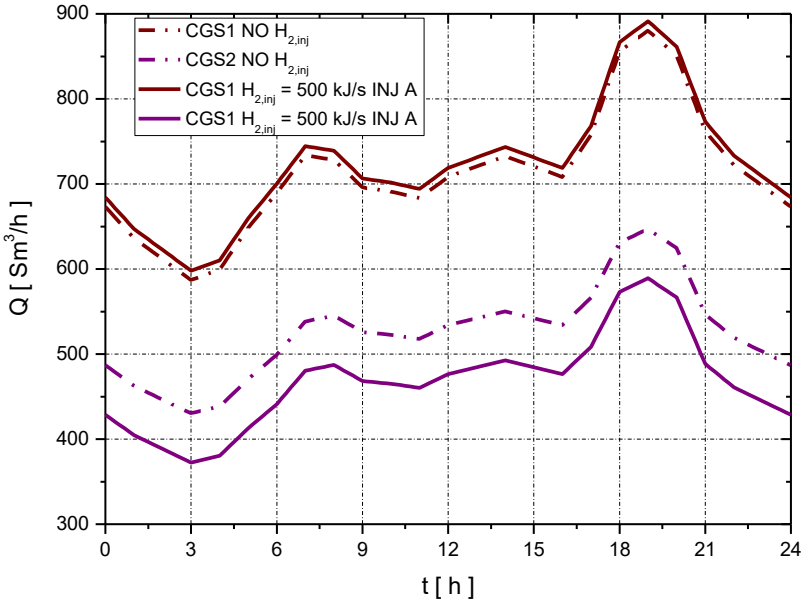

Figure 4.46: Gas flow elaborated by city gate stations and reducing stations during the day.

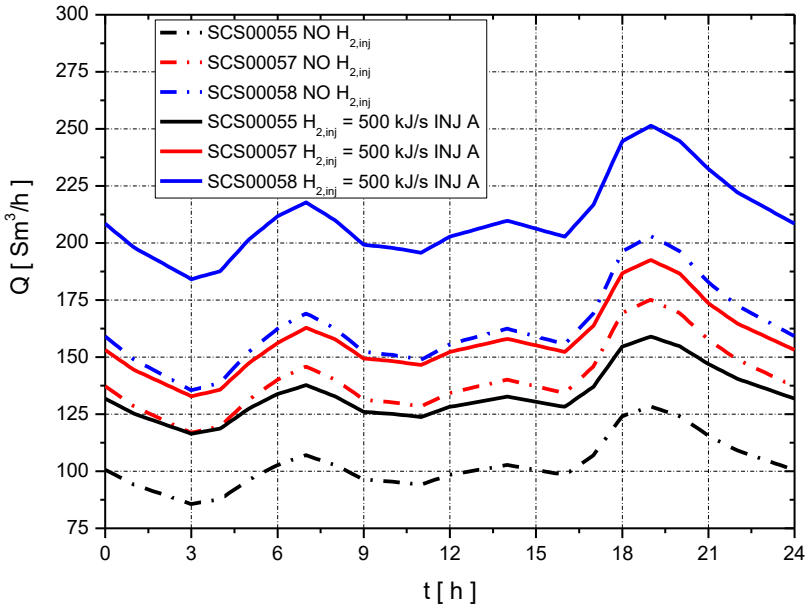

Figure 4.47: Gas flow elaborated by city gate stations and reducing stations during the day.

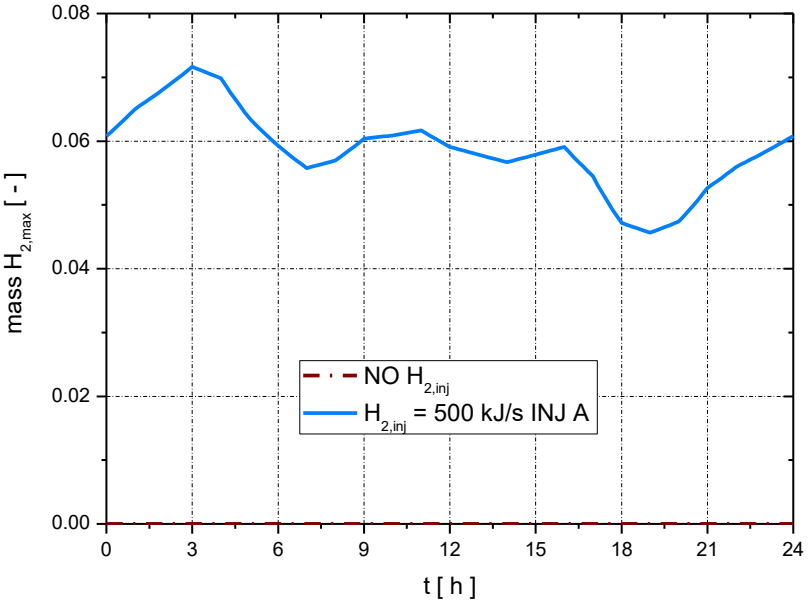

Figure 4.48: Maximum hydrogen mass fraction at demand nodes during the day in the presence of H_2 injection.

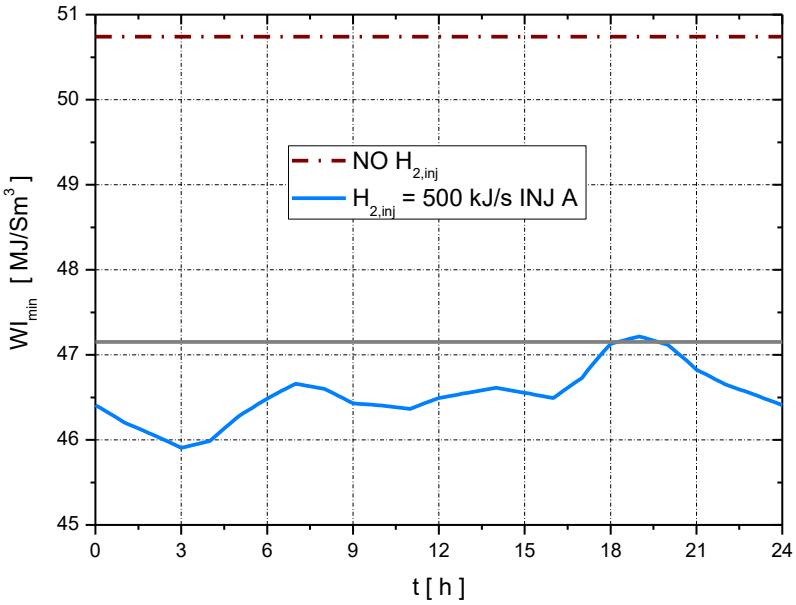

Figure 4.49: Minimum Wobbe index of demand nodes during the day in the presence of H_2 injection.

Figure 4.50 shows hydrogen mass concentration and Wobbe index values of the gas that arrives at the reducing stations affected by the alternative source. The gas arriving at stations SCS00055 and SCS00058 has a different quality compared to the one arriving at station SCS00057. For the third station, the hydrogen mass fraction into the mixture is between 1.83 and 2.62% during the hours of the day. As a consequence, the Wobbe index of the gas elaborated by this station is significantly higher than the values of the others and the minimum allowed value defined ($47.2\ MJ/Sm^3$). Minimum pressure increases and maximum velocity decreases when lower gas demand is required and vice versa (figure 4.51). As shown in the steady-state analysis the effect of H_2 on medium-pressure and velocity is limited. The differences with respect to the scenario without hydrogen injection are up to 10%.

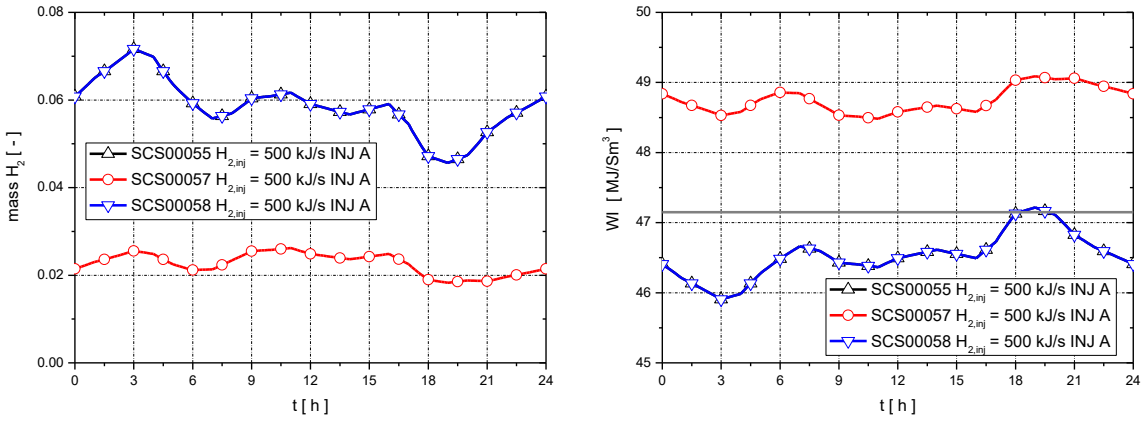

Figure 4.50: H_2 mass fraction and Wobbe index at reducing stations during the day in the presence of H_2 injection.

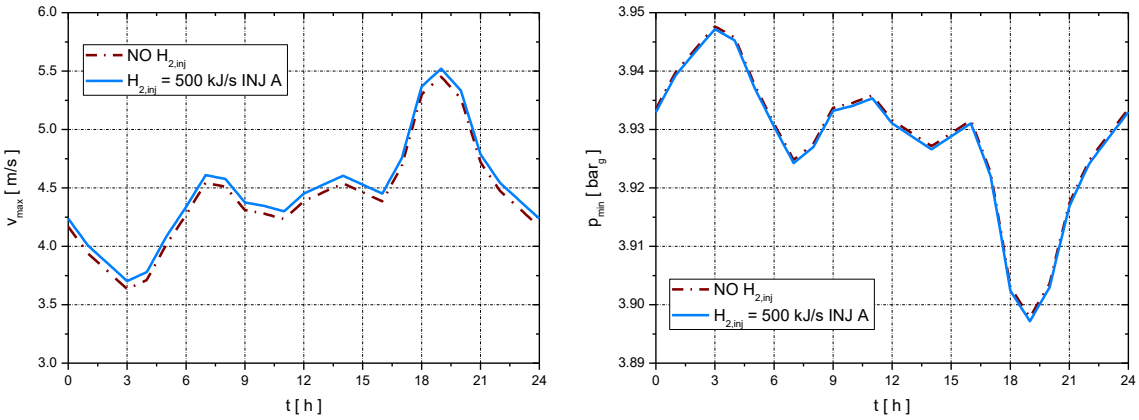

Figure 4.51: Maximum flow velocity and minimum pressure during the day in the presence of H_2 injection.

Bibliography

[4.1] ARERA, the Italian Regulatory Authority for Energy, Networks and Environment, https://www.arera.it.

Conclusion

Increasing worldwide energy demand requires the replacement of high-carbon fossil fuels with clean and alternative ones to limit the chances of climate collapse. In this scenario, natural gas supplies approximately 30% of total energy demand and it is forecasted to become the primary energy source in the next years. Furthermore, the introduction and use of green and zero-carbon fuels, such as biogas, hydrogen and synthetic natural gas, is necessary to achieve emission targets defined by the EU 2050 long-term strategy.

Gas distribution networks, contrary to gas transport pipelines, are usually composed of more than one city gate stations and a large number of pipes, valves and demand nodes. Moreover, there are intermediate and final reducing stations which divide the infrastructure into medium-pressure and low-pressure subnetworks. They provide gas to users at the required pressure levels and manage the system efficiently. In a typical gas distribution network, there are known the pressure at source nodes, where the gas is injected, and the gas flow withdrawn at demand nodes, where industrial and residential customers are connected. The main purpose of a gas distribution company is to evaluate: gas pressure and composition at each node; velocity and pressure drop of each pipe. These values must be monitored to guarantee an efficient operation of the network, supply the gas demand by customers and respect gas standards.

A one-dimensional gas network tool, named "Gas Network Solver", for the simulation of gas distribution network was developed. After the introduction of the computational program requirements, it was described characteristics and mathematical models of elements of the network. The research focused on the implementation of the gas fluid and pipe models which have the most significant impact on network behaviour. The Papay equation of state and Lucas viscosity equation were selected and developed. These formulations consider also the composition of the mixture to calculate the compressibility factor and the dynamic viscosity of the gas fluid. A fully implicit finite difference method, the first-order in time and the second-order in space, is used to solve 1-D unsteady governing equations for the isothermal gas flow into pipes. Instead, for steady-state simulation, the parabolic Fergusson equation, derived from the momentum and which considers the effect of the pipe inclination, is used to calculate pressure drops. Then, it was implemented a batch tracking algorithm for tracking different gas qualities (natural gas, biogas, hydrogen and synthetic natural gas) into the network.

The tool was developed mainly for modelling and simulating traditional medium-pressure and low-pressure distribution grids in steady-state and dynamic conditions. However, the model has also the possibility to study gas network with multiple gas sources with the purpose of evaluate the impact of green gas injections, such as hydrogen, on characteristics (pressure, higher heating value, Wobbe index, etc.) and composition of the gas delivered to customers, pressure drops and velocity into pipes of the network.

The validation of the gas network model proposed was performed by comparing the results of two test cases with values obtained using a commercial software application named "Scenario Analysis Interface for Energy Systems" (SAInt).

The first test case is a single branch pipeline with one source and one demand nodes. Several inlet pressures, demand gas flows, diameters, lengths, inclinations and gas compositions were simulated to evaluate the accuracy of the steady-state model. Decreasing the pressure of the gas, from 50 to $1\ bar_g$, differences between NWG and SAInt values increase, independently on other parameters of the pipeline. However, deviations are marginal ($< 10\%$) for all simulation performed. After that, two dynamic scenarios with different gas flow demand (industrial and residential) during the day are analysed. Pressure drop evolutions calculated by the Gas Network Solver are in good agreement with results of the SAInt software. However, due to the marginal difference of the steady-state models, deviations of about 5% are evaluated during periods of constant gas flow demand.
Instead, the second test case is a simplified looped medium-pressure distribution network. The gas injected into the network by the city gate station at $5\ bar_g$, flows into six pipes of different lengths and diameters. Then, it arrives at two residential/industrial nodes where is extracted from the network. Supply and demand nodes are located at different altitudes (100, 70 and $115\ m$). The steady-state simulation shows that there are little differences (up to 10%) between pressure values evaluated by the two tools. Due to the different altitude of nodes and so inclination of pipes, the two models show deviation in the calculation of the pressure drops in addition to those of the friction losses illustrated in the first test case. Results of the dynamic simulation are in agreement with values calculated by the SAInt software. The difference of pressure evolution at the residential and industrial demand nodes are respectively lower than 4.5 and 5% for the whole period simulated ($24\ h$).
A third test case of a triangular high-pressure network was modelled and simulated with the purpose of benchmark the tool developed with a network studied by several researchers. The source node injects natural gas at a pressure of $50\ bar_g$ and a temperature of $5\ °C$. Three pipes transport the gas to two demand nodes which require different variable gas demands during the day. The simulation performed shows that results of the Gas Network Solver match with the literature data. Values and time of pressure peaks at demand nodes are correctly predicted.
The Gas Network Solver is applied to analyse a case study on a medium-pressure and low-pressure distribution network located in a hilly area of central Italy. The city gate stations (2) supply the gas industrial (230) and residential (719) demand nodes located in small and medium villages in a total area of about $50\ km$. Due to the different pressure level required by users connected to the grid, 18 reducing stations reduce the pressure from $3.80 \div 3.90\ bar_g$ to $20 \div 27.5\ mbar_g$. There are necessary 778 medium-pressure pipes ($24.30\ km$) to transport the gas from the city gate stations to the MP demand nodes and the reducing stations,778 low-pressure pipes ($54.35\ km$) to connect those reducing stations with the LP demand nodes of the 11 low-pressure subnetworks.
After the simulation of the network, a detailed analysis of the elements (source, pipes, demand nodes) of the medium-pressure network and the low-pressure subnetworks was carried out to illustrate the characteristics of the network and boundary conditions of the problem.
In the present case study, a steady-state simulation of the entire distribution network was performed to analyse its behaviour and identify critical elements in the nominal scenario. The 2 city gate stations supply gas at a pressure of $4\ bar_g$ and a temperature of $15\ °C$. Medium-pressure demand nodes withdraw an amount of gas between 0.2 and $5.7\ Sm^3/h$. Conversely, due to the characteristics of residential demand nodes and high-density distribution of urban gas customers, the gas requested by these nodes achieves values up to $18.8\ Sm^3/h$. Results of the simulation show

that there are no criticalities in the elements of the network. For the medium-pressure network, pressure values ($3.88 \div 3.99\ bar_g$) are higher than the maximum pressure required by industrial users and reducing stations. Flow velocities into MP pipes achieve values up to $5.8\ m/s$, considerably lower than the limit ($25\ m/s$). On the other hand, for the low-pressure subnetworks, the minimum value achieved is $19.27\ mbar_g$, adequately higher than the limit value ($19\ mbar_g$) defined by the gas Regulators. However, due to the structure and characteristics of the low-pressure subnetworks studied, the gas arrives only at about 45% of the nodes at the optimal pressure level ($21 \div 19\ mbar_g$). The gas flow supplied by the 18 reducing stations is up to $203\ Sm^3/h$. However, the high stress of some of the stations (> $100\ Sm^3/h$) is compensated by the greater number of sources in the belonging subnetwork.

A dynamic simulation of the medium-pressure network was performed to investigate the network behaviour during the hours of the day. The 18 reducing stations are converted into 18 demand nodes which withdrawn the gas flow necessary to satisfy the demand of low-pressure users. For the gas consumptions required by the medium-pressure demand nodes and reducing stations are used three profiles (RES, IND1 and IND2) because the real profiles of each demand node are not available/accessible. Results show that the gas stored into the network is limited because of the typically slower gas flow variation during the day and especially for the characteristics of the distribution network studied. Minimum pressure ($3.897\ bar_g$) and maximum flow velocity ($5.46\ m/s$) are achieved at about the $19\ h$ when gas demand by users connected to the network is maximum. Conversely, at the $3\ h$, where gas demand is minimum, the gas flows into pipes at low velocity and so pressure drops are very low.

In the case study, a possible solution to decarbonise the network was analysed. One power-to-gas facility, which produces pure green H_2 fuel is connected to the medium-pressure network. In this scenario, the traditional natural gas is supplied by the 2 city gate stations and green fuel gas (hydrogen) is introduced into the network by the alternative P2G source. Therefore, hydrogen is blended with NG flowing into the pipes of the network and a mixture with a variable composition of these two gases arrives into demand nodes of the network.

The NWG solver is used to simulate the transport of hydrogen into the element of network and evaluate the impact of H_2 injection on network behaviour and composition of the gas delivered to users connected to the grid.

The steady-state analysis was performed to determine the most favourable and unfavourable position for the alternative source and estimate the maximum amount of hydrogen injectable respecting gas standards. Four positions (A, B, C and D) of the hydrogen source and different amount of energy between 100 and $1000\ kJ/s$ were simulated.

Results of the simulations for the injection at node A show differences in the impact of hydrogen injection on Wobbe index, velocity and pressure values of the network's elements between the two ways formulated for modelling users' gas consumptions. Using the traditional flow method that imposes the standard volumetric flow, the energy not supplied to users of the network is up to the 13.4% of the total energy demand. The maximum amounts of hydrogen injectable into the network respecting gas standards is about $410\ kJ/s$ for the energy method and $480\ kJ/s$ for the flow method.

For the four different injection positions, simulations show that maximum H_2 concentrations and minimum WI values achieved in the A, B and C scenarios are quite similar. For these positions, the

maximum amount of H_2 injectable without achieve the minimum allowed WI is $500\ kJ/s$. Instead, when hydrogen is injected at the node D, maximum hydrogen into the mixture achieved is three and four times more than the other cases. Therefore, in this case, it is possible to inject only $180\ kJ/s$ respecting limit WI values. The number of demand nodes and pipes that do not respect gas standards is different for the alternative source position studied. Considering WI, v, p values of the medium-pressure network, the best position is the location A. Conversely, for the A injection position, the minimum number of LP pipe (2) with a value higher than $5\ m/s$ is achieved. The position C has a minimum impact on the pressure value of LP demand nodes, but just with only $500\ kJ/s$, there are some nodes which have a value lower than $19\ mbar_g$. If the location A is selected, the pressure of the gas delivered at demand nodes is lower than the limit only injecting $1000\ kJ/s$.

During the other hours of the day, gas demand by the users is variable and so performances of the network and the impact of the alternative source change. Therefore, dynamic simulations are necessary to predict correctly the behaviour of the network and respect gas standards during all day. The medium-pressure network was simulated in the presence of a hydrogen injection at node A. A constant amount of $500\ kJ/s$ is injected by the alternative source during all hours of the day. Results show that the gas supplied by the city gate station CGS2 decrease because of the use of alternative gas into the network. However, a limited increment of the gas provided by CGS1 is necessary to balance pressures and gas flows of the network. During night hours (minimum gas demand), the percentage of hydrogen injected increases compared to the total energy injected into the network and so the H_2 fraction at demand nodes increases too. As a consequence of the different hydrogen fractions into the network during the day, the Wobbe Index at demand nodes changes. For the scenario studied, if $500\ kJ/s$ of hydrogen is injected, the minimum allowed WI is respected only for the hours of maximum demand $(19, 20\ h)$.

In conclusion, the injection into the existing gas grid, of the hydrogen “green” gas produced by the power to gas technology, is a potential solution to reduce carbon dioxide emissions.

Nevertheless, flow velocity into pipes, pressure and Wobbe index at demand nodes are highly influenced by the amount of hydrogen gas injected into the network.

Gas network simulations are useful to choose an appropriate position of the alternative source and so reduce the impact on the network. The number of elements which do not respect gas standard is also important to select the best location. In some case, the minimum WI, p and maximum v achieves could be the same, but the H_2 injection could influence a larger or smaller area. It is possible to blend with the natural gas considered a maximum hydrogen mass fraction of about 5% without achieves the minimum allowed Wobbe index value defined by the Italian gas standard. However, this H_2 concentration in some cases does not guarantee the respect of pressure and velocity limits.